

**Assessing the Effectiveness of Limestone from Oterkpolu Area in the Eastern region of  
Ghana as a Suitable Adsorbent for Water Defluoridation**

A thesis presented to the:

DEPARTMENT OF NUCLEAR SCIENCE AND APPLICATIONS

SCHOOL OF NUCLEAR AND ALLIED SCIENCES

UNIVERSITY OF GHANA

By

ERIC KWABENA DROEPENU; 10506650

B.Ed. Science (University of Education, Winneba), 2007

In partial fulfillment of the requirements for the degree of

**MASTER OF PHILOSOPHY**

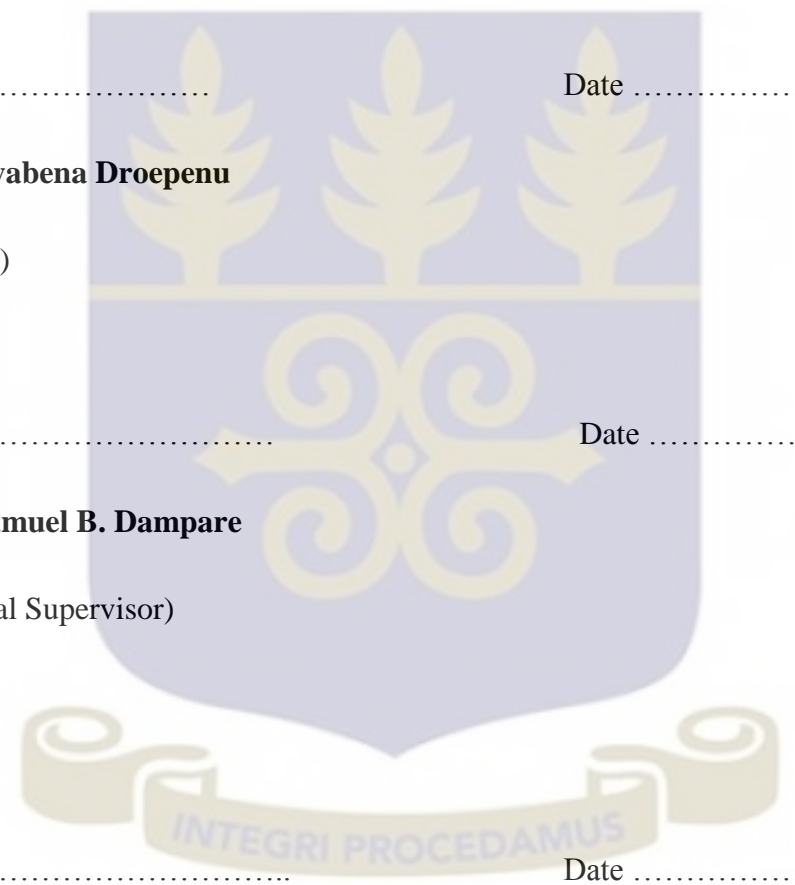
IN

NUCLEAR AND ENVIRONMENTAL PROTECTION

JULY, 2016.

## DECLARATION

This is to certify that this thesis is the result of research work undertaken by **Eric Kwabena Droepenu** towards the Degree of M.Phil. Nuclear and Environmental Protection in the Department of Nuclear Science and Applications, School of Nuclear and Allied Sciences (SNAS), University of Ghana, Legon, under the supervision of **Prof. Samuel B. Dampare** and **Dr. Dennis K. Adotey**.



..... Date .....

**Eric Kwabena Droepenu**  
(Student)

..... Date .....

**Prof. Samuel B. Dampare**  
(Principal Supervisor)

..... Date .....

**Dr. Dennis K. Adotey**  
(Co-Supervisor)

## **DEDICATION**

This work is dedicated to my whole family and friends.



## ACKNOWLEDGMENTS

My first and foremost thanks and appreciation go to the Most High God for Protecting and Guiding me, giving me the Sound Health, Wisdom and Knowledge throughout this research work. May His Sovereign Name be Praised now and forever more.

With maximum respect and standing ovation, I sincerely salute my two able and indefatigable supervisors, Prof. Samuel B. Dampare and Dr. Dennis K. Adotey for working tirelessly day and night, painstakingly going through my write up. Actually, their constructive criticism, corrections, encouragement and pieces of advice they bestowed on me have contributed immensely in coming up to this far.

My special thanks also go to Mr. John Senu, Mr. Courage Argbey, Mr. Nash O. Bentil and Miss Ruby Torto, all of Nuclear Chemistry and Environmental Research Centre, GAEC for their skilled technical assistance. The following also deserve special thanks for their enormous and selfless services rendered. They include; Mr. David Okoh Kpeglo of Radiation Protection Institute, GAEC, Mr Ekow Quagraine and Mr. Isaac Baidoo of GHAR-1- Reactor Centre, GAEC, Dr. Martin Egblewogbe, Miss Beatrice Agyapomah, Mr. Emmanuel Abitty, Mr Peter Duduchoge, Mr. Sedem Garr and Mr. Emmanuel Awunyo of the Earth Science and Physics Department, UG, Legon, and the management of the Limestone Companies (Agyapaado, Love and Fanj) contracted by GHACEM for granting the permission to have access to Oterkpolu site for sampling.

Finally, my profound gratitude goes to my wife, Mrs. Veronica Adae-Dropenu, my parents, brothers, and Staff of Benkum Senior High School, Larteh-Akuapem, for their encouragement during the course of this study. May God be gracious unto them



and lift His light of countenance upon them all and be a blessing to this present and future generations.



## TABLE OF CONTENT

DECLARATION .....	ii
DEDICATION .....	iii
ACKNOWLEDGMENTS .....	iv
TABLE OF CONTENT .....	vi
ABSTRACT.....	1
CHAPTER ONE .....	3
INTRODUCTION .....	3
1.1 Background to the Study.....	3
1.2 RESEARCH PROBLEM.....	8
1.3 RESEARCH OBJECTIVES .....	10
1.3.1 Principal Objective.....	10
1.3.2 Specific Objectives .....	10
1.4 JUSTIFICATION .....	10
CHAPTER TWO .....	12
LITERATURE REVIEW .....	12
2.1 Water occurrence in Ghana.....	12
2.2 Importance of fluoride and its environmental occurrence .....	12
2.3 Fluoride in Bongo .....	14
2.4 Chemistry of fluoride.....	16
2.5 Fluoride in humans and its health effects .....	17
2.5.1 Fluoride intake and metabolism.....	17
2.5.2 Health effects of fluoride ingestion.....	18
2.6 Defluoridation techniques/methods .....	21
2.6.1 Precipitation method .....	22

2.6.2 Chemical method .....	23
2.6.3 Adsorption/Ion-exchange method.....	23
2.6.3.1 Adsorption.....	24
2.6.3.2 Types of Adsorption .....	25
2.6.3.3 Factors affecting Adsorption.....	25
2.7 Use of limestone as an adsorbent.....	30
2.8 Natural Background Radioactivity .....	30
2.8.1 Terrestrial Radionuclides .....	31
2.8.2 Cosmogenic Radionuclide .....	33
2.8.3 Artificial (Man-made) Radionuclide.....	34
2.8.4 Transport, Fate and Distribution of Radionuclides in the Environment .....	34
2.8.5 Effects of Radiation on Humans .....	35
2.8.6 Methods of Assessing NORMs.....	35
CHAPTER THREE .....	36
MATERIALS AND METHODS.....	36
3.1 The Study Area .....	36
3.1.1 Geographical location of Yilo Krobo-Oterkpolu.....	36
3.1.2 Oterkpolu Limestone Deposits .....	38
3.1.3 Commercial Mining of Oterkpolu Limestone.....	38
3.2 Reconnaissance Survey.....	39
3.2.1 Ethical Approval .....	39
3.2.2 Site Visitation.....	39
3.2.3 Identification of Limestone during Site Visit .....	39
3.3 Collection of Limestone.....	40
3.4 Sample Preparation and Analytical Methodology Development.....	41

3.4.1 General Overview of Experimental Work .....	41
3.4.2 Sample Preparation .....	43
3.4.2.1 Mineralogy Using Petrographic Thin Section .....	43
3.4.2.2 Determination of Mineral Composition Using X-Ray Diffraction (XRD) .....	45
3.4.2.3 Assessment of Radiological Risk Posed by Oterkpolu Limestone .....	47
3.5 Development of Limestone Defluoridation Technique using Batch Analysis ..	53
3.5.1 Preparation of Limestone Samples .....	53
3.5.2 Batch Adsorption Experiment.....	54
3.6 Application of Developed Technique .....	58
3.6.1 Collection of Water Samples from Bongo District.....	58
3.6.2 Determination of Physico-chemical Parameters .....	60
3.6.2.1. Determination of pH .....	60
3.6.2.2 Determination of Electrical conductivity (EC), Total Dissolved Solid (TDS), Turbidity, Colour and Salinity .....	60
3.6.3 Column Adsorption Experiments .....	61
3.6.4 Determination of Cations .....	62
3.6.4.1 Magnesium ( $Mg^{2+}$ ).....	63
3.6.4.2 Determination of As by HG-AAS.....	65
3.6.5 Determination of Anions.....	66
3.6.5.1 Determination of Fluoride ( $F^-$ ), Chloride ( $Cl^-$ ), Phosphate ( $PO_4^{3-}$ ), sulphate ( $SO_4^{2-}$ ) and Nitrate ( $NO_3^-$ ) using ICS-90 Chromatographic System ..	66
CHAPTER FOUR.....	68
RESULTS AND DISCUSSION .....	68
4.1 Petrographic Thin Section.....	68
4.1.1 Sample EKL R <sub>1</sub> 02.....	69

4.1.2 Sample EKL D01 .....	69
4.2 XRD Analysis .....	70
4.2.1 Limestone Samples EKL- R <sub>1</sub> 02 and EKL-D01 .....	71
4.3 Radiological Safety of the Limestone Samples .....	71
4.3.1 Activity Concentration of Naturally Occurring Radionuclides in Limestone Sample.....	71
4.4 Batch Adsorption Experiment.....	74
4.4.1 General Procedure.....	74
4.4.2 Effect of Varying Residence Time on Residual Fluoride Adsorption in 1 mg/L Fluoride Solution.....	75
4.4.3 Effect of Varying Residence Time on Residual Fluoride Adsorption in 5 mg/L Fluoride Solution.....	83
4.4.4 Effect of Varying Residence Time on Residual Fluoride Adsorption in 10 mg/L Fluoride Solution.....	89
4.4.5 Effect of Grain Size on Percentage Mean Fluoride Adsorption .....	96
4.4.5.1 Effect of Grain Size on Percentage Mean Fluoride Adsorption for Sample (EKL-R <sub>1</sub> 02) in 1 mg/L NaF Solution.....	96
4.4.5.2 Effect of Grain Size on Percentage Mean Fluoride Adsorption for Sample (EKL-D01) in 1 mg/L NaF Solution.....	98
4.4.5.3 Effect of Grain Size on Percentage Mean Fluoride Adsorption for Sample (EKL-R <sub>1</sub> 02) in 5 mg/L NaF Solution.....	99
4.4.5.4 Effect of Grain Size on Percentage Mean Fluoride Adsorption for Sample (EKL-D01) in 5 mg/L NaF Solution.....	100
4.4.5.5 Effect of Grain Size on Percentage Mean Fluoride Adsorption for Sample (EKL-R <sub>1</sub> 02) in 10 mg/L NaF Solution.....	101
4.4.5.6 Effect of Grain Size on Percentage Mean Fluoride Adsorption for Sample (EKL-D01) in 10 mg/L NaF Solution.....	102
4.4.6 Effect of Fluoride Concentration Variation on Percentage Mean Fluoride Adsorption.....	103

4.4.7 Effect of pH of Fluoride - Limestone Mixture on Percentage Mean Fluoride Adsorption.....	105
4.4.8 Effect of Varying Adsorbent Dose on Percentage Mean Fluoride Adsorption.....	106
4.5 Column Adsorption Experiment .....	109
4.5.1 Anion Analysis from Column Adsorption Experiment .....	110
CHAPTER FIVE .....	114
CONCLUSION AND RECOMMENDATIONS .....	114
5.1 CONCLUSION.....	114
5.1.1 Mineralogy.....	114
5.1.2 Radiological Safety.....	115
5.1.3 Particle Size - % Adsorption.....	115
5.1.4 Resident Time - % Absorption .....	116
5.1.5 Adsorbent Dose - % Adsorption .....	116
5.1.6 Fluoride Concentration - % Adsorption.....	117
5.1.7 pH - % Adsorption of Mixture (Limestone - Fluoride solution) .....	117
5.1.8 Column Adsorption.....	118
5.2 RECOMMENDATIONS.....	119
REFERENCES .....	120
APPENDIX A.....	137
APPENDIX B: Petrographic Thin Section of limestone samples .....	144
APPENDIX C: Activity Concentrations of Samples.....	149
APPENDIX D: Batch Adsorption Analysis.....	155
APPENDIX E: Preparation of NaF solutions .....	158
APPENDIX F: Ion Chromatography .....	160

APPENDIX G: Standard Calibration Curve.....	161
APPENDIX H: Batch Adsorption Analysis .....	163





## LIST OF TABLES

<b>2.1:</b> Fluoride concentration in drinking water and its health effects .....	<b>14</b>
<b>2.2:</b> Fluoride concentration distribution in groundwater (upper regions, Ghana) .....	<b>16</b>
<b>2.3:</b> Fluoride composition in some major mineral .....	<b>17</b>
<b>2.4:</b> Fluoride content in some food crops in Bongo district .....	<b>21</b>
<b>3.1:</b> Concentration (prepared and measured) of standard solutions using Ion Chromatograph .....	<b>56</b>
<b>4.1:</b> Percentage composition of mineralogical content of selected samples .....	<b>67</b>
<b>4.2:</b> Comparism of reported activity concentrations with the present study .....	<b>72</b>
<b>4.3:</b> Absorbed Dose and Radioactivity Indices associated with Oterkpolu limestone samples .....	<b>73</b>
<b>4.4:</b> Percentage fluoride adsorption for 1 mg/L fluoride solution .....	<b>103</b>
<b>4.5:</b> Percentage fluoride adsorption for 5 mg/L fluoride solution .....	<b>104</b>
<b>4.6:</b> Percentage fluoride adsorption for 10 mg/L fluoride solution .....	<b>104</b>
<b>4.7:</b> pH variation of $F^-$ - Limestone mixture with % mean fluoride adsorption .....	<b>106</b>
<b>4.8:</b> Variation of Adsorbent Dose on % Fluoride Adsorption for sample EKL-R <sub>102</sub> .....	<b>107</b>
<b>4.9:</b> Variation of Adsorbent Dose on % Fluoride Adsorption for sample EKL-D01 .....	<b>107</b>
<b>4.10:</b> Physico-chemical and anion analysis of water samples from Bongo district .....	<b>110</b>
<b>4.11:</b> Summary of the effect of co-existing anions in the water samples before and after the defluoridation process .....	<b>113</b>



## LIST OF FIGURES

<b>2.1:</b> Fluoride concentration in some soil samples in the Bongo district of Ghana .....	<b>15</b>
<b>2.2:</b> Stages of dental fluorosis .....	<b>19</b>
<b>2.3:</b> Skeletal fluorosis .....	<b>20</b>
<b>2.4:</b> Effect of contact time on the removal of fluoride from natural groundwater sample .....	<b>27</b>
<b>2.5:</b> Effect of adsorbent dose on the removal of fluoride by gypsiferous limestone .....	<b>28</b>
<b>2.6:</b> The effect of pH of the solution on fluoride removal .....	<b>28</b>
<b>2.7a:</b> Scheme of Uranium decay (U-238) series .....	<b>32</b>
<b>2.7b:</b> Scheme of Thorium decay (Th-232) series .....	<b>33</b>
<b>3.1:</b> Map of study area showing the location of Oterkpolu and limestone deposit .....	<b>37</b>
<b>3.2:</b> Packaging of identified limestone samples for transportation to the lab at GAEC .....	<b>40</b>
<b>3.3a:</b> General Experimental framework .....	<b>41</b>
<b>3.3b:</b> Detailed work layout of the study .....	<b>42</b>
<b>3.4a:</b> Cutting of limestone into slabs .....	<b>44</b>
<b>3.4b:</b> Canada Balsam .....	<b>44</b>
<b>3.4c:</b> Grinding wheel .....	<b>45</b>
<b>3.4d:</b> Petrographic Microscope .....	<b>45</b>
<b>3.5a:</b> Crushing with Fritsch Pulverisette 2 Jaw Crusher .....	<b>46</b>
<b>3.5b:</b> Milling with Fritsch Pulverisette 2 Mortar Grinder .....	<b>46</b>
<b>3.5c:</b> Sieving sample with 63 $\mu$ m mesh .....	<b>46</b>

<b>3.5d:</b> Pulverized and homogenized samples .....	<b>47</b>
<b>3.5e:</b> Tools for transforming powdered samples to pellets .....	<b>47</b>
<b>3.5f:</b> XRD Diffractometer .....	<b>47</b>
<b>3.6a:</b> Packaging of limestone sample in a 1L Marinelli beaker .....	<b>50</b>
<b>3.6b:</b> HPGe Gamma detector for NORMs measurement .....	<b>50</b>
<b>3.7a:</b> Shaking sample with Retsch AS 200 Vibratory Shaker .....	<b>53</b>
<b>3.7b:</b> Sieved limestone samples .....	<b>53</b>
<b>3.8a:</b> Eluent standard solution .....	<b>54</b>
<b>3.8b:</b> Regenerant standard solution .....	<b>54</b>
<b>3.9a:</b> Weighing of limestone sample .....	<b>57</b>
<b>3.9b:</b> Magnetic stirrer of mixture .....	<b>57</b>
<b>3.9c:</b> IC for F <sup>-</sup> measurement .....	<b>57</b>
<b>3.10:</b> Uncapped boreholes at two affected communities in the Bongo District .....	<b>58</b>
<b>3.11a:</b> Mini-Column bed filled with adsorbent .....	<b>61</b>
<b>3.11b:</b> Aliquots taken from the different mini-column beds .....	<b>61</b>
<b>3.12a:</b> Samples being prepared for digestion .....	<b>62</b>
<b>3.12b:</b> Samples on hot plate during digestion .....	<b>62</b>
<b>3.13:</b> Example of a Chromatographic spectrum obtained .....	<b>66</b>
<b>4.1:</b> Photomicrograph of sample EKL- R <sub>1</sub> 02 .....	<b>69</b>
<b>4.2:</b> Photomicrograph of sample EKL D01 .....	<b>69</b>
<b>4.3:</b> Diffractogram of limestone sample EKL-R <sub>1</sub> 02 (A) and EKL-D01 (B) .....	<b>71</b>
<b>4.4:</b> Plot of activity concentration against limestone type .....	<b>71</b>
<b>4.5:</b> Plot of residual fluoride concentration against time for 10 g mass	

[500-1000 $\mu\text{m}$ ] sample in 1 mg/L NaF Solution .....	74
<b>4.6:</b> Plot of residual fluoride concentration against time for 50 g mass	
[500-1000 $\mu\text{m}$ ] sample in 1 mg/L NaF Solution .....	75
<b>4.7:</b> Plot of residual fluoride concentration against time for 100 g mass	
[500-1000 $\mu\text{m}$ ] sample in 1 mg/L NaF Solution .....	76
<b>4.8:</b> Plot of residual fluoride concentration against time for 10 g mass	
[1000-2000 $\mu\text{m}$ ] sample in 1 mg/L NaF Solution .....	77
<b>4.9:</b> Plot of residual fluoride concentration against time for 50 g mass	
[1000-2000 $\mu\text{m}$ ] sample in 1 mg/L NaF Solution .....	78
<b>4.10:</b> Plot of residual fluoride concentration against time for 100 g mass	
[1000-2000 $\mu\text{m}$ ] sample in 1 mg/L NaF Solution .....	79
<b>4.11:</b> Plot of residual fluoride concentration against time for 10 g mass	
[2000-6350 $\mu\text{m}$ ] sample in 1 mg/L NaF Solution .....	80
<b>4.12:</b> Plot of residual fluoride concentration against time for 50 g mass	
[2000-6350 $\mu\text{m}$ ] sample in 1 mg/L NaF Solution .....	80
<b>4.13:</b> Plot of residual fluoride concentration against time for 100 g mass	
[2000-6350 $\mu\text{m}$ ] sample in 1 mg/L NaF Solution .....	81
<b>4.14:</b> Plot of residual fluoride concentration against time for 10 g mass	
[500-1000 $\mu\text{m}$ ] sample in 5 mg/L NaF Solution .....	82
<b>4.15:</b> Plot of residual fluoride concentration against time for 50 g mass	
[500-1000 $\mu\text{m}$ ] sample in 5 mg/L NaF Solution .....	83
<b>4.16:</b> Plot of residual fluoride concentration against time for 100 g mass	
[500-1000 $\mu\text{m}$ ] sample in 5 mg/L NaF Solution .....	84
<b>4.17:</b> Plot of residual fluoride concentration against time for 10 g mass	
[1000-2000 $\mu\text{m}$ ] sample in 5 mg/L NaF Solution .....	84

<b>4.18:</b> Plot of residual fluoride concentration against time for 50 g mass	
[1000-2000 $\mu\text{m}$ ] sample in 5 mg/L NaF Solution	.....85
<b>4.19:</b> Plot of residual fluoride concentration against time for 100 g mass	
[1000-2000 $\mu\text{m}$ ] sample in 5 mg/L NaF Solution	.....86
<b>4.20:</b> Plot of residual fluoride concentration against time for 10 g mass	
[2000-6350 $\mu\text{m}$ ] sample in 5 mg/L NaF Solution	.....86
<b>4.21:</b> Plot of residual fluoride concentration against time for 50 g mass	
[2000-6350 $\mu\text{m}$ ] sample in 5 mg/L NaF Solution	.....87
<b>4.22:</b> Plot of residual fluoride concentration against time for 100 g mass	
[2000-6350 $\mu\text{m}$ ] sample in 5 mg/L NaF Solution	.....88
<b>4.23:</b> Plot of residual fluoride concentration against time for 10 g mass	
[500-1000 $\mu\text{m}$ ] sample in 10 mg/L NaF Solution	.....89
<b>4.24:</b> Plot of residual fluoride concentration against time for 50 g mass	
[500-1000 $\mu\text{m}$ ] sample in 10 mg/L NaF Solution	.....90
<b>4.25:</b> Plot of residual fluoride concentration against time for 100 g mass	
[500-1000 $\mu\text{m}$ ] sample in 10 mg/L NaF Solution	.....90
<b>4.26:</b> Plot of residual fluoride concentration against time for 10 g mass	
[1000-2000 $\mu\text{m}$ ] sample in 10 mg/L NaF Solution	.....91
<b>4.27:</b> Plot of residual fluoride concentration against time for 50 g mass	
[1000-2000 $\mu\text{m}$ ] sample in 10 mg/L NaF Solution	.....92
<b>4.28:</b> Plot of residual fluoride concentration against time for 100 g mass	
[1000-2000 $\mu\text{m}$ ] sample in 10 mg/L NaF Solution	.....92
<b>4.29:</b> Plot of residual fluoride concentration against time for 10 g mass	
[2000-6350 $\mu\text{m}$ ] sample in 10 mg/L NaF Solution	.....93
<b>4.30:</b> Plot of residual fluoride concentration against time for 50 g mass	

[2000-6350 $\mu\text{m}$ ] sample in 10 mg/L NaF Solution .....	94
<b>4.31:</b> Plot of residual fluoride concentration against time for 100 g mass	
[2000-6350 $\mu\text{m}$ ] sample in 10 mg/L NaF Solution .....	95
<b>4.32:</b> Plot of % mean adsorption against mass of sample EKL-R <sub>1</sub> 02	
in 1 mg/L .....	96
<b>4.33:</b> Plot of % mean adsorption against mass of sample EKL-D01	
in 1 mg/L .....	97
<b>4.34:</b> Plot of % mean adsorption against mass of sample EKL-R <sub>1</sub> 02	
in 5 mg/L .....	98
<b>4.35:</b> Plot of % mean adsorption against mass of sample EKL-D01	
in 5 mg/L .....	100
<b>4.36:</b> Plot of % mean adsorption against mass of sample EKL-R <sub>1</sub> 02	
in 10 mg/L .....	101
<b>4.37:</b> Plot of % mean adsorption against mass of sample EKL-D01	
in 10 mg/L .....	102
<b>4.38:</b> Plot of % fluoride adsorption for varying fluoride concentrations .....	105
<b>4.39:</b> Plot of % fluoride adsorption against varying mass of samples .....	108
<b>4.40:</b> Plot of residual fluoride concentration against time for water	
sample BNB6 .....	111
<b>4.41:</b> Plot of residual fluoride concentration against time for water	
sample BNB8 .....	111

## LIST OF ACRONYMS

<b>AED</b>	Annual Effective Dose
<b>CEIA</b>	Centre for Environmental Impact Analysis
<b>DW</b>	Dry Weight
<b>EC</b>	Electrical Conductivity
<b>EKA</b>	Eric Kwabena Agyapaado
<b>EKL</b>	Eric Kwabena Love
<b>EPA</b>	Environmental Protection Agency
<b>HPGe</b>	High Purity Germanium
<b>IQ</b>	Intelligent Quotient
<b>LACOSREP</b>	Land Conservation and Smallholder Rehabilitation Project
<b>MSP</b>	Monosodium Phosphate
<b>NaF</b>	Sodium Fluoride
<b>NORMs</b>	Naturally Occurring Radioactive Materials
<b>NTU</b>	Nephelometric Turbidity Unit
<b>PHC</b>	Population and Housing Census
<b>PSU</b>	Practical Salinity Unit
<b>PTS</b>	Petrographic Thin Section
<b>TDS</b>	Total Dissolved Solids
<b>TENORM</b>	Technologically Enhanced Naturally Radioactive Materials
<b>VOC</b>	Volatile Organic Compound
<b>WHO</b>	World Health Organization
<b>XRD</b>	X-Ray Diffraction



## ABSTRACT

Fluoride-contamination of groundwater [above the World Health Organization (WHO) recommended limit of 1.5 mg/L] in the Upper East and Northern regions of Ghana is a well-known problem. Fluoride is, however, beneficial to humans if present in drinking water at levels between 0.7 – 1.5 mg/L. Although, there are some efficient methods for defluoridation of drinking water using various adsorbents, the magnitude of the problem has made it imperative to develop economically viable water defluoridation techniques using readily available natural resource as adsorbent. This will complement the existing defluoridation techniques in order to alleviate the difficulty faced by inhabitants of the affected communities. In addition, a method which is cost effective, easy to use by a layman, does not add other contaminants to water, and efficient in the long term is highly desirable. In this study, the effectiveness of readily available limestone from Oterkpolu (Yilo-Krobo district, Eastern region of Ghana) as fluoride adsorbent was assessed. A drinking water defluoridation technique was subsequently developed using the limestone with various grain sizes (i.e., 500 – 1000  $\mu\text{m}$ , 1000 – 2000  $\mu\text{m}$  and 2000 – 6350  $\mu\text{m}$ ) through Batch Adsorption Experiment (using NaF solution concentrations of 1, 5 and 10 mgF/L), followed by Column Adsorption Experiment using fluoride contaminated groundwater water samples from Bongo district. This was achieved through the geochemical and mineralogical characterization of Oterkpolu limestone using X-ray Powder Diffraction (XRD) and Petrographic Thin Section (PTS). In addition, the radiological risk associated with the use of the limestone for water defluoridation was assessed through the determination of the activity concentration of the Naturally-Occurring Radioactive Materials (NORMs) using a High-Purity Germanium (HPGe)  $\gamma$ -ray detector [ $\gamma$ -ray spectrometry], and computed Annual Effective Dose (AED). The

study also evaluated the fluoride adsorption efficiency (Sorption capacity and % Adsorption) of different limestone types from Oterkpolu with respect to varying: (i) adsorbent dose (ii) particle sizes of the adsorbent (limestone) (iii) residence time (iv) fluoride concentration. The developed technique was applied to fluoride contaminated water samples collected from affected the communities (Bongo district) through a Column Adsorption Experiment. From the Batch Adsorption Experiment, the maximum percentage adsorption of fluoride was 57.27%, 62.96% and 50.96% (for 1, 5 and 10 mg/L respectively) for sample EKL-R<sub>1</sub>02 at the 60<sup>th</sup> minute. These results were recorded for 1000 – 2000 µm limestone grain size. The mean activity concentrations for <sup>238</sup>U, <sup>232</sup>Th and <sup>40</sup>K were found to be  $2.0 \pm 1.5$ ,  $1.7 \pm 1$  and  $21.9 \pm 13.4$  Bq/kg respectively for the limestone samples from Oterkpolu. The calculated Annual Effective Dose of the adsorbent (0.027 mSv/yr) was lower than the recommended 0.40 mSv/yr proposed by United Nations Scientific Committee on the Effects of Atomic Radiation (UNSCEAR). Mineralogically, (PTS and XRD analysis), the limestone sample is made up of 96% calcite and 4% quartz (PTS) and 83% calcite, 11% serandite and 6% silicon oxide (XRD). This indicates high calcite content in the sample which suggests that, it is an effective material for fluoride adsorption. The application of the developed methodology (Column Adsorption Analysis) yielded 80% and 67% fluoride removal from two groundwater water samples (BNN8 and BNB6) respectively from the Bongo district of the Upper East region of Ghana. Thus, the fluoride levels in the 330 mL samples were reduced from 7.5 and 6.2 mg/L to 1.5 and 2.0 respectively. The variation was as a result of co-existing anions present in the water sample. The results suggest that Oterkpolu limestone can be used effectively for the removal of fluoride ions in fluoride-contaminated groundwater in general and from the northern regions of Ghana in particular Bongo district.



## CHAPTER ONE

### INTRODUCTION

#### 1.1 Background to the Study

Water is an essential natural resource for sustaining life and the environment. The suitability of water for domestic, industrial or agricultural purpose depends on its chemical composition. Freshwater for use by humans occurs as surface water and groundwater (Meenakshi and Maheshwari, 2006). Though groundwater contributes only 0.6% of the total water resources on earth, it is the major and the preferred and only available source of drinking water in rural as well as some urban areas in developing countries (Meenakshi and Maheshwari, 2006).

Preference for groundwater stems from the fact that it is generally of better quality and less polluted (MacDonald *et al.*, 2000). Groundwater has excellent natural microbiological quality and generally adequate chemical quality for most uses (MacDonald *et al.*, 2000). Groundwater is believed to be more potable and safer than surface water due to the protective qualities of the soil cover (Mishra *et al.*, 2005). Though the initial cost for the construction of boreholes and hand-dug wells to harness groundwater are high, the operational costs are generally low as no chemical treatment is required (chemical treatment increases the operational cost for surface water). The cost of treating surface water is twice that of developing groundwater resources in communities with less than 5000 people (Dapaah-Siakwan and Gyau-Boakye, 2000).

Fluoride (F<sup>-</sup>) contamination of groundwater has been recognized as a serious problem worldwide (Meenakshi, and Maheshwari, 2006). Fluoride is classified as one of the contaminants of water for human consumption by the World Health Organization

(WHO), in addition to arsenic and nitrate, which cause large-scale health problems (Bhatnagara *et al.*, 2011). Elevated fluoride concentrations in groundwater occur in various parts of the world (Gaciri and Davies, 1993; WRC Report, 2001). Fluoride is widely distributed in the geological environment (Abe *et al.*, 2004) and generally released into the groundwater by slow dissolution of fluorine-containing rocks (Banks *et al.*, 1995). Various minerals, like fluorite, biotites, topaz, and their corresponding host rocks such as granite, basalt, syenite, and shale, contain fluoride that can be released into groundwater (Edmunds *et al.*, 2005; Apambire *et al.*, 1997; Reddy *et al.*, 2003). Therefore, groundwater is a major source of human intake of fluoride. Besides the natural geological sources for fluoride enrichment in groundwater, various industries are also contributing to fluoride pollution to a great extent (Reardon and Wang, 2000).

Fluoride is thus considered beneficial in drinking water at levels of about 0.7 mg/L but harmful once it exceeds 1.5 mg/L, which is the World Health Organisation (WHO) recommended limit (WHO, 1985; Smet, 1990) and also the Australian recommended limit (Mohapatra *et al.*, 2009). The difference between desirable doses and toxic doses of fluoride is ill-defined, and fluoride may therefore be considered as an essential mineral with a narrow margin of safety (WHO, 1984).

Fluoride in drinking water has a profound effect on teeth and bones. Fluoride displaces hydroxide ions from hydroxyapatite,  $\text{Ca}_5(\text{PO}_4)_3\text{OH}$ , which is the principal mineral constituent of teeth (in particular the enamel) and bones, to form the harder and tougher fluoroapatite,  $\text{Ca}_5(\text{PO}_4)_3\text{F}$ . Up to a small level this strengthens the enamel. However, fluoroapatite is an order of magnitude less soluble than hydroxyapatite, and at high fluoride concentration the conversion of a large amount of the hydroxyapatite

into fluoroapatite makes the teeth (after prolonged exposure, and the bones denser, harder and more brittle. In the teeth, this causes mottling and embrittlement, a condition known as dental fluorosis. With prolonged exposure at higher fluoride concentrations, dental fluorosis progresses to skeletal fluorosis (Dissanayake, 1991; Mohapatra *et al.*, 2009).

Owing to the high toxicity of fluoride to mankind, there is an urgent need to treat fluoride-contaminated drinking water to make it safe for human consumption. Several techniques have been developed for removal of fluoride from drinking water. The most commonly used methods for the defluoridation of water are adsorption, ion exchange, precipitation, Donnan dialysis and electrodialysis (Mohan and Pittman, 2007; Streat *et al.*, 2008; Ahamad and Jawed, 2012). Among the various methods used for water defluoridation, the adsorption process is widely used; because it offers satisfactory results and seems to be a more attractive method for the removal of fluoride in terms of cost, simplicity of design and operation (Tripathy *et al.*, 2004; Hichour *et al.*, 2000; Ruiz *et al.*, 2003; Srimurali *et al.*, 1998; Reardon and Wang, 2000; Vaaramaa and Lehto, 2003; Singh *et al.*, 1999; Amor *et al.*, 2001).

Various conventional and non-conventional adsorbents have been assessed for the removal of fluoride from water. these include activated alumina, amorphous alumina, activated carbon and low-cost adsorbents such as calcite, clay, charcoal, tree bark, saw dust, coffee husk, activated coconut shell carbon, activated saw dust, rice husk, groundnut husk and rare earth oxides (Srimurali *et al.*, 1998; Reardon and Wang, 2000; Ghorai and Pant, 2004; Li *et al.*, 2001; Ramos *et al.*, 1999; Fan *et al.*, 2003; Tripathy *et al.*, 2004; Reardon and Wang, 2000). The removal efficiency and applicability of the existing fluoride removal methods often depend on various factors

such as specific mineral concentrations in water, geographical and economic conditions, and availability of materials used for the removal. Some of the methods commonly used in most countries, adds harmful aluminium to water and need adjustment of pH (Suresh and Dutta, 2010; Meenakshi, and Maheswari, 2006).

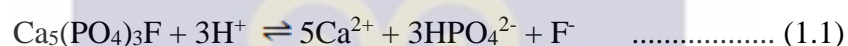
Although, there are some efficient methods for defluoridation of drinking water, a method which is cost effective, does not add other contaminants to water, economically viable, can be easily used by a layman and efficient in the long term is highly desirable (Suresh and Dutta, 2010).

Over the past two decades, there has been a massive development of hand-dug wells and boreholes for use by people living in rural communities, especially in the Northern and the two Upper regions of Ghana. District Assemblies, the Community Water and Sanitation Agency (CWSA) of Ghana, non-governmental agencies (NGOs) notably ActionAid and World Vision have assisted most rural communities in Northern Ghana to enjoy safe and portable drinking water, as well as water for agricultural purposes through the provision of boreholes and hand-dug wells. This has helped alleviate poverty as the people mostly farmers have water all year round for their agricultural activities, in addition to improving the quality of drinking water.

Notwithstanding, groundwater in some parts of northern Ghana have high levels of fluoride (above 4.5 mg/L) (Anongura *et al.*, 2003; Apambire *et al.*, 1997; Anongura, 1995; Anim-Gyampo *et al.*, 2012). Communities affected by the high fluoride levels include Bongo, Tongu, Talensi and Bolgatanga districts (Upper East region). Others are, Gushiegu, Karaga, Saboba, Yendi and Chereponi districts (Northern region). Bongo, the worst affected community, has high cases of dental fluorosis, with Bongo

township as the most affected. Available statistics indicate that about 63% of fluorosis cases were recorded in children from Bongo township, with about 9% of fluorosis cases in children outside Bongo township [fluoride concentrations outside Bongo township are generally below the WHO recommended level of 1.5 mg/L (Frimpong *et al.*, 2013)].

Fluoride contamination of groundwater in Bongo and catchment area may be attributed to the geology of the area (granitoid rocks) (Brindha and Elango, 2013). As a result of weathering, the granitoid rocks dissolves, leading to the leaching of fluoride bearing materials (Fluorite and Apatite) into groundwater thereby elevating the fluoride levels (Nagendra Rao, 2003). This is illustrated in Equation 1.1 (release of fluorite due to weathering of apatite [ $\text{Ca}_5(\text{PO}_4)_3\text{F}$ ]):



To help alleviate the high fluoride contents in waters from the Bongo district, a Project called “Sustainable Small Town Rural Water Supply System” jointly funded by the World Bank and the Ghana Government was initiated (GNA, 2014). Apart from this project, Non-Governmental Organisations (NGO) such as Rural Aid (a British NGO), World Vision International Ghana, European Union Micro-Projects Programme, ActionAid and the LACOSREP-II (Land Conservation and Smallholder Rehabilitation Project Phase II) have also provided quite a number of water and sanitation facilities in the district (GNA, 2014; Citifmonline.com, 2014).

The Centre for Environmental Impact Analysis (CEIA) of the University of Cape Coast, Ghana, designed a local water project to reduce the high level of fluoride and iron in water at the Bongo district using local materials such as clay and laterite. According to the study, the technique removed about 75.3-85.6% fluoride, bringing it



to the WHO acceptable range of 1.5 mg/L. Despite its high efficiency in fluoride removal, there is the introduction of iron into the water which is also of immense concern. The introduction of iron (Fe) may be due to the high iron oxide and aluminium content of clay and laterite.

In view of the pervasive nature of the high fluoride contents in groundwater in the Upper East and Northern regions of Ghana, it has become imperative to help alleviate the fluoride problem in the affected communities by developing an economically viable water defluoridation technique using limestone as the adsorbent. The developed limestone-based method will complement existing defluoridation techniques being used by the inhabitants of the affected communities.

## **1.2 RESEARCH PROBLEM**

Groundwater is the main source of drinking water for majority of the communities in Northern Ghana and other parts of the world. Due to the geology of the area [(presence of granitoid rocks containing fluoride-bearing minerals (Fluorite and Apatite) in the case of Ghana] weathering of the rocks leads to the dissolution and leaching of fluoride into groundwater, thereby increasing the levels of fluoride. This has resulted in increasing reported cases of dental fluorosis among children in affected communities in Northern Ghana.

As a result of the elevated fluoride levels in groundwater, drilled boreholes and hand-dug wells are often abandoned in spite of the large amount of money spent in drilling. School children walk long distances in search of water with acceptable fluoride levels. Often these children abandon the classroom. The issue of elevated fluoride levels

constitutes a major setback in the socio-economic development of the people living in the affected communities. Therefore, provision of safe drinking water to the affected communities has become a matter of high priority to Governmental Agencies, Environmentalists and Medical Practitioners. To help alleviate the fluoride problem in the affected communities, there is an urgent need for the development of drinking water defluoridation techniques using locally-available fluoride adsorbents. Limestone or calcite, which is abundant in the severely fluoride-affected areas, is one of the potential materials for removal of fluoride; and has reportedly been used as adsorbent for fluoride removal (Suresh and Dutta, 2010). Accordingly, a defluoridation method using this low cost and readily available material (limestone) can be suitable for the affected areas in the Upper East and Northern regions of Ghana, considering Ghana's large limestone deposits (8-10 million tonnes) [Iddrisu, 1987]. Ghana's limestone deposits can be found in Otekpulu (Yilo Krobo district, Eastern Region), Nauli (Jomoro district, Western Region), and Bongo-Da (Nalerigu district, Northern Region), Limestone occurrences have been reported in the Buipe and Daboya (Northern Region of Ghana), Anyaboni (Upper Manya Krobo, Eastern Region), Sadan-Abetifi (Ashanti Region), and Du area (Upper Eastern Region) [Afenya, 1982; Kesse, 1975, 1985; Iddrisu, 1987]. Meanwhile no work has been done on these limestones to assess their effectiveness as a suitable adsorbent for removal of fluoride from drinking water.

### **1.3 RESEARCH OBJECTIVES**

#### **1.3.1 Principal Objective**

The main objective of the study is to assess the effectiveness of limestone from Oterkpolu (a town in the Yilo-Krobo district, Eastern region of Ghana) as fluoride adsorbent and develop a drinking water defluoridation technique using the limestone.

#### **1.3.2 Specific Objectives**

The specific objectives of the study are:

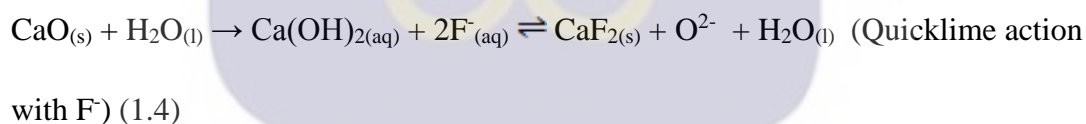
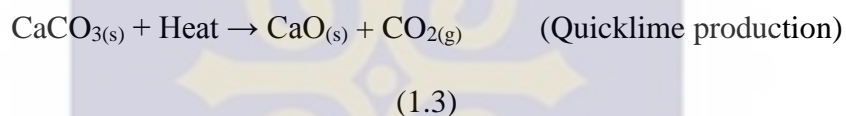
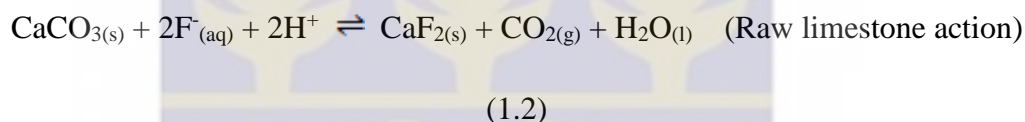
- i. to characterize Oterkpolu limestone geochemically and mineralogically;
- ii. to assess the Radiological Risk and Safety associated with the use of Oterkpolu limestone for water defluoridation [Activity Concentration(AC) and hence the Annual Effective Dose (AED)];
- iii. to assess the fluoride adsorption efficiency (Sorption capacity and % Adsorption) of different limestone types from Oterkpolu (in a Batch Adsorption Experiment) with respect to varying:
  - (a) adsorbent dose;
  - (b) particle sizes of the adsorbent (limestone);
  - (c) residence time; and,
  - (d) fluoride concentration.
- iv. to apply the developed defluoridation technique to fluoride-contaminated water samples from Bongo district.

### **1.4 JUSTIFICATION**

Most rural communities in the northern regions of Ghana depend on groundwater for both domestic and agricultural purposes. Majority of the water from the dug wells in



northern part of Ghana contains excess fluoride. Consequently, most of the wells have been abandoned, and this has caused huge financial deficit to the government and the affected communities (Atipoka, 2009). Such communities are also faced with the problem of looking for alternative sources of water. In view of the fluoride contamination problem, a user-friendly and cost effective technology is needed to defluoridate water using readily available and cheap natural raw materials. The use of limestone as a defluoridation material has been reported to be relatively efficient as compared to other methods. The reaction between Calcite (in limestone) with fluoride is very effective in defluoridation of water removal according to the reactions:



Oterkpolu limestone samples were used for this study because it is the only limestone deposit in Ghana being mined currently for commercial purposes.

## CHAPTER TWO

### LITERATURE REVIEW

#### 2.1 Water occurrence in Ghana

Water is an essential natural resource for sustaining life and is among nature's most valuable gifts. Once viewed as an infinite and bountiful resource, today, water often defines the limits of human, social, and economic development of a region. The Environmental Protection Agency (EPA) of Ghana in 1995 estimated that fresh water resources of Ghana have been estimated to about 40 million-acres and these are derived from the following sources: rainfall, rivers, streams, springs, lakes and groundwater from various aquifers. One of the main sources of freshwater for sustaining life on earth is groundwater. Unfortunately, groundwater is either being increasingly depleted for irrigation of crops, industrial, or other uses, or is becoming contaminated with various pollutants.

Urban dwellers are more likely to have access to safe drinking water than rural dwellers at 91% and 69% respectively (GSS, 2011). Consequently, dependency on unsafe water sources is higher in the rural areas (<http://www.water.org>). Even with this statistics, it continues to dwindle due to factors such as rainfall variability (partly due to climatic changes), rapid population growth, increased environmental degradation and pollution of most water bodies (Dwamena-Boateng *et al.*, 2011).

#### 2.2 Importance of fluoride and its environmental occurrence

Fluoride is a pale yellow green corrosive gas which cannot be found naturally in the environment in its elemental form. This is because it is highly electronegative and

very reactive. Due to its small radius, it forms Ligands with organic and inorganic compounds in the soil, rocks, air, plants, animals etc. As a result, some of these compounds are soluble in water; both surface and groundwater (WHO, 1984).

Fluorine rich minerals such as Fluorite ( $\text{CaF}_2$ ), Cryolite ( $\text{Na}_3\text{AlF}_6$ ), and Fluoroapatite [ $\text{Ca}_{10}(\text{PO}_4)_6\text{F}_2$ ] undergoes weathering which accumulate in water and soil (Murray, 1986). Water with high pH is believed to have high concentration of fluoride (Fawell *et al.*, 2006). It is also noted that fluoride occurrence and their high concentration in water may be contributed by other factors such as Total Dissolved Solids (TDS), Alkalinity, Hardness and Geochemical composition of the aquifers (WHO, 1984; Mohan and Karthikeyan 1997; Abdelgawad *et al.*, 2009; Meenakshi and Maheshwari, 2006).

Moreover high concentrations of fluoride in water can also be attributed to anthropogenic sources. These are discharges of agricultural and industrial products such as glass, electronics, steel, aluminium, pesticides and fertilizers (Pietrelli, 2005), ceramics (Ponsot *et al.*, 2013), coal fired power station, oil refineries etc (Shen *et al.*, 2003; Bhatnagar *et al.*, 2011).

Fluoride therefore has both beneficial and detrimental effects on human health in terms of prevalence of dental caries, skeletal fluorosis and bone fractures, reproductive and immunological defects (Harrison, 2005; Valdez-Jimenez *et al.*, 2011; Browne *et al.*, 2005, Ayoob and Gupta, 2006).

Dissanayake (1991) presented a typical fluoride concentration in drinking water and its associated health effects in the table below;

**Table 2.1: Fluoride concentration in drinking water and its health effects**

F <sup>-</sup> Concentration(mg/L) in drinking water	Potential health effect
a) < 0.5	Minimal effect in prevention of dental caries
b) 0.5 – 1.5	Beneficial effect in preventing dental caries
c) 1.5 – 4.0	Dental fluorosis
d) 4.0 – 10.0	Dental and skeletal fluorosis
e) > 10.0	Crippling fluorosis

The amount of fluoride increases in the bones up to the age of 55 years but children are the most affected and remained crippled or deformed when high amount of fluoride is ingested (WHO, 1984).

### 2.3 Fluoride in Bongo

Fluoride occurrence in groundwater is mainly controlled by two factors; geology and climate. The northern part of Ghana is mainly arid zone dominated by granitoid rocks underlining the geology. The upper regions are therefore considered as the most likely areas with high fluoride prevalence.

Bongo district has an elevated fluoride in groundwater ranging between 1.7-4.0 mg/L (Atipoka, 2009). The district has 335 wells (boreholes, hand-dug wells and scoop wells) with depth ranging from 10-35 meters deep. Out of this number of boreholes, 35 are capped due to high fluoride content (Atipoka 2009).

Apart from fluoride ingestion from water, soil is another medium from which plants and animals directly or indirectly derive their nutrients and food (Smedley *et al.*, 1995; Pelig-Ba, 1987). As such, man consumes these products thereby increasing the fluoride concentration in the body. However information regarding the concentration of fluoride in the surrounding cultivated soils of the area is not widely publicised as that of water. In view of this no attention has ever been drawn to other sources except in water.

But in a study by Abugri and Pelig-Ba (2011) on assessment of fluoride in tropical soils, samples were collected from selected communities known to have high fluoride concentration in their groundwater sources based on previous studies (Smedley *et al.* 1995; Apambire *et al.*, 1997; Pelig-Ba, 1998). The physical parameters considered were pH, soil depth and specific electrical conductivity of all the soil samples. The soil samples showed various concentrations of fluoride as indicated in the figure below.

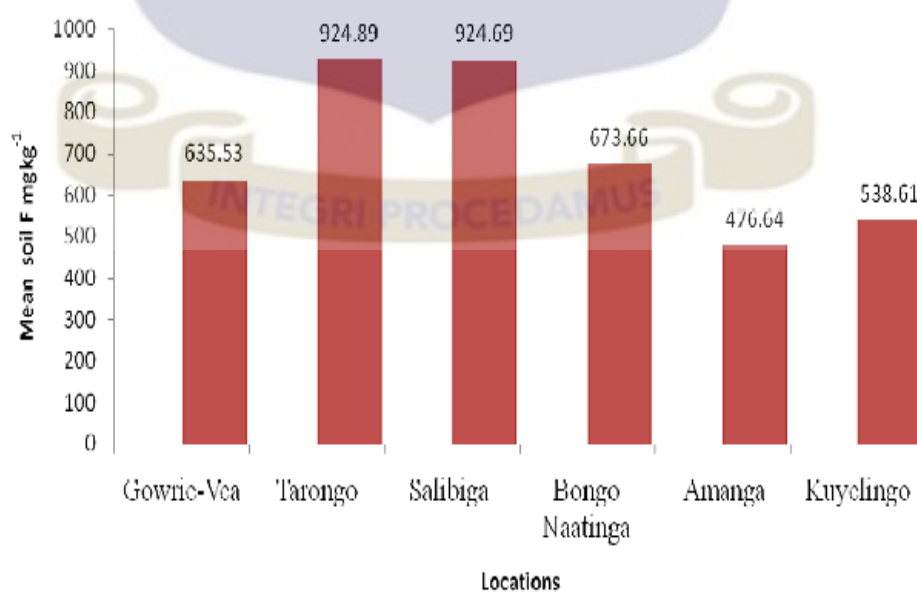


**Fig 2.1** Fluoride concentration in some soil samples in the Bongo district of Ghana

Apambire *et al* (1997) also investigated the distribution of fluoride in groundwater of the Upper Regions of Ghana and the results presented in the table below.

**Table 2.2: Fluoride concentration distribution in groundwater (upper regions, Ghana)**

Total No. of wells studied in entire Upper Regions	No. of Bongo granite wells	Range of Fluoride Conc. obtained (mg/L)
49	0	0.11 – 0.25
133	0	0.26 – 0.50
88	7	0.51 - 1.00
16	16	1.01 - 1.50
24	24	1.51 - 2.00
14	14	2.01 - 2.50
23	23	2.51 - 3.00
12	12	3.01 - 3.50
7	7	3.51 - 4.00
5	5	4.01 - 4.60
<b>Total</b>	<b>371</b>	<b>108</b>

## 2.4 Chemistry of fluoride

Fluoride belongs to the group of halogens (Group VII) on the periodic table with atomic number 9 and an oxidation number of -1. With an electron affinity of  $83.5 \pm 2$  kcal/g-atom, it is highly electronegative and very reactive to all elements except Oxygen and Nitrogen (Greenwood and Earnshaw, 1998; Macomber, 1996).

Fluorine is characterised by a pungent odour and strongly irritant and very corrosive. Low calcium and high bicarbonate alkalinity favours high fluoride content in groundwater (Meenakshi and Maheshwari, 2006). It occurs in sedimentary and



igneous rocks and associated with volcanic activities and with thermal water with high pH. The major minerals which contain fluoride are in Table 2.3.

**Table 2.3: Fluoride composition in some major mineral**

Mineral	Chemical formula	% fluoride
Sellaite	$\text{MgF}_2$	61
Villiamite	$\text{NaF}$	55
Fluorite (fluoraspars)	$\text{CaF}_2$	49
Cryolite	$\text{Na}_3\text{AlF}_6$	45
Bastnaesite	$(\text{Ce}, \text{La})(\text{CO}_3)\text{F}$	9
Fluorapatite	$\text{Ca}_3(\text{PO}_4)_3\text{F}$	34

[Source: Rao, 2003]

Fluoride forms very strong bonds with carbon making it resistant to chemical and biological attack but can be substituted for hydrogen atoms and hydroxyl ions in molecules.

## **2.5 Fluoride in humans and its health effects**

### **2.5.1 Fluoride intake and metabolism**

Fluoride ingested in small amount has beneficial effects on the rate of occurrence of dental caries among children (Mahramanlioglu *et al.*, 2002). But on the contrary, excessive exposure to fluoride in drinking water leads to various health effects such as osteoporosis, arthritis, brittle bones, cancer, infertility, brain damage, Alzheimer syndrome and thyroid disorder (chinoy, 1991; Harrison, 2005; Xiang, 2003).

A survey conducted in 1993 for 1,558 students in the Bongo district recorded 62% of the students (966 students) suffering from dental fluorosis (Duah, 2002).

When tooth enamel which is made up of crystalline hydroxyapatite  $2[\text{Ca}_5(\text{PO}_4)(\text{OH})]$ , gets into contact with food or water containing fluoride, the ion gets incorporated into the apatite crystal lattice of the calciferous tissue enamel during its formation. The hydroxyl ion gets substituted by the fluoride ion since the fluoroapatite is more stable than the hydroxyapatite.



When fluoride in water is taken into the body system, about 50% of the fluoride is retained onto the teeth surface (surface uptake). The remaining 50% gets to the stomach as Hydrofluoric acid (HF). As a result of the acidic nature of the stomach, the HF diffuses into the blood plasma which is distributed to all parts of the body. Fluoride that is not absorbed into the blood stream as a result of high pH disrupts oxidative phosphorylation, glycolysis, coagulation and neurotransmission leading to gastro-intestinal irritation or corrosive effects (Islam and Patel, 2007; 2011).

The absorbed fluoride (from the blood plasma) which is now available to the skeletal structures are retained and stored in proportions that increase with age and intake resulting in skeletal fluorosis. Meanwhile soft tissues do not retain fluoride (Raymond, 1999).

### 2.5.2 Health effects of fluoride ingestion

It is well known that toxicity is determined by the dosage that the body takes as proposed by the Swiss Physician, Paracelsus (1493-1541). The body needs fluoride to build strong dental structures but when it exceeds the maximum permissible limit of



1.5 mg/L (WHO, 2008), it results in negative effects ranging from dental caries to brain defects.

Dental fluorosis is defined as hypomineralization of the enamel characterised by greater surface and subsurface porosity than in normal enamel as a result of excess fluoride intake during the period of enamel formation (Browne *et al.*, 2005).

Dental caries also known as tooth decay on the other hand is a breakdown of the teeth due to activities of bacteria. This occurs due to acid made from food debris or sugar on the tooth surface. Minerals are added to and lost from a tooth's enamel layer through two processes, demineralization and remineralisation. Minerals are lost (demineralization) from the tooth's enamel layer when acids formed from plaque bacteria and sugars in the mouth attack the enamel. Minerals (fluoride, calcium, and phosphate) are redeposited (remineralisation) onto the enamel layer from the foods and waters consumed. Too much demineralization without enough remineralisation leads to tooth decay.

The figure below shows the various stages of dental fluorosis.



**Fig 2.2** Stages of dental fluorosis [source: [http://en.m.wikipedia.org/wiki/dental\\_fluorosis](http://en.m.wikipedia.org/wiki/dental_fluorosis)]

Skeletal fluorosis affects both children and adults. It fully shows up when the disease attains an advanced stage (osteoporosis). The gradual intake and storage of fluoride increases bone formation in trabecular bones which exerts a greater response in the axial skeleton than in the appendicular. This could even lead to osteosarcoma (bone cancer) (Meenakshi Maheshwari, 2006)



**Fig 2.3** skeletal fluorosis [source: [source: http://en.m.wikipedia.org/wiki/skeletal\\_fluorosis](http://en.m.wikipedia.org/wiki/skeletal_fluorosis)]

According to the US Research Council, 2006, fluorides have the ability to interfere with the brain tissues resulting in mental retardation ( $IQ < 70$ ). Even in endemic areas, it could affect the development of children's intelligence (Xiang, 2003).

Ingestion of fluoride is not only through drinking water but some foods such as fish and other seafood (Shomar *et al.*, 2004). This research is corroborated by Abugri and Pelig-Ba, 2011 when they determine the level of fluoride ( $F^-$ ) in cultivated soils in the Bongo district and its implication to crops. The  $F^-$  content in the soils ranged from 219.26 to 1163.01 mg/kg dry weight (DW). Table 2.4 gives the fluoride content in some food crops in the Bongo district (unpublished document) by Asamoah-Antwi Dinah.

**Table 2.4: Fluoride content in some food crops in the Bongo district**

PLANT SAMPLES	Ca <sup>2+</sup> (mg/kg)	Mg <sup>2+</sup> (mg/kg)	F <sup>-</sup> (mg/kg)
Bito (Amanga)	24.047	4.86	263.90
Bito (Bongo central)	24.038	8.51	213.45
Millet (Bongo central)	40.078	6.08	267.26
Okro (Bongo central)	22.023	4.25	208.97
Millet (Tapentin)	22.043	4.86	223.54
Okro (Tapentin)	20.039	4.86	196.64
Guinea corn (Tapentin)	26.051	4.86	278.48
Groundnut (Tapentin)	24.027	7.29	228.03
Groundnut (Navrongo)	22.009	2.43	126.01
Bito (Navrongo)	18.035	2.43	87.89
Okro (Navrongo)	20.039	3.65	113.68

[The F<sup>-</sup> levels in plants were beyond the maximum F<sup>-</sup> level recommended in food stuffs (0.2-0.5 mg/kg) (US EPA, 1989; 1995; 2003, WHO, 2001; 2002).]

Tea drinks have a very high fluoride levels and when consumed regularly, results in high risk of fluoride toxicity (skeletal fluorosis) [Xiang, 2003]. According to a survey carried out in the US, the fluoride content in tea ranges from 0.1- 4.2 ppm with an average of about 3 ppm (Levy and Guha-Chowdhury, 1999).

## 2.6 Defluoridation techniques/methods

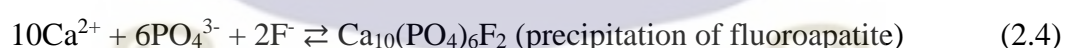
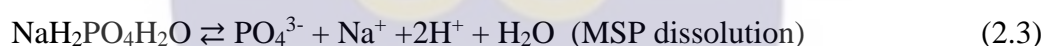
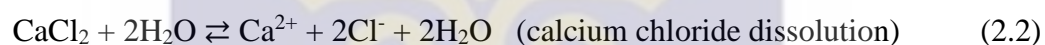
To mitigate the problem of fluoride contamination in water, many methods have been developed. It has been concluded that the selection of treatment process should be site

specific as per local needs and prevailing conditions as each technology has some limitations and no one process can serve the purpose in diverse conditions. The most commonly used ones include precipitation, membrane filtration and adsorption/ion exchange.

### 2.6.1 Precipitation method

This method involves the addition of calcium and phosphate compounds in contact with an already saturated bone charcoal medium. Calcium fluoride and/or fluoroapatite is precipitated as this method is theoretically feasible, but practically impossible due to slow reaction kinetics.

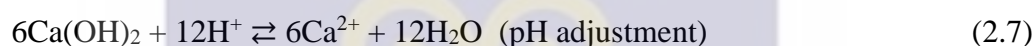
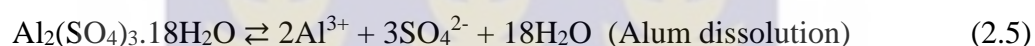
The removal of fluoride from the system is aided by the use of calcium chloride and Sodium Dihydrogenphosphate [Monosodium Phosphate (MSP)] in the following reaction equations.



Though, this method provides a high sorption capacity, the odour and taste of the water is affected due to organic leaching. Also, regular monitoring and maintenance is necessary as the filter needs to be regenerated or replaced. This method has been tested in Tanzania which shows a promising result.

### 2.6.2 Chemical method

This method involves the addition of chemicals (lime, magnesium or aluminium salts along with coagulant materials) to the water to precipitate the fluoride. The process is aluminium sulphate [ $\text{Al}_2(\text{SO}_4)_3 \cdot 18\text{H}_2\text{O}$ ] based coagulation-flocculation sedimentation, where the dosage is designed to ensure fluoride removal from the water. Aluminium hydroxide micro-flocs are produced rapidly and gathered into larger settling flocs with the negatively charged fluoride ions attached (Fawell *et al.*, 2006). The following equations illustrate the removal process.



A large dose of aluminium sulphate is required for this process which makes the medium acidic. Simultaneously, addition of lime is often needed to ensure neutral pH in the treated water and complete precipitation of aluminium. A large sludge is produced which is of a serious environmental health problem due to its toxicity (Fawell *et al.*, 2006). The use of lime and magnesium renders the water unsuitable for drinking due to its high pH. This method is also known as the *Nalgonda Technique* (RGNDWM, 1993).

### 2.6.3 Adsorption/Ion-exchange method

In this method, water is passed or run through a bed column containing defluoridating materials/adsorbents which retains the fluoride by either physical, chemical or ion exchange mechanisms. The material gets saturated after a period of operation and



requires regeneration. Some of the materials used include Activated Alumina, Fly Ash (Chaturvedi *et al.*, 1990), Silica gel (Wasay *et al.*, 1996), Bone charcoal (Bhargava, 1992), Carbon nanotubes (Li, 2003) and some low cost geo-materials including soils (Wang *et al.*, 1995; Wang and Reardon, 2001), Volcanic ash (Srimurali *et al.*, 1998), Zeolites (Onyango *et al.*, 2004) and Macrophyte biomass (Miretzky *et al.*, 2008). Fluoride uptake by the adsorbent is by exchange of metal lattice hydroxyl or other anionic groups with the fluoride.

### **2.6.3.1 Adsorption**

Adsorption is the process through which a substance, originally present in one phase, is removed from that phase by accumulation at the interface of a second (solid) phase (Piero M. Armenante). Crittenden *et al.*, (2005) define adsorption as a mass transfer process which a constituent in a liquid/gas phase is accumulated on a solid/liquid phase and separated from its original environment. The process therefore creates a film of the adsorbate (molecules or atoms being accumulated) on the surface of the adsorbent. Adsorption processes provide a feasible technique for the removal of pollutants from water and waste water (McKay, 1995). In general, adsorption proceeds through the following steps; mass transfer, intra-granular diffusion and physical adsorption.

In principle, adsorption can occur at any solid-fluid interface. Examples include:

gas-solid interface as in the adsorption of a VOC (volatile organic compound) on activated carbon; liquid-solid interface as in the adsorption of fluoride on limestone or activated carbon.



The adsorbate or solute is the materials being adsorbed and the adsorbent is the solid material being used as the adsorbing phase. eg limestone, activated carbon, activated alumina, silica gel.

### 2.6.3.2 Types of Adsorption

The nature of the bonding of the species involved classifies the phenomenon into the two main types. These are;

**Physical adsorption/Physisorption:** In this type of adsorption, the force holding the species together is the weak Van der Waals forces. With this adsorption process, the chemical species of the adsorbate and the surface are left intact.

**Chemical adsorption/Chemisorption:** this type is characterized by covalent bonding or electrostatic force of attraction. This process involves a chemical reaction between the surface and the adsorbate which generates a new chemical bonds at the adsorbant surface.

### 2.6.3.3 Factors affecting Adsorption

#### *Nature of adsorbent*

In adsorption studies, the rate of adsorption depends on many physicochemical features of the adsorbent to achieve a maximum result. These physical features include the surface area of the adsorbent, the porosity, the particle size, the molecular weight of the adsorbent, the solubility and the ionic radii of the species involved.

From reaction kinetics theory, the larger the surface area, the higher the reaction rate. This implies that, the rate of adsorption will increase when the particle size is small or

decreases. This is attributed to the fact that the smaller the particle size, the greater the surface area and the more the number of active sites available for adsorption process for a given amount of adsorbent (Gao *et al.*, 2009). Smaller particle size reduce internal diffusional and mass transfer limitation to the penetration of the adsorbate inside the adsorbent thus equilibrium is more easily achieved and nearly full adsorption capability can be attained. The pore size distribution allows for effective migration of contaminants to the point of adsorption.

The solubility of the adsorbate also plays a major role in the efficiency of adsorption. Higher solubility shows a strong solute-solvent interaction. The increase in the interaction in terms of the bond chain length increases the hydrophobicity of the molecules, hence resulting in a greater adsorption. On the other hand, since fluorine is having a smaller ionic radius, its interaction with positively active sites like calcium ions ( $\text{Ca}^{2+}$ ) becomes very strong and this enhances a greater process of adsorption.

#### ***Contact time or residence time***

As the adsorbent spends more time with the adsorbate, percentage removal also increases initially until an equilibrium is reached. The time to reach equilibrium appears to be independent of the initial fluoride concentration in the range of 5-20 mg/L (Das *et al.*, 2005). Decreasing the contact or residence time results in a premature breakthrough therefore reducing the service time of the bed (Jusoh *et al.*, 2007). The figure below shows the fluoride removal percentage versus contact time by Fufa (2014).

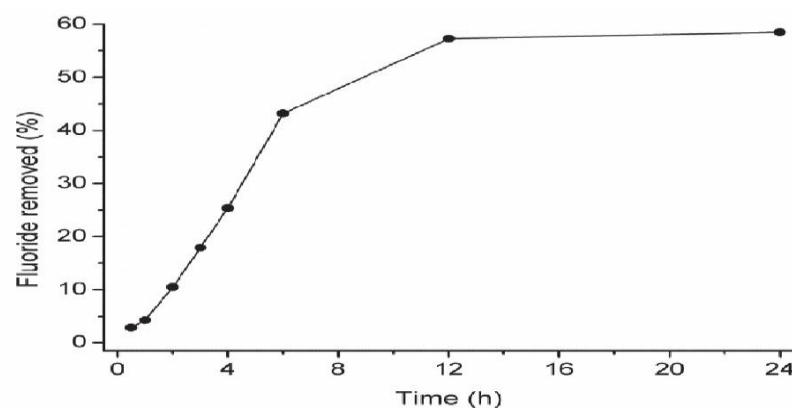


**Fig 2.4:** Effect of contact time on the removal of fluoride from natural groundwater sample.

### *Dose of adsorbent*

The influence of the adsorbent dose on fluoride removal can be looked at from two different perspectives. As the dose is increased, it also increases the active sites of the adsorbent which significantly increases the adsorption rate. However, as the dose significantly increases, the adsorption rate tends to decrease which may be due to the overlapping of the active sites thereby decreasing the surface area of the adsorbent.

A study carried out by Fufa (2014) using gypsiferous limestone in the removal of fluoride in water by varying the adsorbent from 1-20 g/L while keeping the other experimental conditions constant shows a significant increase of fluoride removal up to 60% of the 11.28 mg/L of the fluoride at an adsorbent dose of 15 g/L.

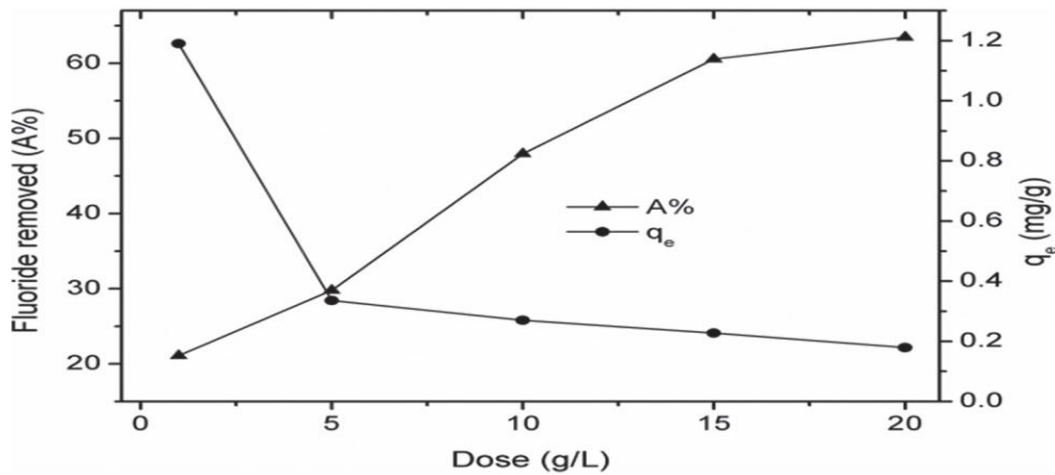


**Fig 2.5:** Effect of adsorbent dose on the removal of fluoride by gypsiferous limestone

### *Effect of pH*

The pH of a medium is important in predicting the efficiency of adsorption since hydrogen ion ( $H^+$ ) and hydroxide ions ( $OH^-$ ) are adsorbed relatively strongly. In an acidic medium, high quantity of particles are adsorbed since the positively charged adsorbent attracts fluoride ions electrostatically than in an alkaline medium since  $OH^-$  compete with the fluoride ions leading to a lower defluoridation.

Figure 2.6 is the results from a survey from Tor, (2006) of fluoride removal using montmorillonite

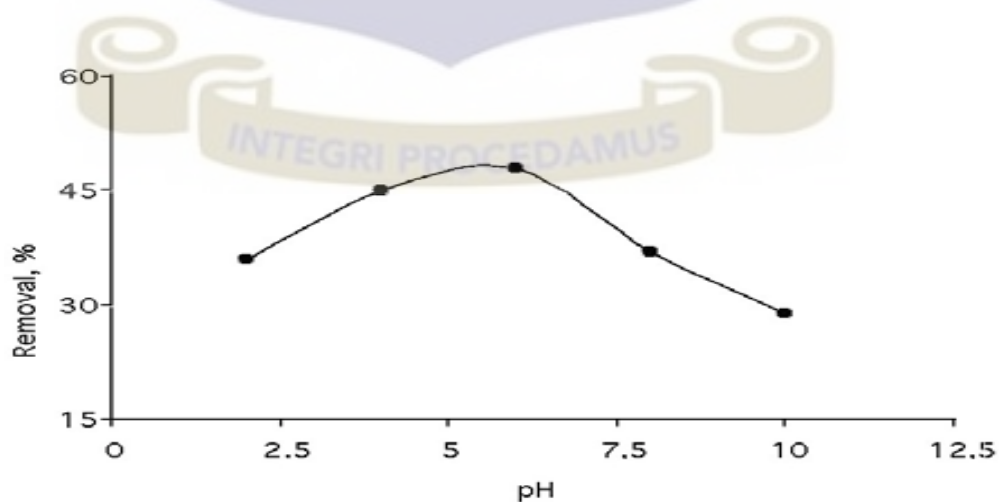


**Fig 2.6.** Effect of pH of the solution on fluoride removal,

### ***Effect of interfering ions***

Groundwater contaminated with fluoride comes along with other anions such as chlorides, nitrates, bicarbonates and phosphates. The impact of interfering ions present in water on fluoride adsorption by activated carbon adsorbent follows the order;  $\text{PO}_4^{3-} > \text{HCO}_3^- > \text{SO}_4^{2-} > \text{NO}_3^- > \text{Cl}^-$  (Suneetha *et al.*, 2015). Previous research by Onyango *et al.*, (2004) also indicated that chloride and nitrate ions has less interferences on fluoride adsorption as compared to sulphate ions. According to Suneetha, the alkalinity of the bicarbonate reduces the active sites on the active carbon thereby decreasing the percentage of fluoride removal.

Tchomgui-Kamga *et al.*, (2010), also have the assertion that sulphates, bicarbonates, nitrates, phosphates and calcium ions at a concentration of 100 mg/L have no significant effect on fluoride removal. But chlorides have a greater deal of influence because of their ionic radii [ $\text{Cl}^- = 3.32\text{\AA}$  and  $\text{F}^- = 3.52\text{\AA}$ ]. Because of their radii, they are able to have higher mobility through the aqueous matrix and penetrate the adsorbent structure offering stronger competition for adsorptive sites thereby reducing the fluoride adsorption.

### ***Effect of flow rate***

Slower flow rate produces higher empty bed contact time and the adsorbate takes longer time to diffuse onto the solid phase of the adsorbing media. The shape of the breakthrough curve from lower flow rates are more approximate to the ideal breakthrough curve than the fast flow rate. The breakthrough curve for fast flow rates deviates more from the ideal breakthrough curve and thus results in a larger root mean square error value (Jusoh *et al.*, 2007).

## **2.7 Use of limestone as an adsorbent**

Limestone is a sedimentary rock largely made of mineral calcite (more than 50%) and aragonite (Folk, 1974). Other sedimentary rocks like carbonate rocks are dominated by dolomite [ $\text{CaMg}(\text{CO}_3)_2$ ]. Most limestone is composed of grains of marine organisms such as coral or foraminifera. These organisms secrete shells made of aragonite or calcite before when they die. Some limestones do not consist of grains but are formed by chemical precipitation of its minerals (Dunham, 1962). Another class of limestone also forms through evaporation. These are the stalactites, stalagmites and other cave formations (speleothems). They are formed as a result of droplets of water seeping down the fractures or other pore spaces in a cave ceiling where the water evaporates. Over time, the evaporative process results in an accumulation of icicle-shaped calcium carbonate on the cave ceiling. Limestone often contains variable amounts of silica and varying amounts of clay, silt and sand carried by rivers.

All limestone contains at least a few percent of other materials such as quartz, feldspar, clay minerals, pyrites, siderites and other minerals (Folk, 1974). The calcium carbonate content of limestone gives it a property that is often used in rock identification-effervescence in contact with dilute hydrochloric acid.

## **2.8 Natural Background Radioactivity**

Natural radioactivity originates from outer space and the earth's crust (cosmogenic and terrestrial). The parent sources of these radiations of natural origin are those from daughter products of U-238 series, Th-232 series and K-40. In addition to the



Naturally Occurring Radioactive Materials (NORMs) from terrestrial and cosmogenic sources, Technologically Enhanced Naturally Radioactive Materials (TENORM) and man-made radionuclide from the environment due to the proliferation of different nuclear applications.

The natural background radiation levels differ from place to place and are a function of properties of the underlying rocks and of the soil in the location, such as distribution of uranium and radium, porosity, permeability, moisture content as well as meteorological and seasonal variation (Merdanoglu and Altinsoy, 2006; Chowdhury *et al.*, 2004).

### **2.8.1 Terrestrial Radionuclides**

Primordial radionuclides are long-lived species which have been present on earth since its formation about  $4.5 \times 10^9$  years ago and are found around the globe in most rocks. These radionuclides formed from the decay of the Uranium, Thorium and Actinide series are the main sources of terrestrial radionuclides. Other important terrestrial radionuclides include the isotopes of Potassium-40, Vanadium-50, Rubidium-87, Cadmium-113 and Indium-115.

The decay schemes of U-238 and Th-232 (Fig 2.7a and 2.7b) is shown below.

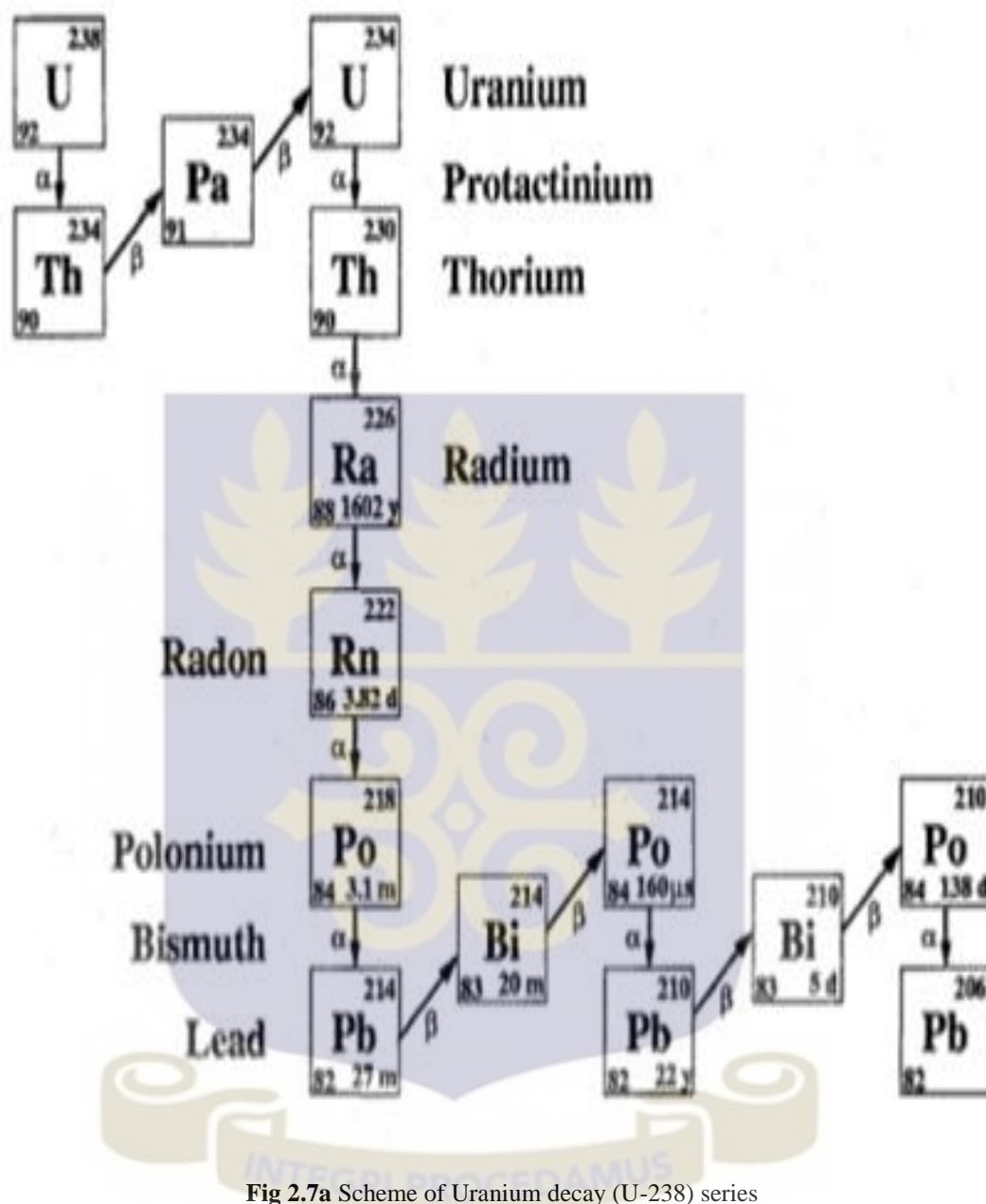


Fig 2.7a Scheme of Uranium decay (U-238) series

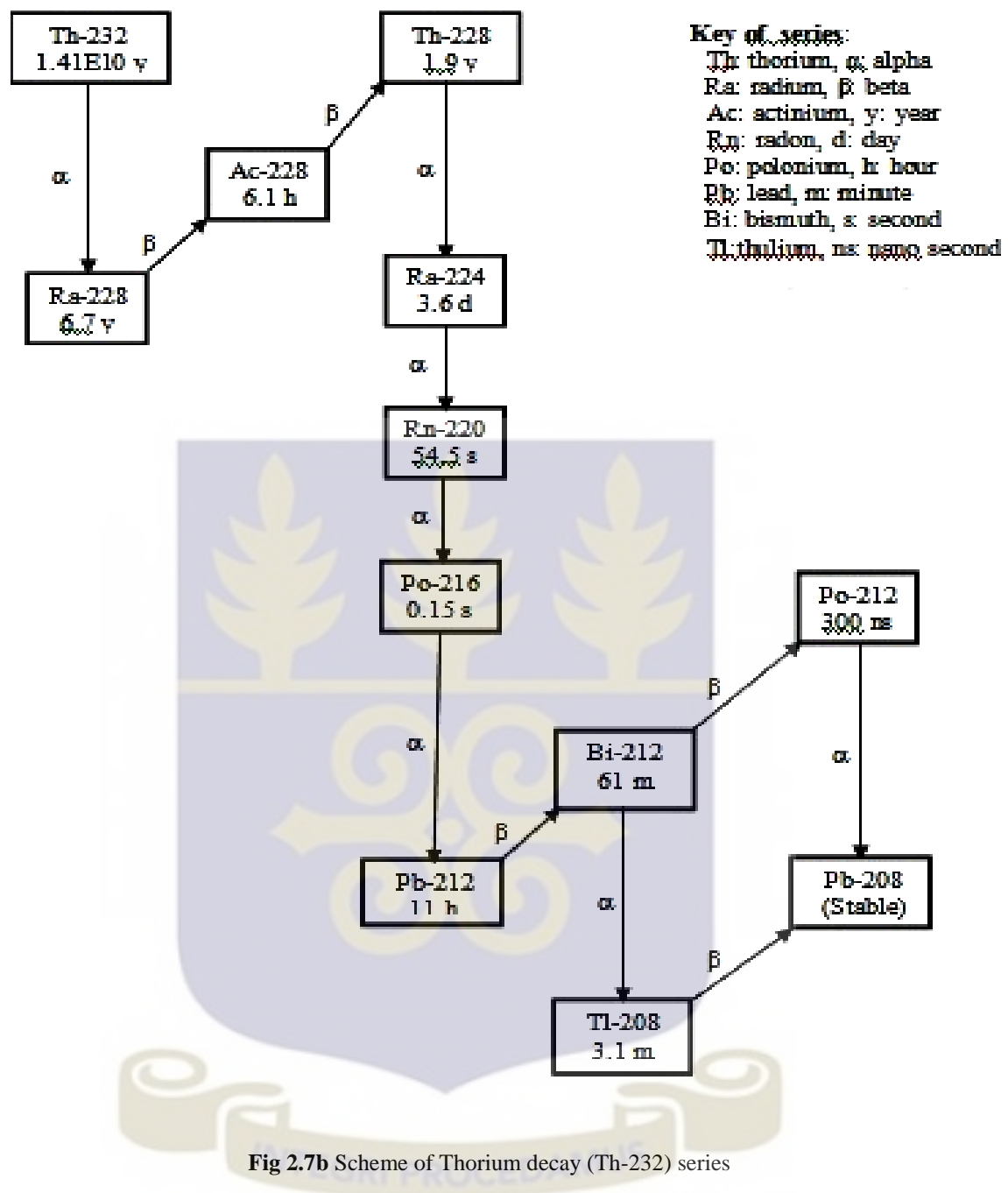


Fig 2.7b Scheme of Thorium decay (Th-232) series

### 2.8.2 Cosmogenic Radionuclide

These are products (isotopes) of interactions of primary and secondary cosmic-ray particles with atomic nuclei (Dunai, 2010). There are both radioactive and stable cosmogenic isotopes. These include  $^3\text{H}$ ,  $^{10}\text{Be}$ ,  $^{41}\text{Ca}$ ,  $^{53}\text{Mn}$ ,  $^{36}\text{Cl}$ ,  $^{26}\text{Al}$ ,  $^{14}\text{C}$ ,  $^{32}\text{P}$ , which are produced by the interaction of galactic cosmic rays with the earth's atmosphere.

Cosmic radiation is a mixture of many different types of radiation such as photons, alpha particles, electrons and other high energy particles. At the earth's surface, more than 98% of the cosmogenic nuclide production arises from secondary cosmic-ray particles (Masarik and Beer, 1999).

### **2.8.3 Artificial (Man-made) Radionuclide**

Through man's potential exploration of radioactivity in such fields like medicine, military, mining and power generation, there is the introduction of radiations order than the natural ones into the environment which have increased the natural background levels leading to enhanced concentration of natural radionuclides generally referred to us Technologically Enhanced Naturally Occurring Radioactive Materials (TENORMs).

### **2.8.4 Transport, Fate and Distribution of Radionuclides in the Environment**

The parent source of natural radionuclides (uranium and thorium series) in the earth crust release radioactive isotopes which dissolve into surrounding aquifers or readily absorbed by surrounding soil particles like clay, noted for its high absorption and ion exchange capacity (Emeka, 2010). Hence, clays have higher concentrations of radioactive isotopes than that found in sand-stones (Solomon *et al.*, 2002). Other radioisotope like radon gas, recognized as carcinogenic is soluble in water under high pressure finds its way to the surface of the earth through geological faults and cracks. These characteristics of radon were used to find geological faults and to predict seismic activities in some regions of the world (Singh *et al.*, 2009; Bhongsuwan *et al.*, 2011; Virk *et al.*, 2000; H. Climent *et al* 1999).

The fate and distribution of radionuclides in the atmosphere depends on the chemical and physical form of the radionuclide. Some radionuclides attaché readily to aerosol particles and are carried by wind. These are inhaled directly or are deposited on plants and find their way into the food chain.

#### **2.8.5 Effects of Radiation on Humans**

Effects of NORMs account for about 80% of man's exposure to natural radiation and the second leading cause of cancer after tobacco (USEPA, 2006; UNSCEAR, 2000). Long term exposure of these radionuclides has several health effects such as chronic lung diseases, acute leucopenia, anaemia and necrosis of the mouth (Ramasamy et al 2009).

#### **2.8.6 Methods of Assessing NORMs**

Radioactive contamination in soil and water can be determined by several laboratory methods. However, type of site, level of contamination at the site and the specific analysis needed will determine the type of methodology that will be appropriate (USEPA, 2006). The different types of determinations include; Liquid Scintillation Counting, Gas Extraction, Gamma Spectrometry and Alpha Spectrometry.

## CHAPTER THREE

### MATERIALS AND METHODS

This chapter consists of seven (6) sections (Sections 3.1 to 3.6). Section 3.1 describes the study area (geographical location, the limestone deposit, and mining of the limestone). Section 3.2 is a description of the Application for Ethical Clearance to enter the concession, and Reconnaissance Survey undertaken (visit to Oterkplolu limestone deposit, identification of limestone deposits). In Section 3.3, the collection of the limestone samples was described. General sample preparation is described in Section 3.4. In Section 3.5, the development of the limestone defluoridation technique using Batch Adsorption experiments are described. Application of the developed technology is described in Section 3.6.

#### 3.1 The Study Area

##### 3.1.1 Geographical location of Yilo Krobo-Oterkpolu

Oterkpolu, (6° 12' 0" North; 0° 70' 0" West), is a small farming community and one of the twenty-two (22) communities located in the Yilo Krobo Municipality (between latitude 6°00'N and 0°30'N and longitude 0°30'E - 1°00'W) [Population & Housing Census, 2010]. Oterkpolu is about 1.5 km off the Koforidua-Asesewa main road. The estimated population of Oterkpolu is about 1.7% (1500 people) of the estimated 87,847 population of the Yilo Krobo Municipality (Population & Housing Census, 2010). The Municipality covers an estimated area of 1201 sq km and is predominantly rural (more than 67% of its population live in rural communities). The major economic activities in the Municipality are Agriculture, Trading and Small Scale



Industrial activities (like Beads Making) [Population & Housing Census, District Analytical Report, (2010), Yilo Krobo Municipal].

Somanya is the administrative capital of the Yilo Krobo Municipality. The municipality shares boundaries (Fig 3.1) with New Juabeng and East Akim Municipalities to south- west, Fanteakwa to the west, Lower and Upper Manya Krobo to the north and east respectively, Akuapem North and Dangme West municipalities to the south (Population & Housing Census, District Analytical Report, (2010), Yilo Krobo Municipal).

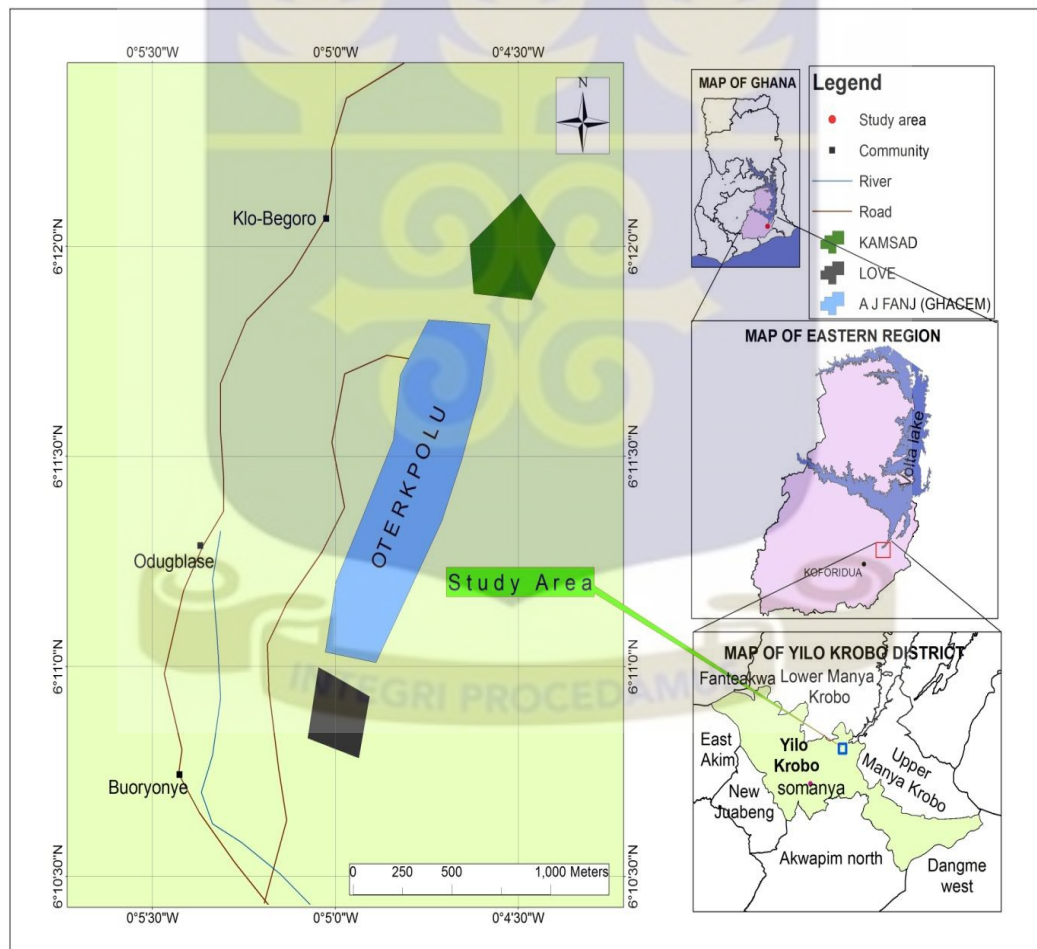


**Fig 3.1** Map of study area showing the location of Oterkpolu and the limestone deposit

The municipality is about 80% mountainous with numerous valleys. This is made up of the Akuapem Range stretching from the southwest to northeast across the municipality. The Togo series (including quartzites, phyllites, sandstones, phyllonites and sandy-shales) forms the rocks of the range peaking at an average height of between 300-500 meters above sea level (MOFA, 2015).

### **3.1.2 Oterkpolu Limestone Deposits**

The limestone deposit is located about 6.5 km east of Oterkpolu township (about 25 km from Koforidua, the Eastern regional capital). The limestone occurs within the arenaceous rocks of the Lower Voltaian range. The limestone is overlain by brown sandstone containing small iron-rich concretions which are weathered out to give a characteristic pitted surface with a purplish coloured transition zone at the base of the limestone (Atiemo, 2012). The rocks dip eastward into the hillside with local variation occurrences due to folding. Investigations by the Ghana Geological Survey have estimated the limestone reserve at Oterkpolu to be over 3.7 million tonnes (Kesse, 1985).



### **3.1.3 Commercial Mining of Oterkpolu Limestone**

After 1916, when the Buipe limestone deposit was discovered in Ghana, subsequent discoveries also led to that of Oterkpolu limestone (Pozzolanic material). This limestone mine went commercial in the year 2004 when Heidelberg Cement Group, producers of Ghana cement (GHACEM) set up a US\$ 2million plant at Yongwase-Krobo in the Eastern region to produce cement from limestone (Business & Financial

Times, BF&T, 2013). With the rapid expansion of Ghana's economy with respect to the construction industry, GHACEM has contracted three mining companies (A. J. Fanj, Kamsad and Love) to mine the Limestone for the cement industry.

### **3.2 Reconnaissance Survey**

#### **3.2.1 Ethical Approval**

Ethical approval/approval to enter the Oterkpolu limestone concession was sought from and granted by the Management of the three limestone mining companies contracted by GHACEM to mine the limestone at Oterkpolu.

#### **3.2.2 Site Visitation**

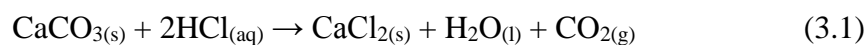
A site inspection was undertaken with the assistance of some Engineers and Geologist of the limestone mining companies (after ethical approval was granted).

The visit to the limestone deposit was to identify the type of limestone available at the concession, to identify the equipment needed for sampling, and, to locate areas within the concession where samples will be collected.

#### **3.2.3 Identification of Limestone during Site Visit**

Limestone is a sedimentary rock composed largely of the minerals, calcite ( $\text{CaCO}_3$ ) and aragonite. The minerals are different crystal forms of calcite. To identify limestone, the reaction between carbonate ( $\text{CO}_3^{2-}$ ) and dilute hydrochloric acid, ( $\text{H}^+$ ) used generally by Geologists in limestone identification was used. The evolution

(effervescence) of the Carbon (IV) Oxide (CO<sub>2</sub>) gas (fizzy reaction) indicates the presence of calcite (CaCO<sub>3</sub>).



Each fresh limestone samples from the different locations were first taken and tested using the reaction between carbonate and dilute acid {hydrochloric acid [10% (*v/v*) HCl]}.

### 3.3 Collection of Limestone

The limestone samples were carefully identified and collected (Fig 3.2). Each limestone sample was labelled and first bagged in a High Density Polythene (HDPE) Woven Bag Sack with liners to prevent weathering. The limestone samples were then transported to the laboratories of the Ghana Atomic Energy Commission (GAEC) in Kwabenya, Accra.



**Fig 3.2** Packing of identified limestone samples for transportation to GAEC

### 3.4 Sample Preparation and Analytical Methodology Development

#### 3.4.1 General Overview of Experimental Work

The experimental framework for the study is illustrated in Figure 3.3a (General Framework) and Figure 3.3b (scheme for development of water defluoridation technology).

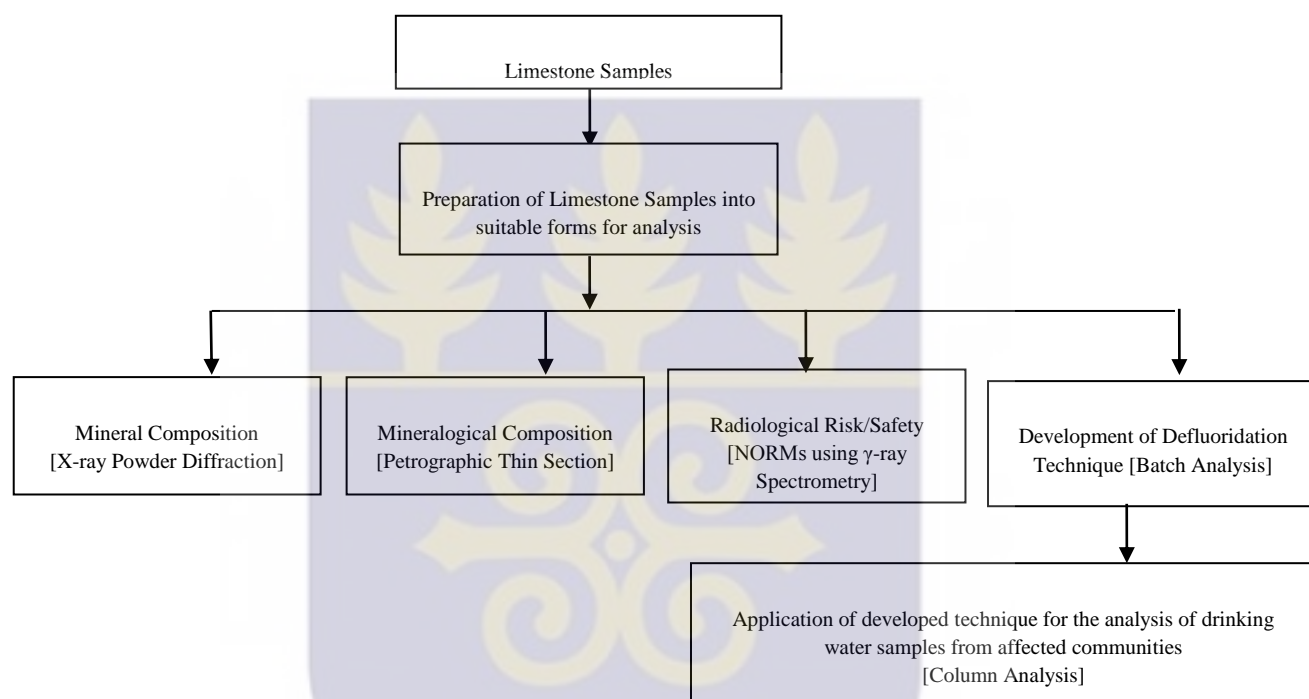


**Fig 3.3a** General Experimental Framework

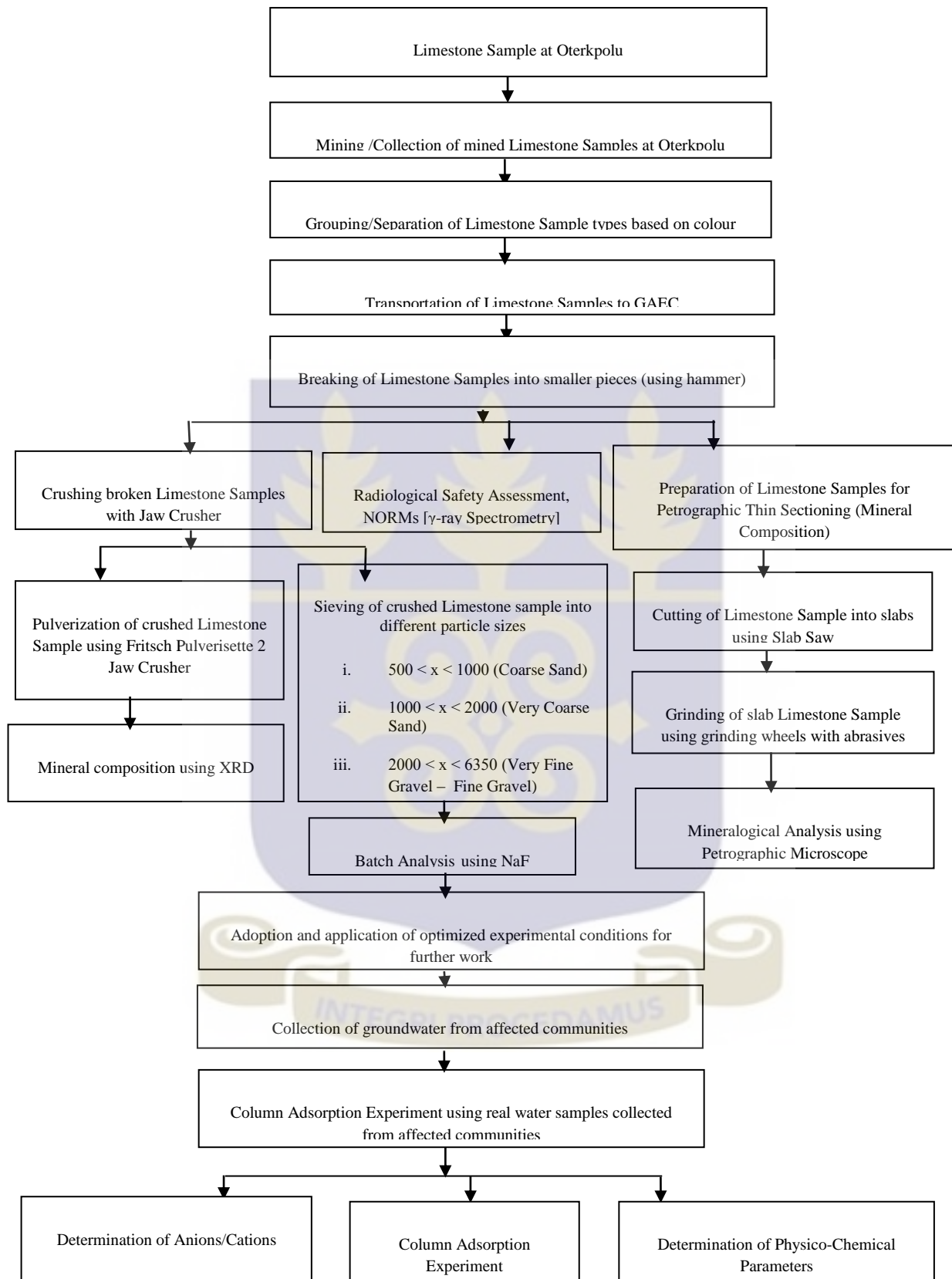


**Fig 3.3b** Detailed work layout of the study



### **3.4.2 Sample Preparation**

#### **3.4.2.1 Mineralogy Using Petrographic Thin Section**

##### ***Instrumentation***

Slab saw, Grinding wheel, Microscope Glass Slide, Leica DM 750P Petrographic Microscope (Leica, Germany)

##### ***Chemicals***

Canada balsam (a yellowish resin obtained from the balsam fir and used for mounting preparations on microscope slides) [Sinus Biochemistry & Electrophoresis GmbH, Germany]

##### ***Principle***

In optical mineralogy and petrography, a thin section is a laboratory preparation of a rock, mineral, soil, pottery, bones, even metal sample for use with a polarizing Petrographic microscope, electron microscope and electron microprobe.

A thin sliver of rock is cut from the sample with a slab saw and ground optically flat. It is then mounted on a glass slide and then ground smooth using progressively finer abrasive grit until the sample is only 30  $\mu\text{m}$  thick. Typically, quartz is used as the gauge to determine thickness as it is one of the most abundant minerals. When placed between two polarizing filters set at right angles to each other, the optical properties of the minerals in the thin section alter the colour and intensity of the light (as seen by the viewer). As different minerals have different optical properties, most rock forming minerals can be easily identified using the Michel-Lévy Interference Colour Chart (a tool used to identify minerals in Thin Section using a Petrographic Microscope).

### ***Experimental Procedure***

The limestone sample was cut into slabs with a slab saw (Fig 3.4a). The limestone slab was glued onto a microscope glass slide with Canada balsam (an epoxy and a hardener) (Fig 3.4b) for a firm grip. To ensure complete and even grinding, the specimen (limestone slab on the glass slide) was held on a grinding wheel (Fig 3.4c) and moved back and forth slowly with the right abrasive and grounded. The process was repeated with finer abrasives to get the right thickness (30  $\mu\text{m}$ ) for the specimen. It was then dried for about five (5) minutes and a cover slip was adhered to the surface of the grounded specimen to protect the section from damage; and also to increase the microscopic clarity. The specimen was placed and examined under a Leica DM 750P Petrographic Microscope (Fig 3.4d) to obtain the characteristics of the rock (which reflect its properties) and hence identify rock type with the aid of the Michel- Lévy Interference Colour Chart.



**Fig 3.4a** Cutting of Limestone into slabs

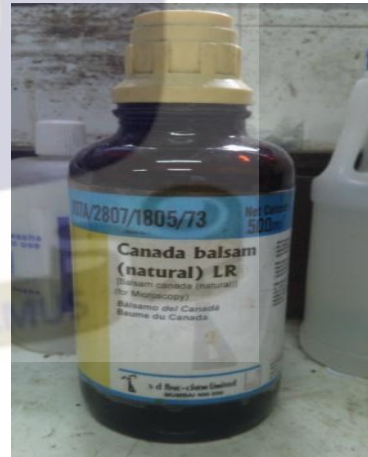


**Fig 3.4b** Canada Balsam



**Fig 3.4c** Grinding wheel



**Fig 3.4d** Petrographic Microscope

### **3.4.2.2 Determination of Mineral Composition Using X-Ray Diffraction (XRD)**

#### ***Instrumentation:***

Empyrean Series2 x-ray Diffractometer (XRD) [PANalytical, Netherlands], Fritsch Mortar Grinder Pulverisette 2 (Fritsch GmbH, Germany), Fritsch Jaw Crusher Pulverisette 2 (Fritsch GmbH, Germany), Rock-breaking hammer, Standard metal sample press

#### ***Principle***

This analytical technique is used for phase identification of a crystalline material and can provide information on unit cell dimensions. The technique is based on constructive interference of monochromatic X-rays and a crystalline sample. The X-rays are generated by a cathode ray tube, filtered to produce monochromatic radiation, collimated to concentrate, and directed towards the sample. The interaction of the incident rays with the samples produces constructive interference (and a diffracted ray) when conditions satisfy Bragg's Law;

$$n \cdot \lambda = 2d \sin \theta \quad (3.2)$$

where,

$\lambda$  is the wavelength of the wave,  $\theta$  is the angle between the incident rays and the surface of the crystal,  $d$  is the spacing between layers of the atom and  $n$  is an integer.

This law relates the wavelength of the electromagnetic radiation to the diffraction angle and the lattice spacing in a crystalline sample. The diffracted X-rays are then detected, processed and counted. By scanning the sample through a range of  $2\theta$  angles, all possible diffraction directions of the lattice should be attained due to the random orientation of the powdered material. A conversion of the diffraction peaks to  $d$ -spacings allows identification of the mineral because each mineral has a set of unique  $d$ -spacings as compared with standard reference patterns.

### ***Experimental Procedure***

Limestone samples were broken into smaller fragments with a rock-breaking hammer, and further crushed with a Jaw Crusher Pulverisette 2 (Fig 3.5a). The crushed sample was further milled in Mortar Grinder Pulverisette 2 (Fig 3.5b). The powdered sample was passed through a 63  $\mu\text{m}$  sieve to obtain a finely powdered homogenous limestone sample (Fig 3.5c). Aliquots of the finely powdered sample were used for the analysis.





**Fig 3.5a** Crushing with Fritsch Pulverisette 2 Jaw Crusher



**Fig 3.5b** Milling with Fritsch Pulverisette 2 Mortar Grinder



**Fig 3.5c** Sieving of samples with a 63 µm mesh

The powdered limestone samples (Fig 3.5d) were transformed into pellets using standard metal sample press (Fig 3.5e). The pellets were loaded into the sample exchanger and transferred to the x-ray Diffractometer (Fig 3.5f).



**Fig 3.5d** Pulverized and homogenized samples

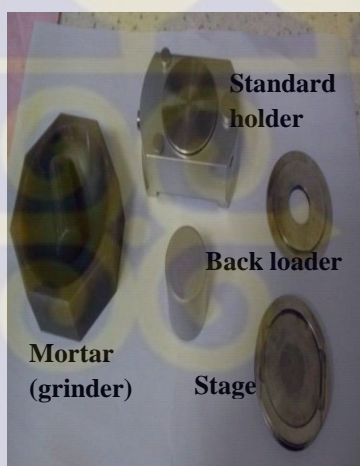


**Fig 3.5e** Tools for transforming powdered samples to pellets



**Fig 3.5f** XRD Diffractometer

### 3.4.2.3 Assessment of Radiological Risk Posed by Oterkpolu Limestone

The radiological risk posed by the limestone was assessed through the determination of the Annual Effective Dose of the naturally-occurring radioactive materials (NORMs). This was achieved through measurement of  $\gamma$ -radiation activity of NORMs on HPGe  $\gamma$ -radiation detector, and hence calculation of Activity Concentration. The activity concentration obtained was used to calculate the Annual Dose Rate (ADR) and subsequently, the Annual Effective Dose (AED).

*Calibration of  $\gamma$ -ray detector*

Prior to the analysis, energy and efficiency calibrations were performed to enable both qualitative and quantitative analysis of the samples. The detector system was calibrated using the multi-nuclide reference standard liquid solution (NW 146). The standard was measured in a 1.0 L Marinelli beaker using a counting time of 36000 seconds. The Standard Certificate (APPENDIX C9) was supplied by Czech Metrology Institute (Inspectorate for Ionizing Radiation, Canberra-Packed Central Europe, Wienersiedlung 6, Austria).

*Energy calibration*

The energy calibration was performed by matching the principal  $\gamma$ -rays in the spectrum of the standard reference material to the channel number of the spectrometer both manually or by software. The formulae relating the energy and the channel number is expressed as

$$E = A_0 + A_1 \cdot \text{CN} \quad (3.3)$$

where,

E is the energy (keV), CN is the channel number for a given radionuclide, and  $A_0$  and  $A_1$  are calibration constants for a given geometry. A graph of energy against channel number is presented in Appendix G3.



***Efficiency calibration***

The efficiency calibration was performed by acquiring a spectrum of the standard until the count rate of total absorption could be calculated with a statistical uncertainty of <1% at a confidence level of 95%.

The net count rate was determined at the photo peaks for all the energies to be used for the determination of the efficiency of the calibration standard at the time of measurement. The efficiency at each energy level was plotted as a function of the peak energy and extrapolated to determine the efficiencies at other peak energies for the measurement geometry used. The efficiency was then related to the count rate and the activity of the standard calculated using Equation 3.4 (Gilmore and Hemingway, 1995).

$$\eta = \frac{N}{P_{\gamma} \times T_c \times A} \quad (3.4)$$

where,

$\eta$  is the efficiency of the detector;  $N$  is the total count under a photo peak;  $P_{\gamma}$  is the gamma ray emission probability for the energy, in a peak range;  $A$  is the activity of the calibration standard for a given radionuclide in Bq at the time of measurement; and,  $T_c$  is the counting time.

The efficiency is related to the energy by the expression.

$$\ln(E) = a_0 + a_1 \ln E_1 + a_2 \ln E_2 \quad (3.5)$$

where,

$a_0$ ,  $a_1$  and  $a_2$  are calibration constants for a given geometry. The efficiency calibration curve is presented in Appendix G4.

From the efficiency calibration curve, the following expression was obtained using a first order polynomial:

$$\ln \eta = 1.239 - 0.995 \ln E_\gamma \quad (3.6)$$

For  $E_\gamma > 100 \text{ keV}$

### ***Experimental procedure***

#### **Sample Preparation**

One (1) kg each of the sieved limestone samples were transferred into 1 litre Marinelli beakers. The beakers were sealed using a paper tape to prevent the escape of gaseous radionuclides in the sample. They are then labelled appropriately for activity concentration measurement as shown in Figure 3.6a. This was left for a period of 30 days to attain secular equilibrium between the long-lived parent nuclides of  $^{226}\text{Ra}$  ( $^{238}\text{U}$ ) and  $^{232}\text{Th}$ , and their short-lived daughters (Darko & Faanu, 2007; Matiullah *et al.*, 2004; Merdanoglu & Altinsoy, 2006). The method of  $\gamma$ -analysis adopted for this work is by using High Purity Germanium (HPGe) Gamma-ray detector as shown in Figure 3.6b.



**Fig 3.6a** Packaging of Limestone Sample in a  
1 L Marinelli beaker

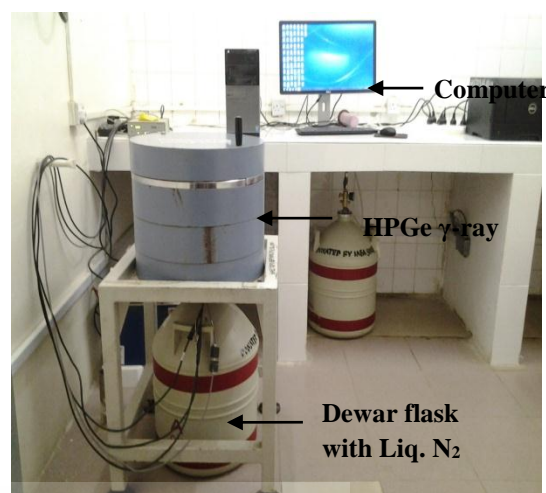


**Fig 3.6b** HPGe Gamma Detector for NORMs  
measurement

### **$\gamma$ -radiation Measurement on the HPGe Detector**

The  $\gamma$ -radiation intensity of the limestone samples were measured on a coaxial HPGe semiconductor  $\gamma$ -ray detector (Fig 3.6b).

The 1 kg finely powdered limestone sample contained in the 1 L Marinelli polyethylene beaker was placed on the coaxial HPGe  $\gamma$ -ray detector and the  $\gamma$ -radiation intensity of NORMs contained in the limestone measured for 36,000 seconds (10 hours).

The  $\gamma$ -radiation activity of the uranium-series were determined using the  $\gamma$ -ray emissions of  $^{214}\text{Pb}$  at 351.9 keV (35.8%) and  $^{214}\text{Bi}$  at 609.3 keV (44.8%) for  $^{226}\text{Ra}$ . For the  $^{232}\text{Th}$ -series, the  $\gamma$ -ray emissions of  $^{228}\text{Ac}$  at 911 keV (26.6%),  $^{212}\text{Pb}$  at 238.6 keV (43.3%) and  $^{208}\text{Tl}$  at 583 keV (30.1%) were used. The  $\gamma$ -radiation activity of  $^{40}\text{K}$  was determined directly from its  $\gamma$ -ray emission line at 1460.8 keV (10.7%).

### Calculation of Activity Concentration

The specific activity concentrations ( $A_{sp}$ ) of  $^{232}\text{U}$ ,  $^{232}\text{Th}$  and  $^{40}\text{K}$  in  $\text{Bq kg}^{-1}$  for the limestone samples (APPENDIX C1-C9) were determined using the Equation 3.7 [Awudu *et al.*, (2010)]:

$$A_{sp} = \frac{N_{sam}}{P_{\gamma} \cdot \eta \cdot T_c \cdot M} \quad (3.7)$$

where,

- $N_{sam}$  - net counts of the radionuclide in the sample
- $P_{\gamma}$  - gamma ray emission probability (gamma yield)
- $\eta$  - total counting efficiency of the detector system
- $T_c$  - sample counting time
- $M$  - mass of sample (kg) or volume (L)

### Calculation of Absorbed Dose Rate (ADR)

From the mean specific concentrations of  $^{232}\text{U}$ ,  $^{232}\text{Th}$  and  $^{40}\text{K}$ , the dose rate was calculated using the relation from Beck *et al.*, (1992);

$$ARD = 0.417C_U + 0.462C_{Th} + 0.604C_K \quad (3.8)$$

where,

$C_U$ ,  $C_{Th}$  and  $C_K$  are the specific concentrations of  $^{238}\text{U}$ ,  $^{232}\text{Th}$  and  $^{40}\text{K}$  in  $\text{Bq/kg}$  respectively.

### Calculation of Annual Effective Dose (AED)

The Annual Effective Dose due to the absorbed dose rate was applied using the conversion factor of 0.7 Sv/Gy (UNSCEAR, 2000);

$$AED = ARD \cdot \frac{8760hr}{yr} \cdot 0.2 \cdot 0.7 \frac{Sv}{Gy} \cdot 10^{-6} \quad (3.9)$$

where,

0.2 is the outdoor occupancy proposed by UNSCEAR, (2000) ; and, 0.7 Sv/Gy is the dose conversion factor.

## 3.5 Development of Limestone Defluoridation Technique using Batch Analysis

### 3.5.1 Preparation of Limestone Samples

#### *Instrumentation*

Jaw Crusher Pulverisette 2 (Fritsch GmbH, Germany), Retsch AS 200 Vibratory Sieve Shaker (Retsch GmbH, Germany)

#### *Experimental Procedure*

Limestone samples were broken into smaller fragments (Suresh and Dutta, 2010; Beraki, 2014) with the Jaw Crusher Pulverisette 2. The crushed limestone samples were then loaded into arranged selected sieves in order of increasing sizes (500, 1000, 2000 and 6350  $\mu\text{m}$ ). The loaded sieves were clamped on the Retsch AS 200 Vibratory Sieve Shaker and agitated for about 15 minutes (Fig 3.7a). The different sieved limestone particles (Fig 3.7b) were stored separately in hermitically-closed polythene bags and labelled. To avoid cross contaminating of one sample with the other, the sieves were washed, dried and cleaned with acetone after sieving each sample.



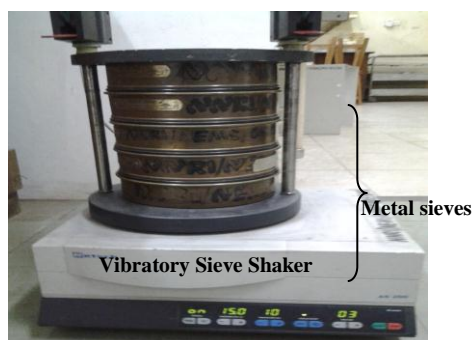


**Fig 3.7a** Shaking sample with Retsch AS 200 Vibratory Shaker

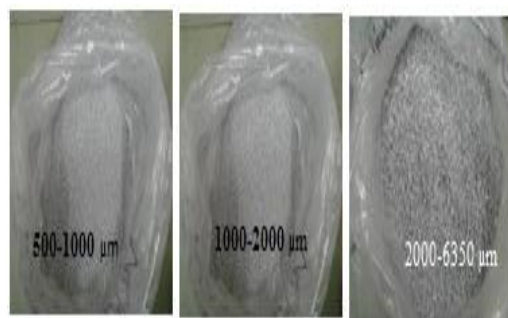


**Fig 3.7b** Sieved limestone Samples

### 3.5.2 Batch Adsorption Experiment

#### *Instrumentation*

A DIONEX ICS-90 Ion Chromatographic System was used for fluoride content determination in Batch Adsorption experiments; as well as fluoride, chloride, nitrate, sulphate and phosphate in the Column Adsorption experiment. The chromatographic system consists of a DIONEX AMMS 300 (4 - mm) Anion Micro-Membrane Suppressor, a DIONEX IonPac AS14A-5  $\mu\text{m}$  Analytical Column ( $3 \times 150 \text{ mm}$ ), a DIONEX IonPac AG14A-5  $\mu\text{m}$  Guard Column ( $3 \times 30 \text{ mm}$ ), and an ICS-900 DS 5 Detection Stabilizer

Acquisition and quantification of the chromatographic spectrum was achieved using the DIONEX CHROMELEON Chromatographic Data Management System Software (Thermo Scientific, USA).

#### *Chromatographic Solutions and Standards*

**Eluent solution:** mixture of 0.16 M  $\text{Na}_2\text{CO}_3$  and 0.02 M  $\text{NaHCO}_3$

**Regenerant solution:** 4 M  $\text{H}_2\text{SO}_4$



**Fig 3.8a** Eluent standard solution



**Fig 3.8b** Regenerant standard solution



**Standard:** Dionex Seven Anion Standard II (Thermo Fisher Scientific, USA)

containing 20 mg/L, with the following composition (99.9 % H<sub>2</sub>O, 20 mg/L F<sup>-</sup>, 100 mg/L Cl<sup>-</sup>, 100mg/L NO<sub>2</sub><sup>-</sup>, 100 mg/L Br<sup>-</sup>, 100 mg/L NO<sub>3</sub><sup>-</sup>, 200 mg/L PO<sub>3</sub><sup>2-</sup>, and 100 mg/L SO<sub>4</sub><sup>2-</sup>)

### *Operating Conditions*

The compressor uses air (Nitrogen gas) drawn from the ambient surroundings.

The flow rates of Eluent and the Regenerant solution are 0.5mL/min respectively.

### *Calibration of Chromatographic System*

Using a pre-washed syringe [1 mL Norm Ject syringe (DIN/EN/ISO 7886-1)], calibration standards of concentrations 5, 10, 15 and 20 mg/L were each injected into the IC and allowed to flow at a rate of 0.5 mL/min to calibrate the ICS-90.

The standards were prepared from Dionex Seven Anion Standard II (Thermo Fisher Scientific, USA) containing 20 mg/L, having the following composition (99.9 % H<sub>2</sub>O, 20 mg/L F<sup>-</sup>, 100 mg/L Cl<sup>-</sup>, 100 mg/L NO<sub>2</sub><sup>-</sup>, 100 mg/L Br<sup>-</sup>, 100 mg/L NO<sub>3</sub><sup>-</sup>, 200 mg/L PO<sub>3</sub><sup>2-</sup>, and 100 mg/L SO<sub>4</sub><sup>2-</sup>).

After the last peak (SO<sub>4</sub><sup>2-</sup>) has appeared and the conductivity signal has returned to the base line, water sample were then injected. The Eluent used for the analyses was a solution of 0.16 M Na<sub>2</sub>CO<sub>3</sub> and 0.02 M NaHCO<sub>3</sub>, while the anion Regenerant used was 4 M H<sub>2</sub>SO<sub>4</sub>.

### *Apparatus/Materials*

Measuring cylinder (50 and 100 mL), Magnetic stirrer (Eisco EI 0112M, India), Beakers, Sampling bottles, 1 mL Syringe (Ningbo Clan Medical Instruments Co, Ltd, India), PTFE Syringe Filter-0.45  $\mu\text{m}$  (Filter-Lab, UK), Volumetric flask (1000 and 100  $\text{cm}^3$ ), Mettler AB204-S analytical balance (Mettler Toledo, )

### *Fluoride Standards*

A Stock solution containing 100 mg/L was prepared by dissolving 0.221 g of anhydrous NaF and diluting to volume (1000 mL) with deionised water. Working standards of concentrations 1, 5 and 10 mg/L were prepared by appropriate dilution of the stock (detailed calculation for the preparation of the stock and working solutions is presented in APPENDIX E1 and E2).

The concentrations of the prepared solutions (stock and dilute) were ascertained using the DIONEX ICS-90 Ion Chromatographic (IC) System. The results are presented in Table 3.1.

**Table 3.1** Concentrations (prepared and measured) of standard solutions using IC

Type of standard	Concentration (mg F/L)			
	Prepared	Measured	(Range)	[No. of determinations]
Stock	100.00	<b>100.83 <math>\pm</math> 0.39</b>	(100.08 - 101.13)	[5]
Working	1	<b>1.06 <math>\pm</math> 0.05</b>	(0.99 – 1.10)	[3]
	5	<b>5.00 <math>\pm</math> 0.03</b>	(4.98 – 5.05)	[3]
	10	<b>10.06 <math>\pm</math> 0.95</b>	(9.95 – 10.16)	[3]

### ***Experimental Procedure***

About 10, 50 and 100 grams aliquots of the raw crushed limestone were for each of the three (3) grain sizes (500-1000, 1000-2000 and 2000-6350  $\mu\text{m}$ ) were respectively weighed into 250 mL beakers using a Mettler AB204-S analytical balance (Fig 3.9a). Each limestone aliquot was mixed with 100 mL of 1, 5 and 10  $\text{mgF}^-/\text{L}$  (Anhydrous Sodium Fluoride ( $\text{NaF}$ ) solution) respectively. This was followed by stirring magnetically for about 90 minutes with an Eisco EI 0112M Magnetic Stirrer (Fig 3.9b). Aliquots of the mixture were taken at 15 minutes intervals and the residual fluoride concentration measured using the DIONEX ICS-90 Ion Chromatographic System (3.9c). A blank was prepared by mixing 10 g limestone with 100 mL of distilled water and agitating it magnetically.



**Fig 3.9a** Weighing of sample



**Fig 3.9b** Magnetic stirrer of mixture

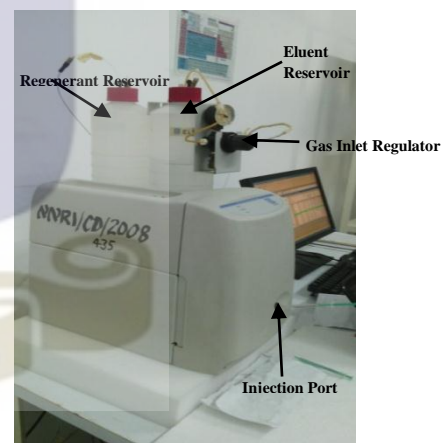


**Fig 3.9c** IC for  $\text{F}^-$  measurement

The defluoridation efficiency of the limestone sample was determined by measuring the initial and residual fluoride concentrations in the various aliquots taken and calculated using equations:

$$\% \text{ Adsorption} = \frac{C_o - C_t}{C_o} \times 100 \quad (3.10)$$

$$\text{Adsorption Capacity} = \frac{C_o - C_t}{M} \times V \quad (3.11)$$

where,

$C_o$  = initial fluoride concentration

$C_t$  = residual fluoride concentration

$M$  = mass of adsorbent used

$V$  = volume of fluoride used in Batch experiment

### 3.6 Application of Developed Technique

The developed defluoridation technique was applied to defluoridate water from Bongo in the Upper region of Ghana, using the Column Adsorption experiment.

#### 3.6.1 Collection of Water Samples from Bongo District

Prior to the collection of the water samples, the sampling bottles (330 mL) were conditioned by first treating with 10% (v/v)  $\text{HNO}_3$  solution for 48 hours, followed by thorough rinsing with double-distilled water (APHA, 1998).

Water samples were collected from five (5) communities (Bongo-Namoa, Bongo-Navorogo, Bongo-Anafobiisi, Bongo-Zuruyi, and Bongo-Soe) in the Bongo district of the Upper East region. A total of 10 samples (from uncapped wells) were collected in

March 2016 (Fig. 3.10). At each sampling point, three replicate samples were taken. Of the three replicate samples, one sample was acidified with 10%  $\text{HNO}_3$  for heavy metals determination. This was done to preserve the water samples and to dissolve the particulate metals into the solution (APHA, 1992).



**Fig 3.10** Uncapped boreholes at two affected communities in the Bongo District

At each sampling point, just before samples were collected from the borehole, the water in the borehole was purged. This is because a fresh water sample is needed to accurately assess groundwater quality. Water standing in a well for a period of time undergoes changes that can affect and alter the water quality. Example of these changes includes temperature, oxidation, biological activity, precipitation of metals and reactions with the well casing. These changes can impact several parameters such as pH, alkalinity, TDS and concentration of metal (USEPA, 1996; Koterba *et al.*, 1995).

After filling the sampling container with the water sample, the container was securely capped, labelled and kept in a thermo-insulated container with some ice packs. The collected samples were transported overnight courier to the laboratories of the Ghana Atomic Energy Commission located at Kwabenya, Accra, for analysis.



### **3.6.2 Determination of Physico-chemical Parameters**

Six (6) physico-chemical parameters, namely pH, Electrical Conductivity (EC), Salinity, Colour, Turbidity and Total Dissolved Solids (TDS) were determined.

#### **3.6.2.1. Determination of pH**

The pH of the water samples was determined using the pH 3110 SET 1 2AA111 multi-fractional meter [Wissenschaftlich Technische Werkstätten (WTW) Germany].

The pH meter was first calibrated using two standard buffer solutions of pH 4.01 and 7.01, respectively. After the calibration, the pH meter was used to determine the pH of the water samples.

About 100 mL of the water sample was transferred into a 250 mL beaker and thoroughly homogenized by swirling. The sensing electrode of the pH meter was placed in the water sample for about five (5) minutes for the reading to stabilize. The pH of the water was then recorded. The calibration of the meter was verified after measuring every four samples. After each reading, the electrode is rinsed with double distilled water and a small portion of the next sample to be determined.

#### **3.6.2.2 Determination of Electrical conductivity (EC), Total Dissolved Solid (TDS), Turbidity, Colour and Salinity**

*Instrument:* HI 991301 pH/EC/TDS/Temperature meters (Hanna Instruments, USA )

*Reagent:* 0.01 M KCl



### *Experimental Procedure*

The Hanna HI 991301 multi-functional conductivity meter was used to determine EC, TDS, Turbidity, Colour and Salinity of the water samples. Prior to measurement, the meter was calibrated using a standard reference solution of 0.01 M KCl solution of known conductivity (1412  $\mu\text{S}/\text{cm}$ ). The electrode was rinsed in distilled water followed by measurement of the parameters in the water sample. The electrode was dipped into the sample and was slowly moved circularly for a minute until digital readout was stabilised.

### **3.6.3 Column Adsorption Experiments**

#### *Apparatus/Materials*

In-house designed mini-column glass bed of diameter 4 cm and varying heights of 20, 30 and 40 cm.

#### *Experimental procedure*

The mini-column glass beds were clamped and loaded with the selected limestone sample (R<sub>102</sub>) of grain size 1000-2000  $\mu\text{m}$  (Fig 3.11a). The bed column was supported and closed at the outlet with cotton wool to prevent the flow of the adsorbent together with the effluent or filtrate.

The bed was rinsed with distilled water and left overnight to ensure a closely packed arrangement of the particles. The Bongo water sample was poured onto the packed limestone in the fixed mini-column bed. Aliquots of filtrate solutions were taken from the outlet of each bed at 15 minutes interval for 90 minutes (Fig. 3.11b). The residual

fluoride concentration was determined using the DIONEX ICS-90 Ion Chromatographic System.



**Fig. 3.11a** Mini-Column bed filled with adsorbents



**Fig 3.11b** Aliquots taken from the different mini-column beds

### 3.6.4 Determination of Cations

The VARIAN AA 250 Fast Sequential (FS) Atomic Absorption Spectrometer equipped with deuterium background corrector was used in the determination of cations in the water samples. The instrument consists of a light source (hollow-cathode lamp), a flame atomizer system (Air-Acetylene), monochromator or filter and adjustable slit (means of isolating an absorption line) and a photoelectric detector with its associated electronic amplifying and measuring equipment.

Water samples meant for cation analysis were acidified with 3.0 mL (10% v/v) concentrated  $\text{HNO}_3$ . This was done to preserve the water samples and to dissolve the particulate metals into the solution (APHA, 1992).

#### *Digestion of Water Samples*

The Reagents used for the digestion of water samples are: 36% (w/v) HCl (AnalaR grade) and 70% (w/v)  $\text{HNO}_3$  (AnalaR grade)

The water samples were digested using the hot plate method. About 40 mL of the water sample was transferred into a borosilicate glass beaker, followed by the addition of 5 mL of aqua regia (4.5 mL HCl to 0.5 mL HNO<sub>3</sub>). The mixture were covered with clean film and placed on the hot plate and digested for 3 hours at a temperature of about 45 °C (Fig 3.12a and 3.12b). The digested samples were cooled, filtered and diluted with double distilled water nominal volume of 30 mL. It is then transferred into labelled test tubes and analyzed using the VARIAN 240FS atomic absorption spectrometer.

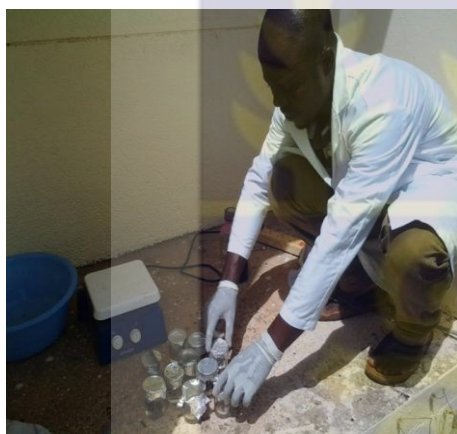


**Fig 3.12a** Samples being prepared for digestion



**Fig 3.12b** Samples on a hot plate during digestion

#### **3.6.4.1 Magnesium (Mg<sup>2+</sup>)**

Magnesium (Mg<sup>2+</sup>) levels in the water samples were determined using the VARIAN AA 250 Fast Sequential (FS) Atomic Absorption Spectrometer.

##### *Reagents*

Lanthanum solution was prepared by dissolving 11.730 g of La<sub>2</sub>O<sub>3</sub> in a minimum volume of 10 % HNO<sub>3</sub> and diluted with distilled water to 1000 mL. This reagent serves as ion suppressant.

### *Experimental Procedure*

Conditions associated with the operation of the AAS used for analysing  $\text{Mg}^{2+}$  in the samples are as follows:

- air-acetylene flame atomizer; air flow rate was 13.50 L/min and acetylene flow rate was 2.00 L/min
- Hollow cathode lamp current and wavelength were 4 mA and 285.2 nm respectively
- Slit width was 0.1 nm

Magnesium calibration standards (0.00, 0.10, 0.20 and 0.50 mg/L) was prepared by appropriate diluting a commercially-available magnesium stock solution. The prepared solution was used to calibrate the instrument (calibration graph in APPENDIX G1). This was followed by sample analysis.

To prepare the samples for analysis, 1 mL of the water sample was transferred into a test tube, followed by the addition of 9 mL lanthanum solution (100 mg/L) was added and thoroughly homogenized by shaking. The prepared samples were then aspirated into the AAS. After every 10 readings a standard (magnesium calibration standard solution) is aspirated as a quality control measure.

### *Calculation*

$[\text{Mg}^{2+}]$  in mg/L in the water samples were calculated from direct reference to the calibration curve according to the equation:

$$[\text{Mg}^{2+}] = \text{Mg}^{2+} \cdot D \quad (3.12)$$

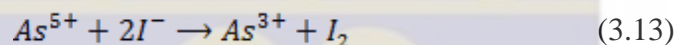
where,

D is the dilution factor ratio

### 3.6.4.2 Determination of As by HG-AAS

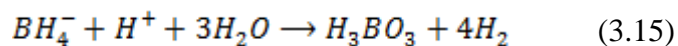
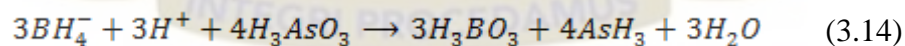
*Reagents:* Hydrochloric acid [AnalaR grade, 50% (v/v)], Sodium borohydride solution [AnalaR grade, 0.5 % (m/v) in 0.5 % (w/v) NaOH], Pre-reducing solution [AnalaR grade, 10 % (w/v) potassium iodide + 10 % (w/v) L-ascorbic acid], and arsenic standard (1000 mg/L)

Prior to analysis of the water samples for arsenic,  $As^{5+}$  was reduced to  $As^{3+}$ . This was achieved by the addition of 4 mL of freshly prepared 5 M KI to the digested sample.



#### *Hydride generation*

The continuous flow approach was used to merge sample solution and reagents. The sample solution of flow rate 0.1 mL/s was mixed with both HCl and  $NaBH_4$  in a polyetheretherketone (PEEK) cross connector and pumped into a reaction coil. During the mixing, arsenic hydride ( $AsH_3$ ) and considerably hydrogen gas ( $H_2$ ) are produced.



The gaseous  $AsH_3$  and  $H_2$  generated were separated from the liquid phase and transferred with a flow argon gas and dried by a stream of nitrogen gas. The liquid goes to waste and the gaseous hydride and hydrogen were swept out of the vapour generation vessel into the atomisation system of the AAS.



### *Calibration*

Calibration standards (0.02, 0.04, 0.08 and 0.10 mg/L) were prepared by appropriate dilution of the commercially-available stock As solution. A calibration graph (absorbance versus concentration of calibrants) was plotted (APPENDIX G2). This was followed by aspirating the KI reduced samples into the AAS.

### *Calculation*

The concentration of As in each water sample obtained from the equation of the regression line of the calibration curve was used to calculate the final concentration of the water samples according to the equation;

$$Final\ conc. (mg/L) = \frac{Conc._{AAS} \times D_f \times Nominal\ volume}{Sample\ weight(g)} \quad (3.16)$$

where,

$D_f$  is dilution factor.

### **3.6.5 Determination of Anions**

#### **3.6.5.1 Determination of Fluoride ( $F^-$ ), Chloride ( $Cl^-$ ), Phosphate ( $PO_4^{3-}$ ), sulphate ( $SO_4^{2-}$ ) and Nitrate ( $NO_3^-$ ) using ICS-90 Chromatographic System**

The set-up and experimental conditions for the ICS-90 Chromatographic System was the same as described during Batch Adsorption Experiment in section 3.5.2.



## Experimental Procedure

### Sample analysis

After calibration, samples were injected into the IC using a 1 mL Norm Ject syringe (DIN/EN/ISO 7886-1). During the injection, uniformity in the injection process is required to give a pulse-free flow. After five (5) to ten (10) sample injections, distilled water was used to flash the system. The chromatographic spectrum obtained showed the peaks for each anion (Fig. 3.13)

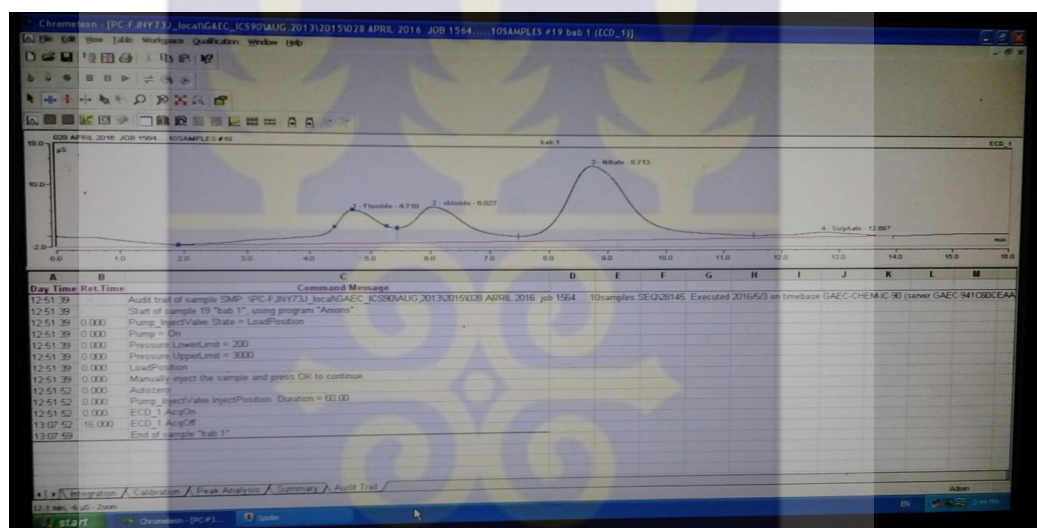


Fig 3.13 Example of a Chromatographic spectrum obtained

## CHAPTER FOUR

### RESULTS AND DISCUSSION

The results obtained from the study are presented and discussed in this Chapter. The discussion is supported by presentation of some of the results in Tables and Figures.

#### 4.1 Petrographic Thin Section

The results of the Petrographic Thin Section conducted on the eight (8) limestone samples from Oterkpolu is presented in Table 4.1.

**Table 4.1: Percentage composition of mineralogical content of selected samples**

Sample	XRD (%)	PTS (%)
EKL-R <sub>1</sub> 02	Calcite (83), SiO <sub>2</sub> (6), Serandite (11)	Calcite (96), Quartz (4)
EKL-D01	Calcite (68), Dolomite (22), SiO <sub>2</sub> (10)	Calcite (85), Quartz (15)
EKA-R02	Calcite (95), SiO <sub>2</sub> (5)	Calcite (71), Quartz (21)
EKA-R01	Calcite (19), Dolomite (22), SiO <sub>2</sub> (17) {K, Na, Al, Fe, Mg, Ti} (42)	Calcite (95), Quartz (5)
EKL-Y03	Calcite (17), SiO <sub>2</sub> (16), Muscovite (23) Ankerite (44)	Calcite (90), Quartz (10)
EKA-Y04	Dolomite (57), SiO <sub>2</sub> (30), Ankarite (7) Muscovite (6)	Calcite (95), Quartz (5)
EKA-B01	Calcite (13), Dolomite (54), SiO <sub>2</sub> (8) Diopside (25)	Calcite (98), Quartz (2)
EKA-Bk03	Dolomite (98), SiO <sub>2</sub> (2)	Calcite (95), Quartz (5)
EKL-Y01	Calcite (28), Dolomite (10), SiO <sub>2</sub> (24) Muscovite (38)	Nil

From the Petrographic Thin Section (PTS) and X-Ray Diffraction analysis, two samples (EKL-R<sub>1</sub>02 and EKL-D01) were selected for the Batch Adsorption Experiment. The selection was based on the high percentage of Calcite and Dolomite mineral content in both analysis and the abundance of the sample. The Calcite had been the major compound (analyte of interest) for the reaction with the fluoride ions.

#### **4.1.1 Sample EKL R<sub>1</sub>02**

##### *Hand Sample*

The rock is grey in colour and fined grained and layered. Iron (Fe), probably present as siderite gives some of the layers a reddish colour. The specimen fizzed with dilute hydrochloric acid indicating the presence of calcite.

##### *Thin Section*

The photomicrograph of the sample (Fig 4.1) revealed the dominance of fined grained calcite with angular quartz grains in the minority. Iron rich bands can be evident. The iron here may exist in the form of siderite. The sample has fractures indicating that, the sample seems to have undergone deformation or alteration.

#### **4.1.2 Sample EKL D01**

##### *Hand Sample*

This sample is grey in colour and finely grained. It is also massive and lacks lamination. Calcite present in the sample fizzes with dilute hydrochloric acid. Crystalline grains of quartz are also visible in hand sample.

### *Thin Section*

The photomicrograph of the sample (Fig 4.2) consists of two layers. One layer contains very fine grains of calcite with a few quartz grains. The other layer has bigger, angular grains of quartz. This layer is still dominated by calcite. This layering could have formed due to an alternation in the phases of deposition of the silicilastic sediments and calcite which make up the rock. The sample has no fractures and does not seem to have undergone deformation or alteration.

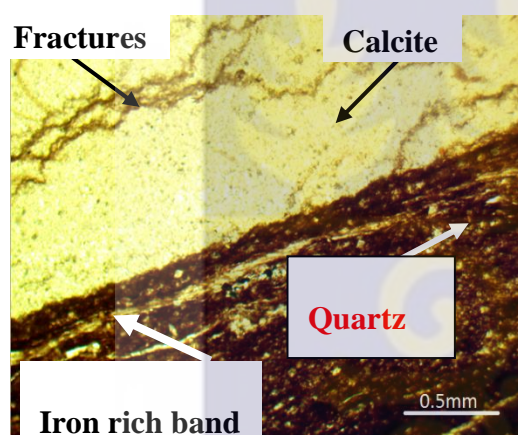


**Fig 4.1:** Photomicrograph of sample EKL R102

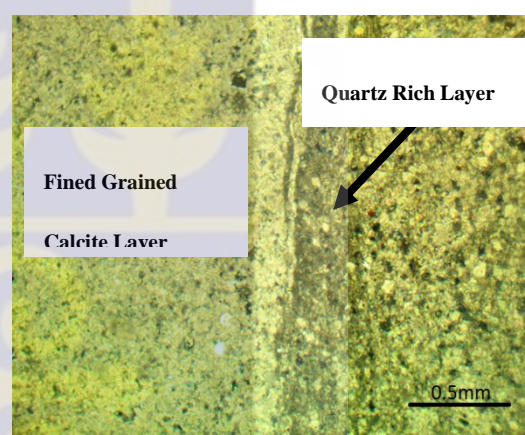


**Fig 4.2:** Photomicrograph of sample EKL D01

### **4.2 XRD Analysis**

In order to determine the mineralogical composition of Oterkpolu limestone, few grams of the different samples were taken and quantitatively analysed by X-ray Diffraction using Diffractometer with copper (Cu) as the anode material, an Alpha 1 wavelength ( $\lambda$ ) of “1.54060”, Alpha 2 wavelength of “1.54443” and K-Beta wavelength of “1.39225”.

From the analysis, two samples (EKL-R<sub>102</sub> and EKL-D01) were selected due to the following criteria:

- High percentage of calcite content for an efficient adsorption reaction with fluoride.
- The abundance of the particular type of sample present.

#### 4.2.1 Limestone Samples EKL- R<sub>1</sub>02 and EKL-D01

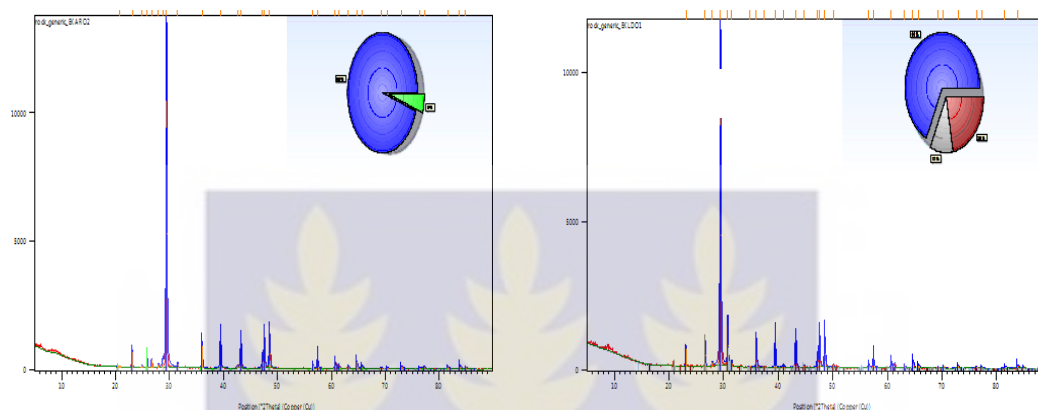


**Fig 4.3** Diffractogram of limestone sample EKL-R<sub>1</sub>02 (A) and EKL-D01 (B)

From the analysis, the sample EKL-R<sub>1</sub>02 is made up of two main minerals; calcium carbonate (calcite) and silicon oxide (quartz). The calcite and silicon oxide constitutes 95% and 5% respectively as per the phase identification of Oterkpolu limestone sample. The highest peak at 2theta (29.4456) was 10343.67 (Fig. 4.3A). On the other hand, sample EKL-D01 is made up of 68% Calcium Carbonate (Calcite), 22% Dolomite (Calcium Magnesium Carbonate) and 10% Silicon Oxide. Its highest peak at 2 theta (2θ) [29.4406] was 8791.41 (Fig. 4.3B). The full peak list of the analysis is presented in Appendix A6 and A9 respectively.

### 4.3 Radiological Safety of the Limestone Samples

#### 4.3.1 Activity Concentration of Naturally Occurring Radionuclides in Limestone Sample

In all the samples from Oterkpolu, the Activity Concentration of K-40 was higher than Th-232 and U-238 (Fig. 4.4). Limestone sample EKA-Bk03 was the only sample



with Activity Concentration of K-40 as low as 5.42 as compared to the highest concentration of 49.40 in EKL-R102.

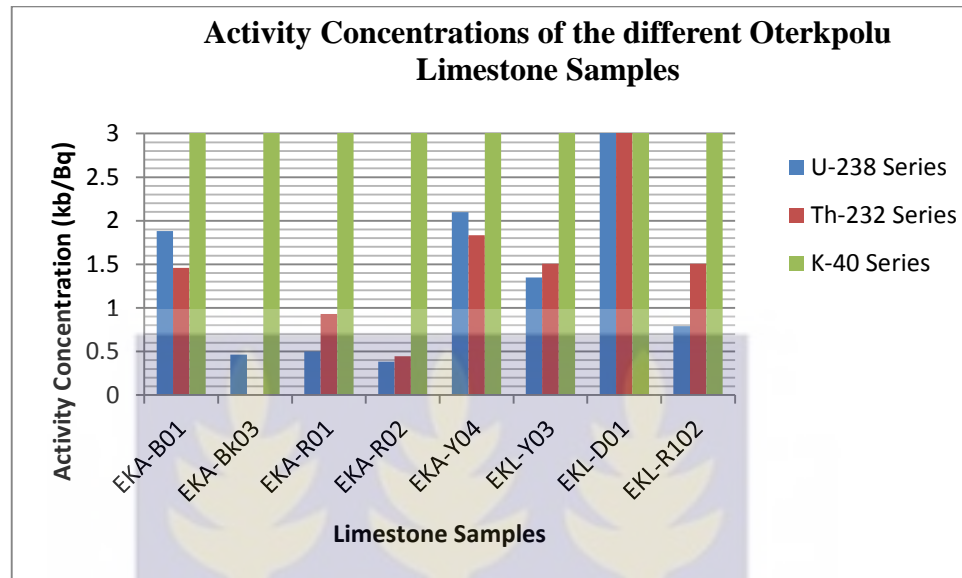


**Fig 4.4** Plot of Activity Concentration against limestone Type.

The mean activity concentration of U-238, Th-232 and K-40 of the different limestone are  $2.0 \pm 1.5$ ,  $1.7 \pm 1$  and  $21.9 \pm 13.4$  respectively.

The average values of concentrations of  $^{238}\text{U}$ ,  $^{232}\text{Th}$  and  $^{40}\text{K}$  in soils worldwide in Bq/kg are 33, 45 and 420 respectively (UNSCEAR, 2000). This indicates that the Activity Concentrations of Oterkpolu limestone is less than the stated values above and the average concentrations reported in similar studies in other parts of the world (India, Serbia, Belgium and Turkey) [Table 4.2].



**Table 4.2: Comparison of Reported Activity Concentrations with the Present Study**

Country	Activity Concentration (Bq/kg)			Nature of sample	Reference
	$^{238}\text{U}$	$^{232}\text{Th}$	$^{40}\text{K}$		
Ghana	?	?	?	Limestone samples from Oterkpolu	This study
Ghana	7.3	6.9	379.9	Sediment from Tono Irrigation Dam	Agalga, 2012
India	7.3	46.8	384.03	Sediments from Ponnaiyar River	Ramasamy <i>et al.</i> , 2009
Serbia	42	36	445	Sediments from Danube	Krmar <i>et al.</i> 2009
Turkey	39	38	573	Sediments from Firtina valley	Kurnaz <i>et al.</i> , 2007

The calculated Annual Effective Dose (AED) of the selected samples (EKL-R<sub>102</sub> and D01) are 0.03 and 0.01 mSv/yr respectively. Notwithstanding, the mean Annual Effective Dose of limestone from Oterkpolu is estimated at 0.013 mSv/yr. This value is lower than the recommended 0.40 mSv/yr according to UNSCEAR, 2000. This means that, the samples are radiologically safe.

Both internal and external hazard indices gave mean values of 0.01 and 0.02 respectively. Exposures at or below the reference level (HI = 1) indicates that no adverse human health effects (non cancer) are expected to occur. Table 4.3 gives a detailed analysis of the various samples.

**Table 4.3: Absorbed Dose and Radioactivity Indices Associated with Oterkpolu Limestone Samples**

Sample ID	ADR(Gy/hr)	Hazard Index		AED(mSv/yr) $\times 10^{-3}$	$^{238}\text{U}/^{232}\text{Th}$ Ratio
		$H_{\text{in}}$	$H_{\text{ex}}$		
EKA-B01	9.0514	19.442	14.361	11.101	0.777
EKA-Bk03	2.4736	3.631	2.379	3.034	0.000
EKA-R01	13.7347	12.748	11.399	16.844	1.866
EKA-R02	6.14168	6.629	5.591	7.532	1.156
EKA-Y04	8.1668	21.452	15.784	10.016	0.874
EKL-Y03	14.7535	19.704	16.054	18.094	1.115
EKL-D01	9.8808	46.622	32.326	12.118	0.761
EKL-R <sub>102</sub>	21.8746	20.360	18.226	26.827	1.910
<b>MINIMUM</b>	<b>2.4736</b>	<b>3.631</b>	<b>2.379</b>	<b>3.034</b>	<b>0.000</b>
<b>MAXIMUM</b>	<b>21.8746</b>	<b>46.622</b>	<b>32.326</b>	<b>26.827</b>	<b>1.910</b>
<b>MEAN</b>	<b>10.7596</b>	<b>18.824</b>	<b>14.515</b>	<b>13.196</b>	<b>1.057</b>
<b>STD. DEV.</b>	<b>5.5761</b>	<b>12.245</b>	<b>8.453</b>	<b>6.839</b>	<b>0.582</b>

#### 4.4 Batch Adsorption Experiment

##### 4.4.1 General Procedure

Each of the two crushed limestone samples (EKL-R102 & EKL-D01) of grain sizes (500-1000  $\mu\text{m}$ , 1000-2000  $\mu\text{m}$  and 2000-6350  $\mu\text{m}$ ) and masses (10 g, 50 g and 100 g) were each combined with 100 mL of approximately 1, 5 and 10 mg/L anhydrous Sodium Fluoride (NaF) solution. Each NaF-Limestone mixture was agitated magnetically with Eisco E0112M Magnetic Stirrer for 90 minutes and aliquots of the

mixture were taken every 15 minutes and the residual fluoride concentration determined with DIONEX ICS-90 Ion Chromatographic System.

Before the agitation of the mixture, the pH of the NaF-Limestone mixture was determined. A blank of limestone-distilled water mixture was also determined for each batch experiment. [Let sample EKL-R102 = **A** and sample EKL-D01 = **B**]

#### 4.4.2 Effect of Varying Residence Time on Residual Fluoride Adsorption in 1 mg/L Fluoride Solution

##### *Batch Adsorption Experiment 1*

A 10 g mass each of the two limestone samples (**A** & **B**) of grain size 500-1000  $\mu\text{m}$  were mixed with 100 mL of 1 mg/L NaF solution. The pH of the each mixture (7.78 and 9.42 respectively) was recorded. A graph of residual fluoride concentration with time for the two limestone type (Fig. 4.5) was plotted.

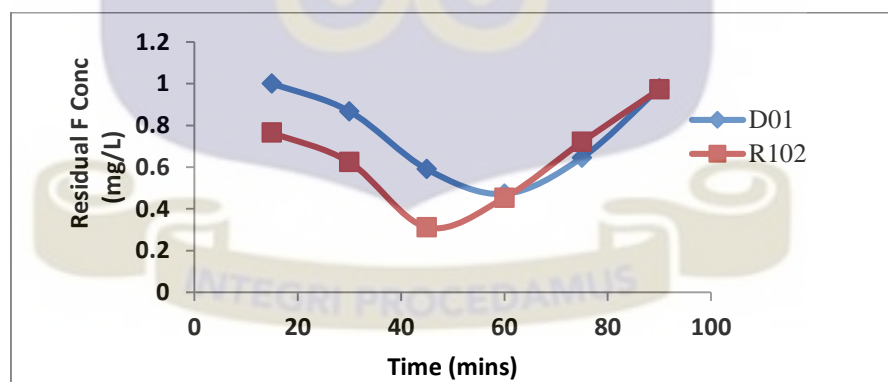


**Fig 4.5** Plot of Residual  $\text{F}^-$  concentration against Time for 10 g mass (500-1000  $\mu\text{m}$ ) samples in 1 mg/L NaF

Sample **A** recorded a maximum residual fluoride concentration of 0.3124 mg/L (71.53%) at the 45<sup>th</sup> minute of the 90 minute duration, while sample **B** gave a

maximum residual fluoride concentration of 0.4721 mg/L (53.85%) at the 60<sup>th</sup> minute (Fig. 4.5).

### *Batch Adsorption Experiment 2*

A 50 g mass each of the two limestone (**A** & **B**) sample of grain size 500-1000  $\mu\text{m}$  were mixed with 100 mL of 1 mg/L NaF solution. The pH of the mixtures was 7.80 and 9.47 respectively. A graph of residual fluoride concentration with time (Fig 4.6) for the two limestone type was plotted.

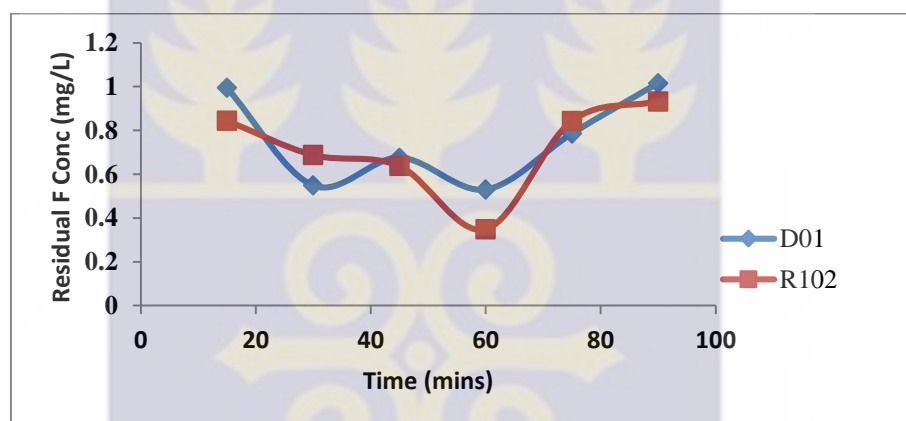


**Fig 4.6** Plot of Residual F<sup>-</sup> concentration against Time for 50 g mass (500-1000  $\mu\text{m}$ ) sample in 1 mg/L NaF

Both samples attained equilibrium at the 60<sup>th</sup> minute but with different residual fluoride concentrations (Fig. 4.6). Samples **A** and **B** recorded residual fluoride concentrations of 0.3487 mg/L (68.22%) and 0.5298 (48.21%) respectively. Fluoride removal was detected to increase with increasing contact time to a point when equilibrium was attained using crushed limestone and fluoride solutions acidified with acetic acid and the other with citric acid (Suresh and Dutta, 2010).

*Batch Adsorption Experiment 3*

A 100 g mass each of the two limestone (**A** & **B**) sample of grain size 500-1000  $\mu\text{m}$  were mixed with 100 mL of 1 mg/L NaF solution. The Ph of the mixtures was 7.80 and 9.50 respectively.

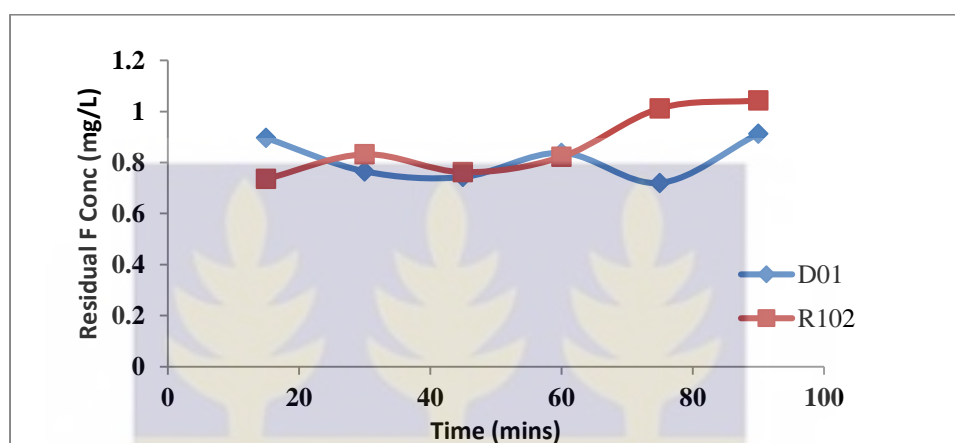


**Fig 4.7** Plot of Residual F<sup>-</sup> concentration against Time for 100 g mass (500-1000  $\mu\text{m}$ ) samples in 1 mg/L NaF

Sample **A** attained equilibrium at the 60<sup>th</sup> minute and sample **B** attained its equilibrium at the 75<sup>th</sup> minute (Fig. 4.7). The residual fluoride concentrations at these equilibrium points are 0.7623 mg/L (30.53%) for sample **A** and 0.7201 (29.61%) for sample **B**.

*Batch Adsorption Experiment 4*

A 10 g mass each of the two limestone (**A** & **B**) sample of grain size 1000-2000  $\mu\text{m}$  were mixed with 100 mL of 1 mg/L NaF solution. The pH of the mixtures was 7.65

and 9.38 respectively. A graph of residual fluoride concentration with time (Fig.4.8) for the two limestone type is illustrated below.

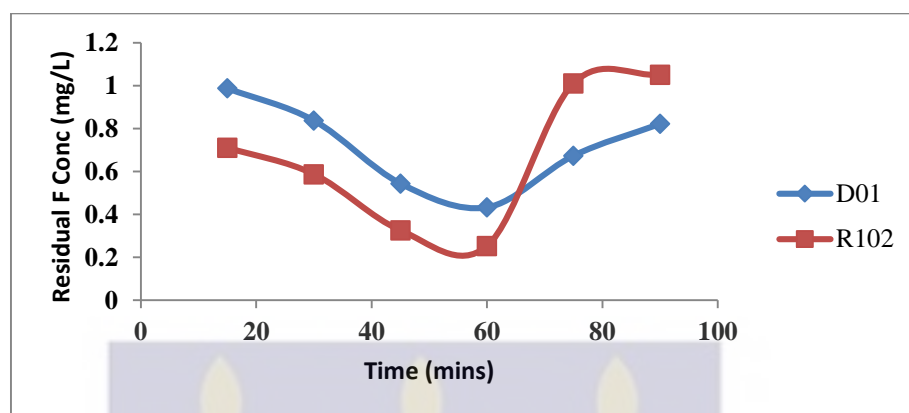


**Fig 4.8** Plot of Residual F<sup>-</sup> concentration against Time for 10 g mass (1000-2000  $\mu\text{m}$ ) samples in 1 mg/L NaF

Both samples attained equilibrium at the 60<sup>th</sup> minute but with different residual fluoride concentrations (Fig. 4.8). Samples **A** and **B** recorded residual fluoride concentrations of 0.2521 mg/L (77.03%) and 0.4329 (57.68%) respectively. The effect of contact time on fluoride adsorption was investigated at different doses and particle size of iron ore. It came out that, the amount of fluoride adsorbed increases with time and reached its steady state in 120 min at which the maximum adsorption efficiency (86%) and maximum adsorption capacity (1.72 mg/g) were achieved (Kebede et al., 2014).

#### *Batch Adsorption Experiment 5*

A 50 g mass each of the two limestone (**A** & **B**) sample of grain size 1000-2000  $\mu\text{m}$  were mixed with 100 mL of 1 mg/L NaF solution. The pH of the mixtures was 7.70



and 9.44 respectively. A graph of residual fluoride concentration with time (Fig. 4.9) for the two limestone type is shown below.

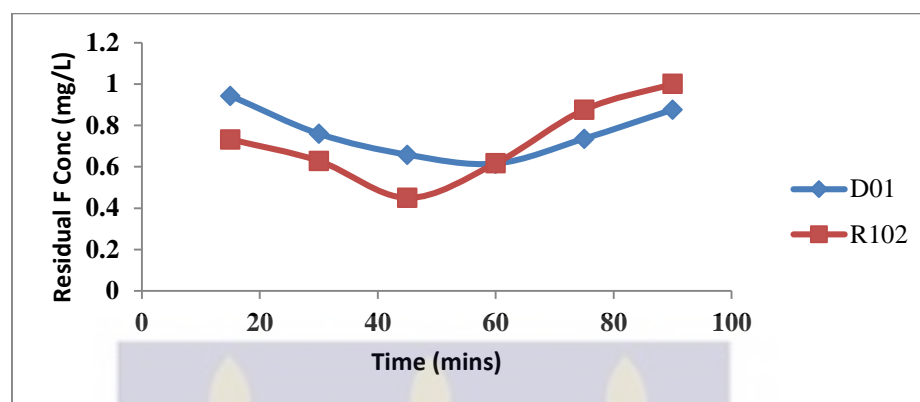


**Fig 4.9** Plot of Residual F<sup>-</sup> concentration against Time for 50 g mass (1000-2000  $\mu$ m) samples in 1 mg/L NaF

Sample **A** recorded a maximum residual fluoride concentration of 0.4502 mg/L (58.97%) at the 45<sup>th</sup> minute of the 90 minute duration, while sample **B** gave a maximum residual fluoride concentration of 0.61531 mg/L (39.85%) at the 60<sup>th</sup> minute (Fig. 4.9). similar work was done on the effect of contact time on fluoride removal from water using aluminium containing compounds (Karthikeyan and Elango, 2007). The result of the equilibrium studies showed that, the removal of fluoride ions increased with time up to 40 min, and after which the increase in agitation time did not alter the fluoride ion uptake due to the attainment of equilibrium.

#### *Batch Adsorption Experiment 6*

A plot of residual fluoride concentration with time (Fig. 4.10) for 100 g mass each of the two limestone (**A** & **B**) sample of grain size 1000-2000  $\mu$ m mixed with 100 mL of

1 mg/L NaF solution is shown below. The pH of the mixtures was 7.79 and 9.50 respectively.

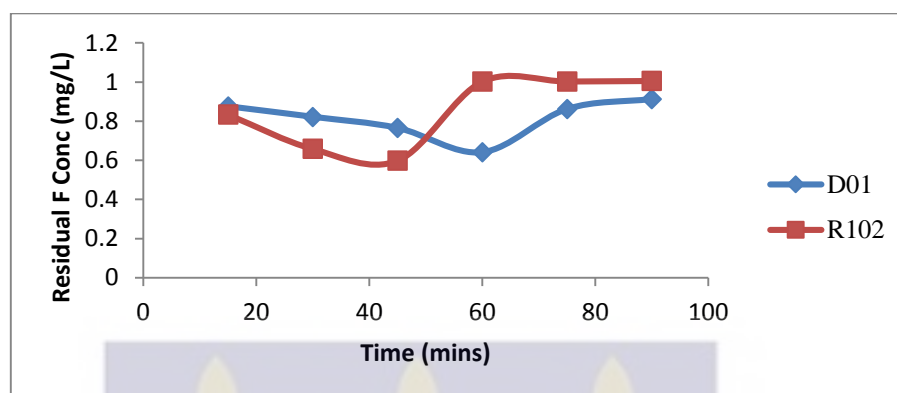


**Fig 4.10** Plot of Residual F<sup>-</sup> concentration against Time for 100 g mass (1000-2000  $\mu$ m) samples in 1 mg/L NaF

Sample **A** recorded a maximum residual fluoride concentration of 0.5983 mg/L (45.48%) at the 45<sup>th</sup> minute of the 90 minute duration, while sample **B** gave a maximum residual fluoride concentration of 0.641 mg/L (37.34%) at the 60<sup>th</sup> minute (Fig. 4.10).

#### *Batch Adsorption Experiment 7*

A plot of graph (Fig. 4.11) shows a 10 g mass each of the two limestone (**A** & **B**) samples of grain size 2000-6350  $\mu$ m mixed with 100 mL of 1 mg/L NaF solution. The pH of the mixtures was 7.73 and 9.39 respectively.

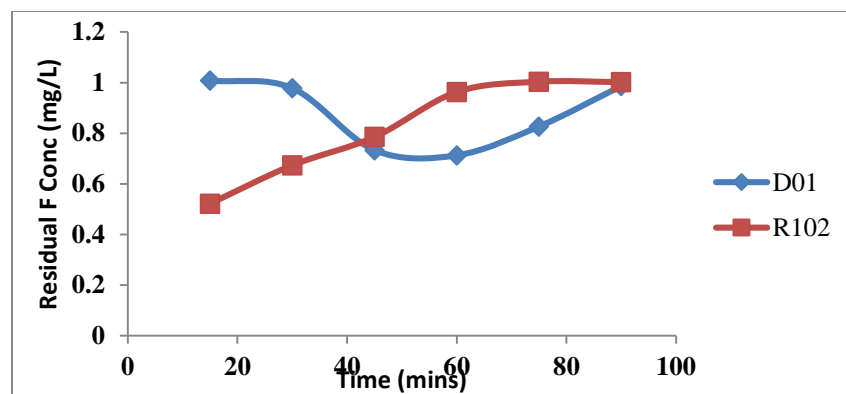


**Fig 4.11** Plot of Residual F<sup>-</sup> concentration against Time for 10 g mass (2000-6350  $\mu\text{m}$ ) samples in 1 mg/L NaF

Sample A shows an appreciable increase in residual fluoride concentration until the 60<sup>th</sup> minute where the concentration became constant. Equilibrium was not established in this respect (Fig. 4.11). Sample B gave a maximum residual fluoride concentration of 0.7126 mg/L (30.34%) at the 60<sup>th</sup> minute.

#### *Batch Adsorption Experiment 8*

A 50 g mass each of the two limestone (A & B) sample of grain size 2000-6350  $\mu\text{m}$  were mixed with 100 mL of 1 mg/L NaF solution and the pH of the mixtures was 7.78 and 9.47 respectively. A plot of residual fluoride concentration with time (Fig. 4.12) for the two limestone type is shown.

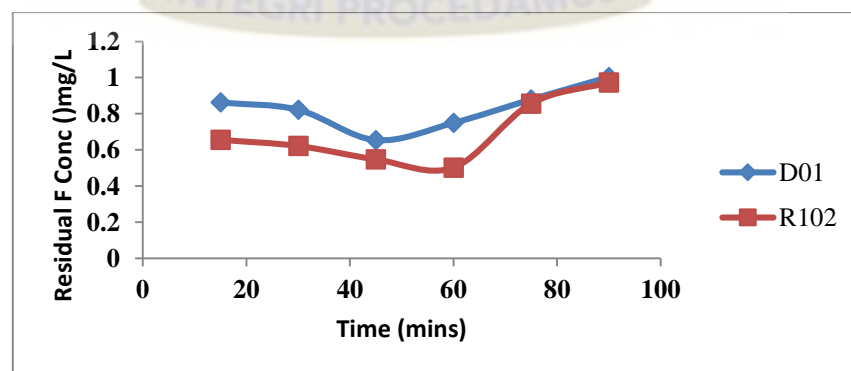


**Fig 4.12** Plot of Residual F<sup>-</sup> concentration against Time for 50 g mass (2000-6350  $\mu\text{m}$ ) samples in 1 mg/L NaF

Sample **A** recorded a maximum residual fluoride concentration of 0.5019 mg/L (54.26%) at the 60<sup>th</sup> minute of the 90 minute duration, while sample **B** gave a maximum residual fluoride concentration of 0.6541 mg/L (36.06%) at the 45<sup>th</sup> minute (Fig. 4.12).

#### *Batch Adsorption Experiment 9*

A plot of residual fluoride concentration with time (Fig. 4.13) for 100 g mass each of the two limestone (**A & B**) sample of grain size 2000-6350  $\mu\text{m}$  mixed with 100 mL of 1 mg/L NaF solution is shown. The pH of the mixtures was 7.80 and 9.50 respectively.

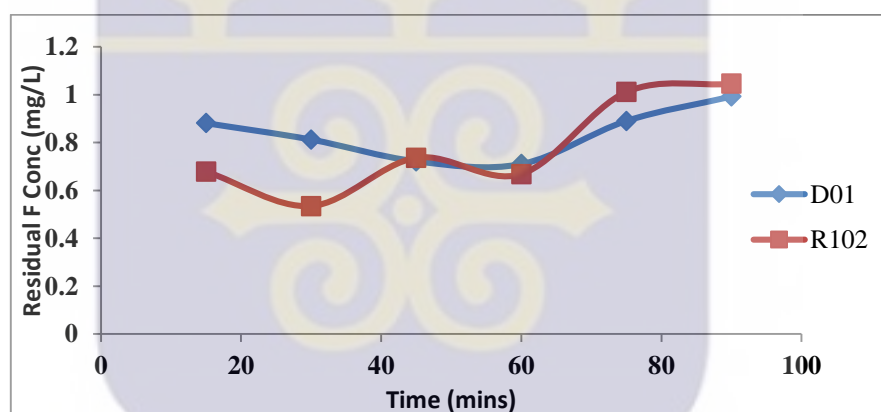


**Fig 4.13** Plot of Residual F<sup>-</sup> concentration against Time for 100 g mass (2000-6350  $\mu\text{m}$ ) samples in 1 mg/L NaF

Sample **A** recorded a reduction of fluoride at two instances. First fluoride reduction occurred at the 30<sup>th</sup> minute with concentration 0.5347 (51.27%) and another reduction at the 60<sup>th</sup> minute of concentration 0.6683 (39.10%). Sample **B** gave a maximum residual fluoride concentration of 0.7104 mg/L (30.56%) at the 60<sup>th</sup> minute (Fig. 4.13).

#### 4.4.3 Effect of Varying Residence Time on Residual Fluoride Adsorption in 5 mg/L Fluoride Solution

##### *Batch Adsorption Experiment 10*

A 10 g mass each of the two limestone (**A** & **B**) sample of grain size 500-1000  $\mu\text{m}$  were mixed with 100 mL of 5 mg/L NaF solution. The pH of the mixtures was 8.15 and 9.20 respectively. A plot of residual fluoride concentration with time (Fig. 4.14) for the two limestone type is shown.

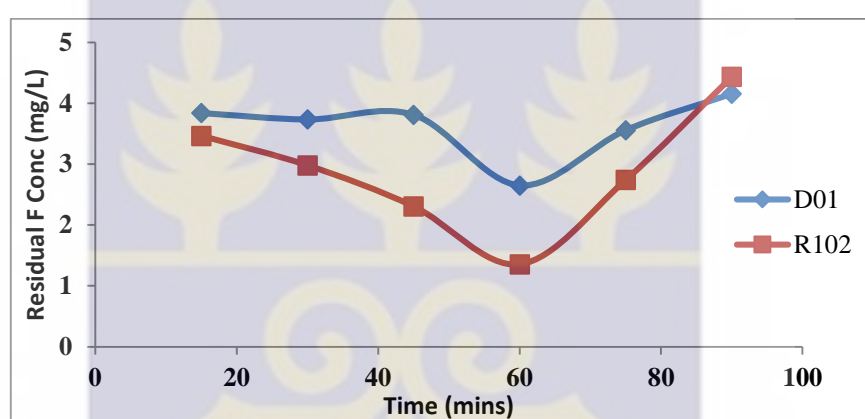


**Fig 4.14** Plot of Residual F<sup>-</sup> concentration against Time for 10 g mass (500-1000  $\mu\text{m}$ ) samples in 5 mg/L NaF

Both sample **A** & **B** attained equilibrium at the 60<sup>th</sup> minutes (Fig. 4.14) with recorded maximum residual fluoride concentration of 1.3547 mg/L (73.18%) and 2.6513 (46.50%) respectively.

##### *Batch Adsorption Experiment 11*

A plot of residual fluoride concentration with time (Fig. 4.15) for 50 g mass each of the two limestone (**A** & **B**) sample of grain size 500-1000  $\mu\text{m}$  mixed with 100 mL of 5 mg/L NaF solution. The pH of the mixtures was 8.32 and 9.47 respectively.

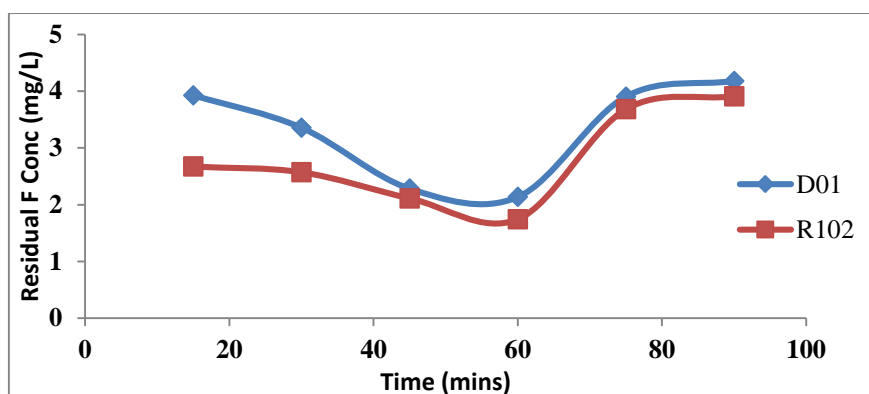


**Fig 4.15** Plot of Residual F<sup>-</sup> concentration against Time for 50 g mass (500-1000  $\mu$ m) samples in 5 mg/L NaF

Both sample **A & B** attained equilibrium at the 60<sup>th</sup> minutes with recorded maximum residual fluoride concentration of 1.7436 mg/L (65.48%) and 2.1373 (56.88%) respectively (Fig. 4.15). Similar work by Yadev et al, 2012, showed a similar trend where the percentage removal of fluoride by four adsorbents at different contact times showed an increase percentage of fluoride removal. However, it gradually approached an almost constant value, denoting attainment of equilibrium at 60, 90, 105 and 75 min for the four adsorbents.

#### *Batch Adsorption Experiment 12*

A 100 g mass each of the two limestone (**A & B**) sample of grain size 500-1000  $\mu$ m were mixed with 100 mL of 5 mg/L NaF solution. The pH of the mixtures was 8.40 and 9.58 respectively.



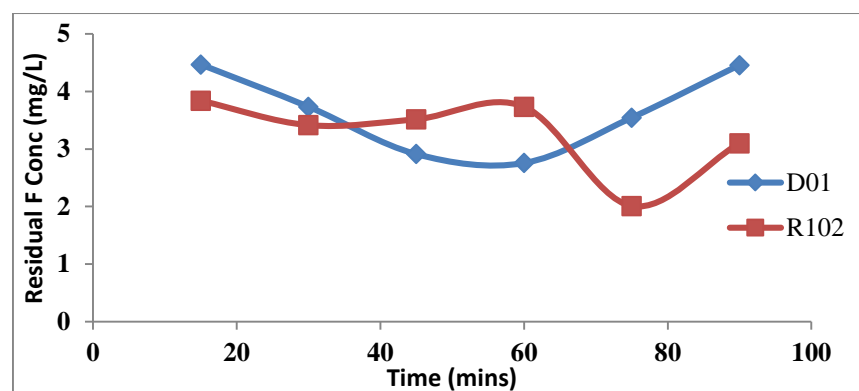


**Fig 4.16** Plot of Residual  $F^-$  concentration against Time for 100 g mass (500-1000  $\mu\text{m}$ ) samples in 5 mg/L NaF

A plot of residual fluoride concentration with time (Fig. 4.16), shows sample **A** recorded a maximum residual fluoride concentration of 2.0094 mg/L (60.21%) at the 75<sup>th</sup> minute of the 90-minute duration, while sample **B** gave a maximum residual fluoride concentration of 2.7571 mg/L (44.37%) at the 60<sup>th</sup> minute.

#### *Batch Adsorption Experiment 13*

A 10 g mass each of the two limestone (**A** & **B**) sample of grain size 1000-2000  $\mu\text{m}$  were mixed with 100 mL of 5 mg/L NaF solution. The pH of the mixtures was 8.38 and 9.53 respectively.

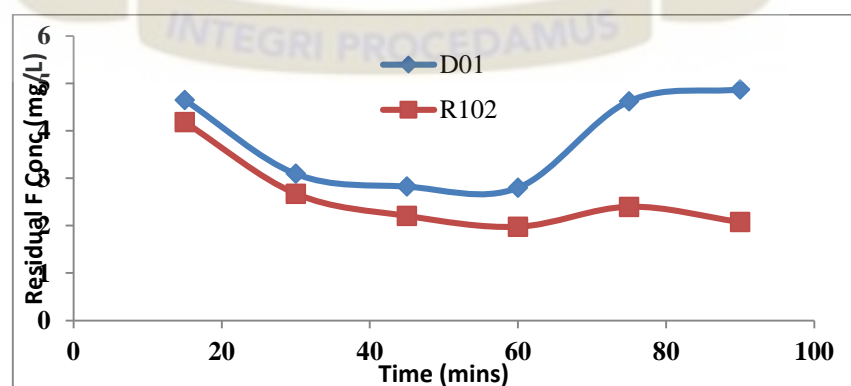


**Fig 4.17** Plot of Residual  $F^-$  concentration against Time for 10 g mass (1000-2000  $\mu\text{m}$ ) samples in 5 mg/L NaF

Both sample **A & B** attained equilibrium at the 60<sup>th</sup> minutes (Fig. 4.17) with recorded maximum residual fluoride concentration of 1.9748 mg/L (60.90%) and 2.8012 (43.48%) respectively.

#### *Batch Adsorption Experiment 14*

A 50 g mass each of the two limestone (**A & B**) sample of grain size 1000-2000  $\mu\text{m}$  were mixed with 100 mL of 5 mg/L NaF solution. The pH of the mixtures was 8.40 and 9.56 respectively.

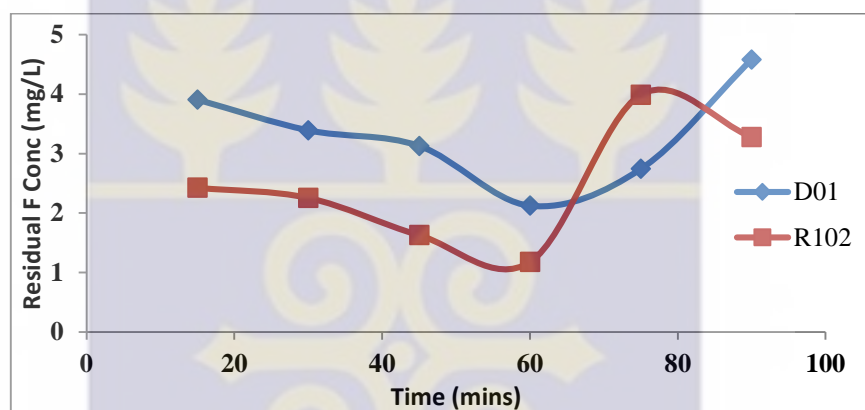


**Fig 4.18** Plot of Residual F<sup>-</sup> concentration against Time for 50 g mass (1000-2000  $\mu\text{m}$ ) samples in 5 mg/L NaF

A plot of residual fluoride concentration with time (figure 4.18), for both sample **A & B** attained equilibrium at the 60<sup>th</sup> minute with recorded maximum residual fluoride concentration of 1.1773 mg/L (76.69%) and 2.1237 (57.15%) respectively.

#### *Batch Adsorption Experiment 15*

A 100 g mass each of the two limestone (**A & B**) sample of grain size 1000-2000  $\mu\text{m}$  were mixed with 100 mL of 5 mg/L NaF solution. The pH of the mixtures was 8.40 and 9.60 respectively.

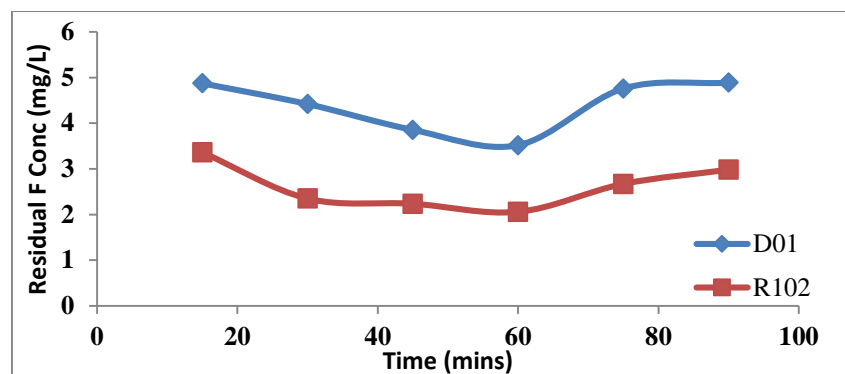


**Fig 4.19** Plot of Residual  $F^-$  concentration against Time for 100 g mass (1000-2000  $\mu\text{m}$ ) samples in 5 mg/L NaF

Both sample A & B attained equilibrium at the 60<sup>th</sup> minute (Fig. 4.19) with recorded maximum residual fluoride concentration of 2.0613 mg/L (59.19%) and 3.5165 (29.05%) respectively.

#### *Batch Adsorption Experiment 16*

A 10 g mass each of the two limestone (A & B) sample of grain size 2000-6350  $\mu\text{m}$  were mixed with 100 mL of 5 mg/L NaF solution. The pH of the mixtures was 8.39 and 9.60 respectively.

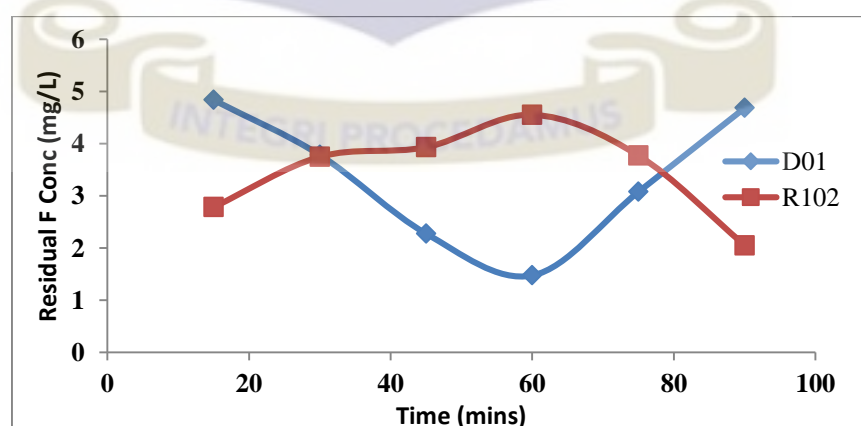


**Fig 4.20** Plot of Residual  $F^-$  concentration against Time for 10 g mass (2000-6350  $\mu\text{m}$ ) samples in 5 mg/L NaF

A plot of residual fluoride concentration with time (Fig. 4.20), for sample **A** shows an appreciable increase in residual fluoride concentration until the 60<sup>th</sup> minute where the concentration gradually reduced to a concentration of 2.0534 at the 90<sup>th</sup> minute. Equilibrium was not established in this experiment. Sample **B** gave a maximum residual fluoride concentration of 1.4776 mg/L (70.19%) at the 60<sup>th</sup> minute.

#### *Batch Adsorption Experiment 17*

A 50 g mass each of the two limestone (**A & B**) sample of grain size 2000-6350  $\mu\text{m}$  were mixed with 100 mL of 5 mg/L NaF solution. The pH of the mixtures was 8.37 and 9.54 respectively.

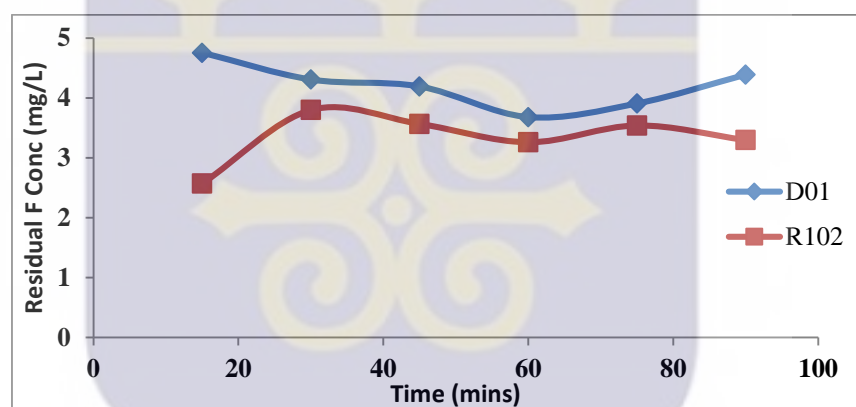


**Fig 4.21** Plot of Residual F<sup>-</sup> concentration against Time for 50 g mass (2000-6350  $\mu\text{m}$ ) samples in 5 mg/L NaF

Both sample **A & B** attained equilibrium at the 60<sup>th</sup> minute (Fig. 4.21) with recorded maximum residual fluoride concentration of 3.2614 mg/L (35.43%) and 3.6808 (25.73%) respectively.

*Batch Adsorption Experiment 18*

A 100 g mass each of the two limestone (**A** & **B**) sample of grain size 2000-6350  $\mu\text{m}$  were mixed with 100 mL of 5 mg/L NaF solution. The pH of the mixtures was 8.40 and 9.60 respectively.

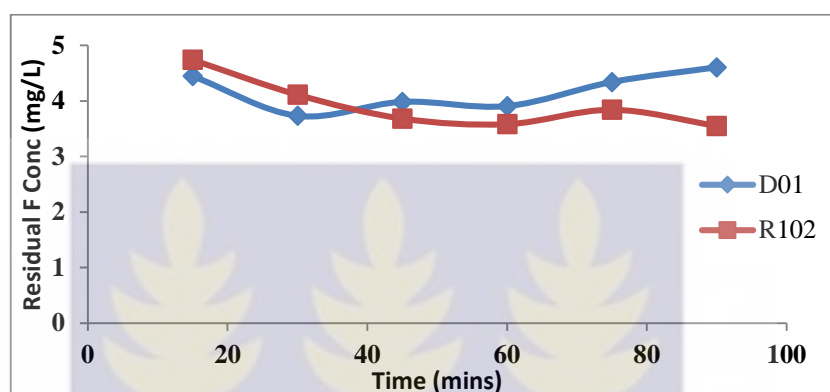


**Fig 4.22** Plot of Residual F<sup>-</sup> concentration against Time for 100 g mass (2000-6350  $\mu\text{m}$ ) samples in 5 mg/L NaF

A plot of residual fluoride concentration with time (Fig. 4.22), shows sample **A** gave a marginal decrease in fluoride concentration of 3.5814 (29.09%) at the 60<sup>th</sup> minute. Sample **B** attained equilibrium at the 30<sup>th</sup> minute with recorded maximum residual fluoride concentration of 3.7315 mg/L (24.71%).

#### 4.4.4 Effect of Varying Residence Time on Residual Fluoride Adsorption in 10 mg/L Fluoride Solution

*Batch Adsorption Experiment 19*

A 10 g mass each of the two limestone (**A** & **B**) sample of grain size 500-1000  $\mu\text{m}$  were mixed with 100 mL of 10 mg/L NaF solution. The pH of the mixtures was 8.32 and 9.44 respectively.

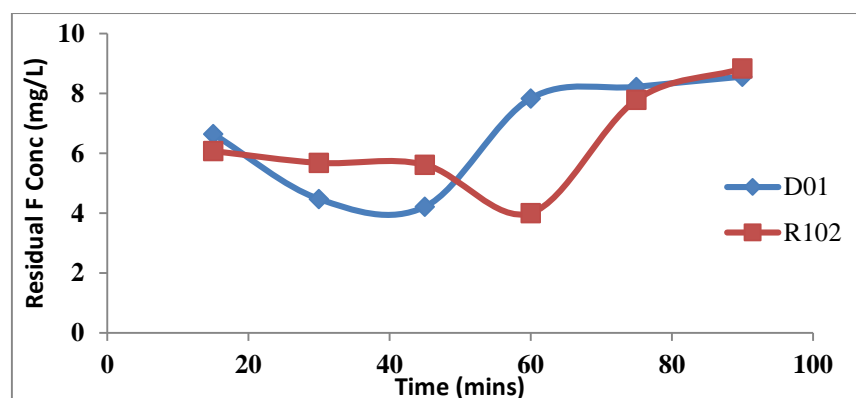


**Fig 4.23** Plot of Residual  $F^-$  concentration against Time for 10 g mass (500-1000  $\mu\text{m}$ ) samples in 10 mg/L NaF

A plot of residual fluoride concentration with time (Fig. 4.23), shows sample **A** recorded a maximum residual fluoride concentration of 4.0029 mg/L (60.65%) at the 60<sup>th</sup> minute of the 90 minute duration, while sample **B** gave a maximum residual fluoride concentration of 4.2127 mg/L (57.67%) at the 45<sup>th</sup> minute. The influence of contact time on the defluoridation capacity of powdered samples of *Citrus limonum* (lemon) leaf by Tomar et al., 2013, showed an increase in fluoride ion removal. Further increase in the contact time did not increase fluoride ion uptake due to sufficient deposition of fluoride ions on the available adsorption sites on the adsorbent materials.

#### *Batch Adsorption Experiment 20*

A 50 g mass each of the two limestone (**A** & **B**) sample of grain size 500-1000  $\mu\text{m}$  were mixed with 100 mL of 10 mg/L NaF solution. The pH of the mixtures was 8.36 and 9.51 respectively.



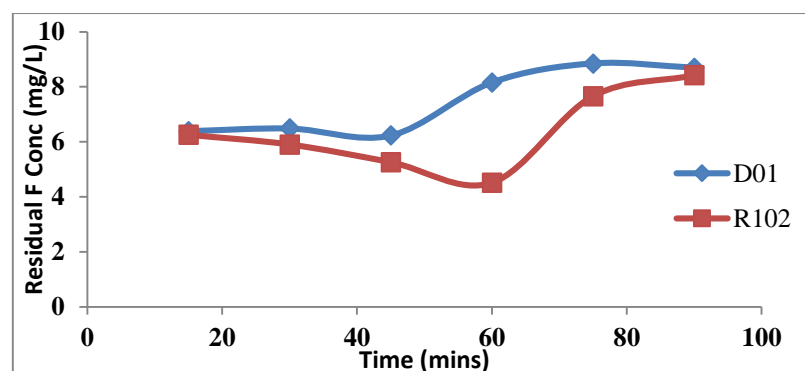


**Fig 4.24** Plot of Residual  $F^-$  concentration against Time for 50 g mass (500-1000  $\mu\text{m}$ ) samples in 10 mg/L NaF

A plot of residual fluoride concentration with time (Fig. 4.24), shows sample **A** recorded a maximum residual fluoride concentration of 4.5077 mg/L (55.69%) at the 60<sup>th</sup> minute of the 90 minute duration, while sample **B** gave a maximum residual fluoride concentration of 6.2341 mg/L (37.36%) at the 45<sup>th</sup> minute.

#### *Batch Adsorption Experiment 21*

A 100 g mass each of the two limestone (**A** & **B**) sample of grain size 500-1000  $\mu\text{m}$  were mixed with 100 mL of 10 mg/L NaF solution. The pH of the mixtures was 8.38 and 9.54 respectively.

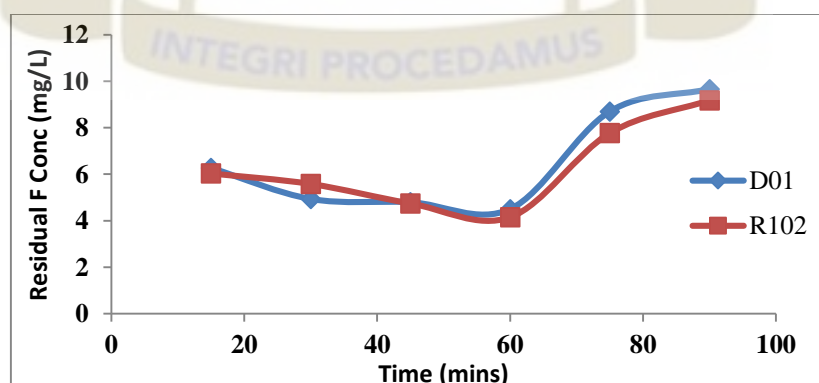


**Fig 4.25** Plot of Residual  $F^-$  concentration against Time for 100 g mass (500-1000  $\mu\text{m}$ ) samples in 10 mg/L NaF

Both sample **A & B** attained equilibrium at the 60<sup>th</sup> minutes (Fig. 4.25) with recorded maximum residual fluoride concentration of 4.1481 mg/L (59.22%) and 4.4943 (54.84%) respectively.

#### *Batch Adsorption Experiment 22*

A 10 g mass each of the two limestone (**A & B**) sample of grain size 1000-2000  $\mu\text{m}$  were mixed with 100 mL of 10 mg/L NaF solution. The pH of the mixtures was 8.27 and 9.47 respectively

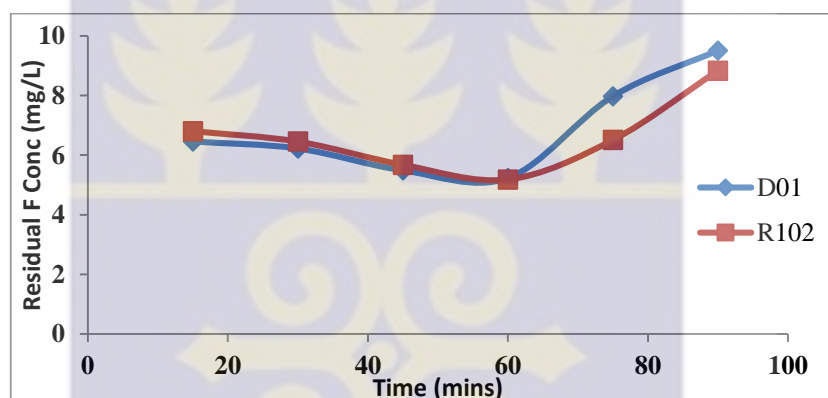


**Fig 4.26** Plot of Residual F<sup>-</sup> concentration against Time for 10 g mass (1000-2000  $\mu\text{m}$ ) samples in 10 mg/L NaF

A plot of residual fluoride concentration (Fig. 4.26), shows both sample **A & B** attained equilibrium at the 60<sup>th</sup> minutes with recorded maximum residual fluoride concentration of 5.1789 mg/L (49.09%) and 5.2282 (47.46%) respectively

#### *Batch Adsorption Experiment 23*

A 50 g mass each of the two limestone (**A & B**) sample of grain size 1000-2000  $\mu\text{m}$  were mixed with 100 mL of 10 mg/L NaF solution. The pH of the mixtures was 8.36 and 9.52 respectively.

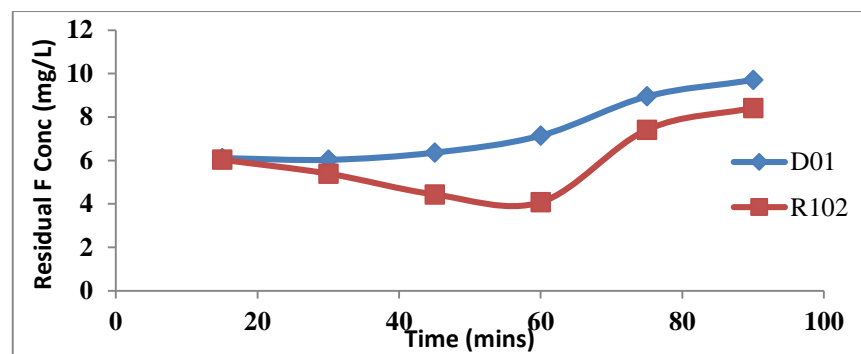


**Fig 4.27** Plot of Residual F<sup>-</sup> concentration against Time for 50 g mass (1000-2000  $\mu$ m) samples in 10 mg/L NaF

Sample **A** attained equilibrium at the 60<sup>th</sup> minute (Fig. 4.27) with recorded maximum residual fluoride concentration of 4.0857 mg/L (59.84%) and sample **B** recorded a marginal residual fluoride concentration of 6.036 (39.35%) at the 30<sup>th</sup> minute of the entire 90 minute duration.

#### *Batch Adsorption Experiment 24*

A 100 g mass each of the two limestone (**A** & **B**) sample of grain size 1000-2000  $\mu$ m mixed with 100 mL of 10 mg/L NaF solution. The pH of the mixtures was 8.40 and 9.58 respectively.

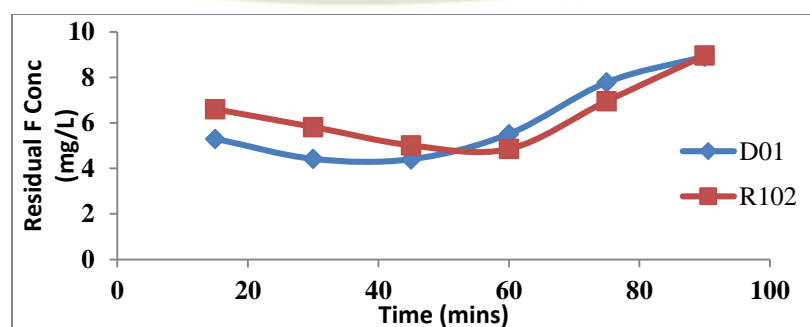


**Fig 4.28** Plot of Residual F<sup>-</sup> concentration against Time for 100 g mass (1000-2000  $\mu$ m) samples in 10 mg/L NaF

A plot of residual fluoride concentration with time (Fig. 4.28), shows sample **A** recorded a maximum residual fluoride concentration of 4.8541 mg/L (52.28%) at the 60<sup>th</sup> minute of the 90 minute duration, while sample **B** gave a maximum residual fluoride concentration of 4.4015 mg/L (55.77%) at the 45<sup>th</sup> minute. The variation of fluoride adsorbed with time is also investigated by Sujana *et al.*, (1997). It was observed that the amount of fluoride adsorbed increases with time as well as concentration. The amount of fluoride adsorbed per gram of sludge increased to attain a constant value after 2 hours.

#### *Batch Adsorption Experiment 25*

A 10 g mass each of the two limestone (**A** & **B**) sample of grain size 2000-6350  $\mu\text{m}$  mixed with 100 mL of 10 mg/L NaF solution. The pH of the mixtures was 8.38 and 9.55 respectively.

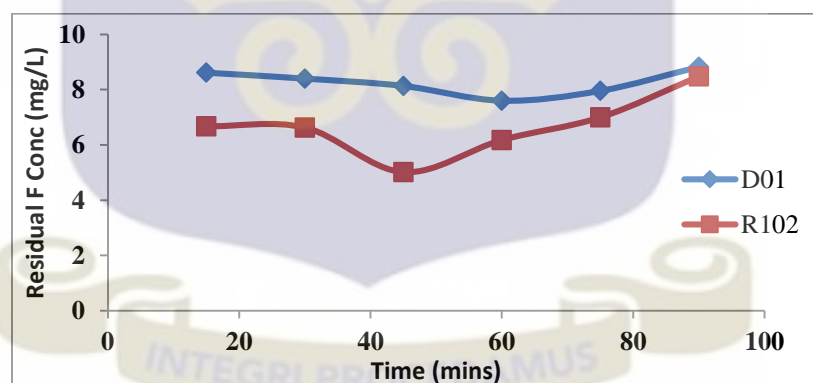


**Fig 4.29** Plot of Residual F<sup>-</sup> concentration against Time for 10 g mass (2000-6350  $\mu\text{m}$ ) samples in 10 mg/L NaF

A plot of residual fluoride concentration with time (Fig. 4.29), indicates sample **A** attained equilibrium at the 45<sup>th</sup> minute with recorded maximum residual fluoride concentration of 5.0143 mg/L (50.71%) and sample **B** recorded a marginal residual

fluoride concentration of 7.5978 (23.65%) at the 60<sup>th</sup> minute of the entire 90 minute duration.

#### *Batch Adsorption Experiment 26*

A 50 g mass each of the two limestone (**A** & **B**) sample of grain size 2000-6350  $\mu\text{m}$  mixed with 100 mL of 10 mg/L NaF solution. The pH of the mixtures was 8.38 and 9.58 respectively.

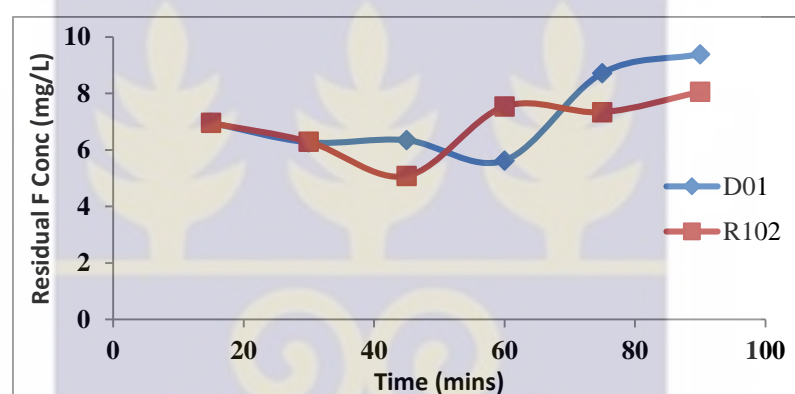


**Fig 4.30** Plot of Residual F<sup>-</sup> concentration against Time for 50 g mass (2000-6350  $\mu\text{m}$ ) samples in 10 mg/L NaF

A residual fluoride concentration with time (Fig. 4.30), shows sample **A** recorded a maximum residual fluoride concentration of 5.0797 mg/L (50.06%) at the 45<sup>th</sup> minute of the 90 minute duration, while sample **B** gave a maximum residual fluoride concentration of 5.6292 mg/L (43.44%) at the 60<sup>th</sup> minute.

#### *Batch Adsorption Experiment 27*

A 100 g mass each of the two limestone (**A** & **B**) sample of grain size 2000-6350  $\mu\text{m}$  mixed with 100 mL of 10 mg/L NaF solution. The pH of the mixtures was 8.40 and 9.60 respectively.

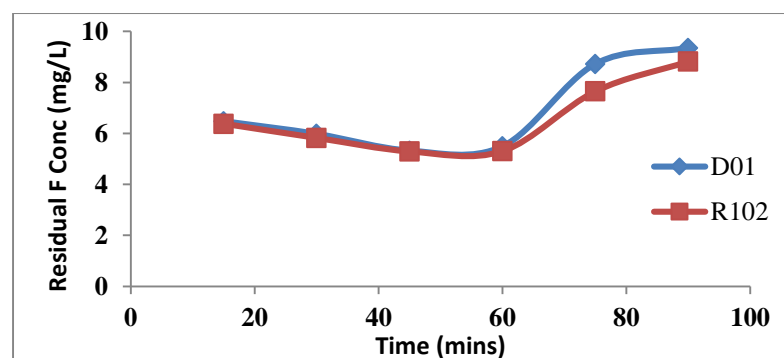


**Fig 4.31** Plot of Residual  $F^-$  concentration against Time for 100 g mass (2000-6350  $\mu m$ ) samples in 10 mg/L NaF

Both sample **A & B** attained equilibrium at the 45<sup>th</sup> minutes (Fig. 4.31) with recorded maximum residual fluoride concentration of 5.2904 mg/L (47.99%) and 5.3254 (46.49%) respectively. From the various results, maximum percentage adsorption of fluoride occurred at the 60<sup>th</sup> minutes for both limestone samples (**A & B**) and NaF concentrations (1, 5 and 10 mg/L). However, there were few that had their maximum percentage adsorption at the 45<sup>th</sup> minute.

#### 4.4.5 Effect of Grain Size on Percentage Mean Fluoride Adsorption

In this experiment, the grain sizes of the different samples are compared and their mean percentage fluoride adsorption compared.

##### 4.4.5.1 Effect of Grain Size on Percentage Mean Fluoride Adsorption for Sample (EKL-R<sub>102</sub>) in 1 mg/L NaF Solution

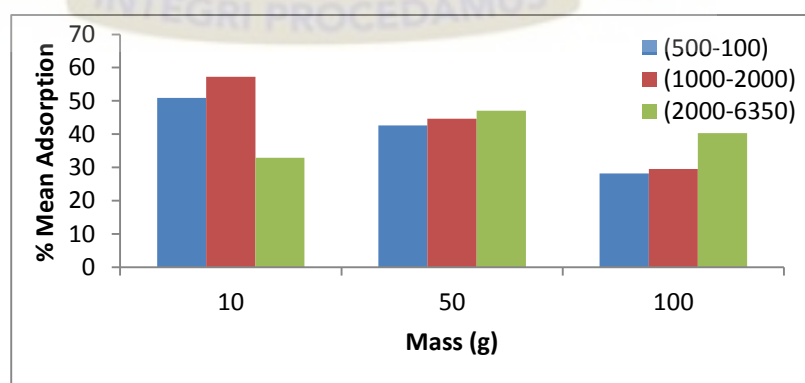


**Fig 4.32** Plot of % Mean Adsorption against Mass of sample EKL-R<sub>102</sub> in 1 mg/L



Grain size of 1000-2000  $\mu\text{m}$  recorded maximum mean fluoride adsorption of 57.27% for the 10 g of the sample while grain size (2000-6350  $\mu\text{m}$ ) recorded maximum mean % adsorption of 47.02% and 40.35% for the 50 and 100 g mass of the sample respectively (Fig. 4.32).

Although large surface area (for grain size 500-1000  $\mu\text{m}$ ) should account for high adsorbing site for high fluoride removal, the above result was due to the crumpling of the sample as a result of the cementing nature (sticky with liquid medium) of the sample. This results in a lesser exposure of the surface area of the sample to the fluoride ions for adsorption. Wang *et al.*, (2012), investigated the impact of the size of reactive materials on iron removal effectiveness. The result indicated that, iron removal efficiencies are strongly affected by particle size. Though larger sized particles removed enough of the 50 mg/L Fe (II) for the final concentration to fall below 0.3 mg/L, smaller sized particles had large surface area leading to higher surface capacity for higher adsorption and reaction (Stumm and Morgan, 1996).

Also, one would expect the smaller particle size to give a greater percentage removal because of the surface area, but as the particle size increases, the number of micro pores on the adsorbent also increases. The increase in micro pores increases the number of accessible sites, hence increase in percentage adsorption, (Eneida *et al.*, 2005)

#### 4.4.5.2 Effect of Grain Size on Percentage Mean Fluoride Adsorption for Sample (EKL-D01) in 1 mg/L NaF Solution

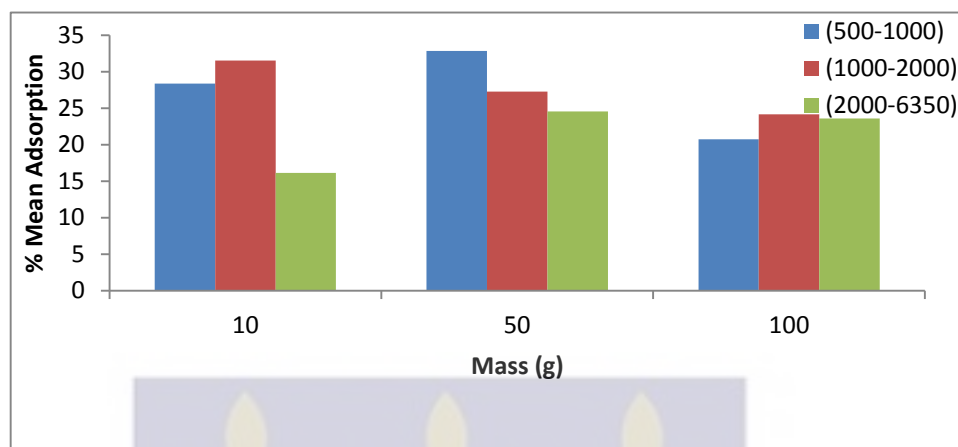


**Fig 4.33** Plot of % Mean Adsorption against Mass of sample EKL-D01 in 1 mg/L

Grain size of 1000-2000  $\mu\text{m}$  recorded maximum mean fluoride adsorption of 31.55% for the 10 g of the sample while grain size (500-1000  $\mu\text{m}$ ) and (1000-2000  $\mu\text{m}$ ) recorded maximum mean % adsorption of 32.86% and 24.15% for the 50 and 100 g mass of the sample respectively (Fig. 4.33).

Although large surface area (for grain size 500-1000  $\mu\text{m}$ ) should have accounted for high adsorbing site for high fluoride removal, the same reason given for sample EKL-R<sub>102</sub> (500-1000  $\mu\text{m}$ ) in section 4.4.5.1 is the same for this sample as well as its result.

Limestone sample EKL-R<sub>102</sub> recorded high fluoride adsorption in the stated grain sizes than sample EKL-D01. This was due to the pH of the limestone-fluoride mixture and the composition of the sample type. More alkaline medium provides more hydroxide ions ( $\text{OH}^-$ ) into the medium where there is a competition between the fluoride ions ( $\text{F}^-$ ) and the hydroxide ions ( $\text{OH}^-$ ) for adsorption sites, (Karthikeyan and Elango, 2007).

Also since sample EKL-D01 have some dolomite minerals in its composition  $[\text{CaMg}(\text{CO}_3)_2]$ , the reactivity of the  $\text{Mg}^{2+}$  with  $\text{F}^-$  is slow as compared to the reactivity of  $\text{Ca}^{2+}$  with  $\text{F}^-$  in solution. This is due to their ionic sizes where  $\text{Ca}^{2+}$  has a bigger ionic size than  $\text{Mg}^{2+}$ .

#### 4.4.5.3 Effect of Grain Size on Percentage Mean Fluoride Adsorption for Sample (EKL-R<sub>102</sub>) in 5 mg/L NaF Solution

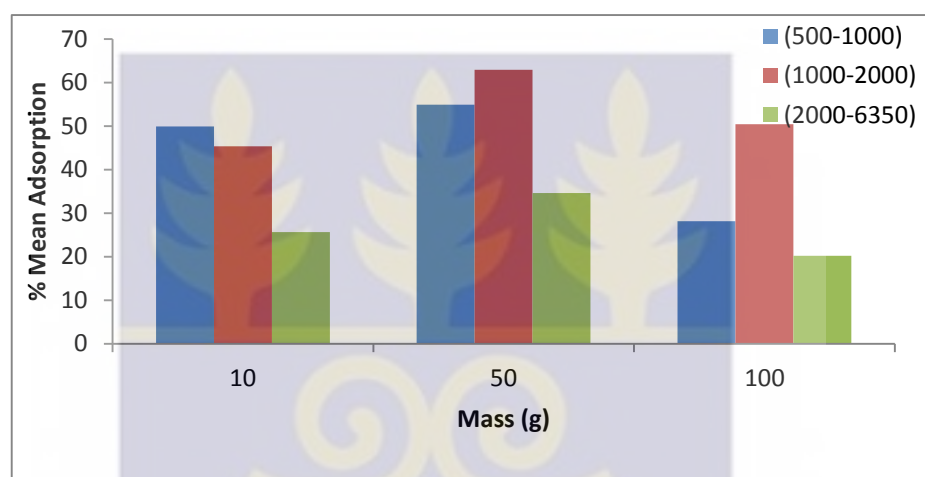


**Fig 4.34** Plot of % Mean Adsorption against Mass of sample EKL-R<sub>102</sub> in 5 mg/L

A plot of percentage mean adsorption against mass (Fig. 4.34), shows grain size (500-1000 μm) recorded maximum mean fluoride adsorption of 49.96% for the 10 g of the sample as against 45.37% and 25.64% for grain sizes 1000-2000 and 2000-6350 μm respectively. This result indicates that, the larger the surface area, the more the adsorption sites for fluoride adsorption. Surface area is closely associated with available adsorption sites and surface reactivity. The more the surface area, the more rapidly the adsorbate gets onto the adsorbent (Wang *et al.*, 2012).

The 50 g mass sample with grain size (1000-2000 μm) recorded maximum mean % adsorption of 62.96% while grain sizes 500-1000 and 2000-6350 μm gave mean % adsorption of 54.96% and 34.66% respectively.

In terms of the 100 g mass, 1000-2000  $\mu\text{m}$  grain size recorded the highest % fluoride adsorption of 50.44%. This is followed by grain size 500-1000 and 2000-6350  $\mu\text{m}$  with % fluoride adsorption of 28.19% and 20.22% respectively.

Grain size (2000-6350  $\mu\text{m}$ ) recorded the minimum percentage fluoride adsorption because, the bigger the grain size, the smaller the surface area for adsorption. The smaller grain size (500-1000  $\mu\text{m}$ ) should have recorded the highest percentage adsorption. This is because, it gives a large surface area as compared to the other grain sizes. But the result does not correlate with the stated assumption. The reason might be due to the stated reason given in Section 4.4.5.1.

#### 4.4.5.4 Effect of Grain Size on Percentage Mean Fluoride Adsorption for Sample (EKL-D01) in 5 mg/L NaF Solution

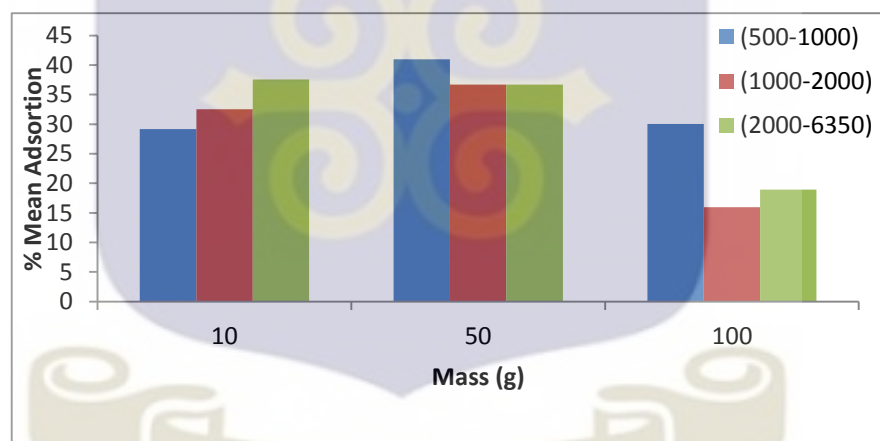


**Fig 4.35** Plot of % Mean Adsorption against Mass of sample EKL-D01 in 5 mg/L

Grain size of 500-1000  $\mu\text{m}$  for both 50 and 100 g mass recorded maximum mean fluoride adsorption of 40.95% and 30.02% respectively (Fig. 4.35). This result shows that, the smaller the grain size, the larger the surface area available for adsorption. An investigation into the use of laterite for the removal of fluoride from contaminated

drinking water indicates that, finer particles have a large surface area resulting in a higher adsorption rate (Sarkar *et al.*, 2006). Although, grain size (2000-6350  $\mu\text{m}$ ) recorded a mean % adsorption of 37.54% for 10 g mass category, this might be attributed to the crumpling of the smaller grain particles together as a result of the cementing nature of the limestone sample.

#### 4.4.5.5 Effect of Grain Size on Percentage Mean Fluoride Adsorption for Sample (EKL-R<sub>102</sub>) in 10 mg/L NaF Solution

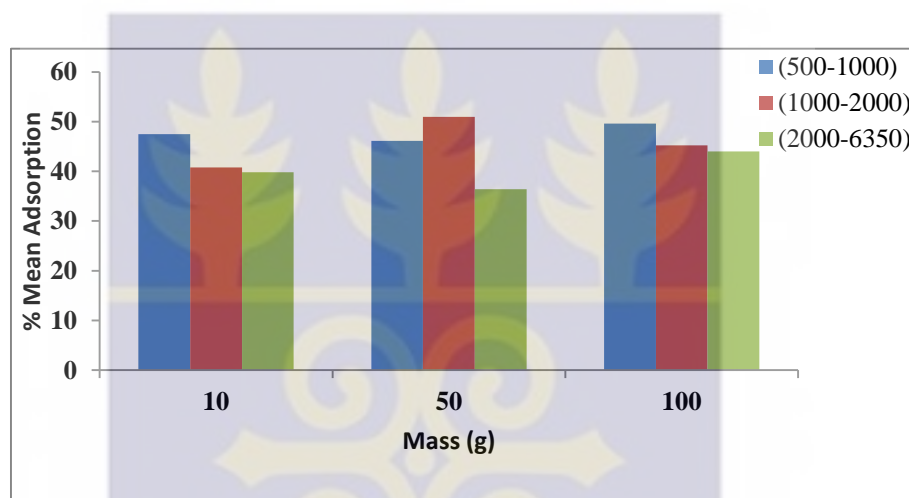


**Fig 4.36** Plot of % Mean Adsorption against Mass of sample EKL-R<sub>102</sub> in 10 mg/L

A plot of percentage mean adsorption against mass for sample EKL-R<sub>102</sub> (Fig. 4.36), shows grain size (500-1000  $\mu\text{m}$ ) for both 10 and 100 g mass recording maximum mean fluoride adsorption of 47.45% and 49.63% respectively. This result shows that, the smaller the grain size, the larger the surface area and hence the more the exposure of active sites of the adsorbent for fluoride adsorption (Wang *et al.*, 2012).

The 50 g mass category shows grain size (1000-2000  $\mu\text{m}$ ) to have recorded the highest mean % adsorption of 50.96%.

#### 4.4.5.6 Effect of Grain Size on Percentage Mean Fluoride Adsorption for Sample (EKL-D01) in 10 mg/L NaF Solution

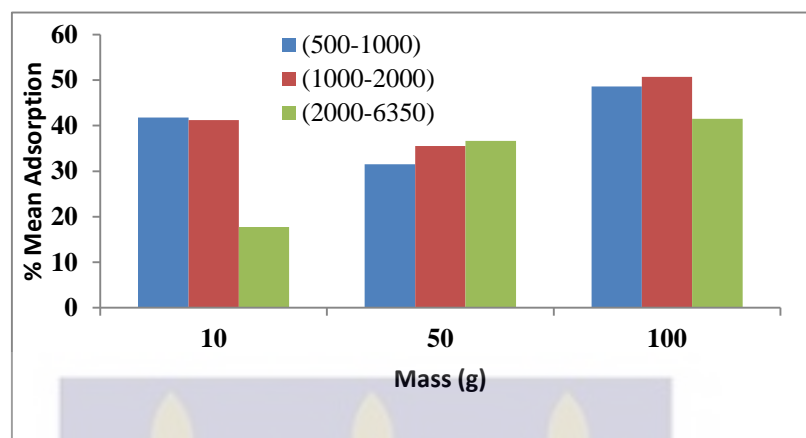


**Fig 4.37** Plot of % Mean Adsorption against Mass of sample EKL-D01 in 10 mg/L

Grain size (500-1000  $\mu\text{m}$ ) recorded maximum mean fluoride adsorption of 41.80% for the 10 g of the sample as against 41.25% and 17.73% for grain sizes 1000-2000 and 2000-6350  $\mu\text{m}$  respectively (Fig. 4.37). This result shows that, the larger the surface area, the more the adsorption sites for fluoride adsorption.

For 50 g mass category, grain size (2000-6350  $\mu\text{m}$ ) recorded the highest mean % adsorption of 36.67% while grain sizes 1000-2000 and 500-1000  $\mu\text{m}$  gave mean % adsorption of 35.51% and 31.50% respectively. This is as a result of the inability of the magnetic rod to stir the fine grained samples in the mixture uniformly. However much surface area is not exposed for grain sizes 500-1000  $\mu\text{m}$  for more adsorption sites to translate into high fluoride adsorption.

In terms of the 100 g mass category, grain size (1000-2000  $\mu\text{m}$ ) recorded the highest % fluoride adsorption of 50.68%. This is followed by grain size 500-1000 and 2000-



6350  $\mu\text{m}$  with % fluoride adsorption of 48.57% and 41.52% respectively. This can also be attributed to the reason stated for the 50 g mass category.

#### 4.4.6 Effect of Fluoride Concentration Variation on Percentage Mean Fluoride Adsorption

The Tables (Table 4.4, 4.5 and 4.6) give the % fluoride adsorption for the different concentrations (1, 5 and 10 mg/L).

**Table 4.4: Percentage fluoride adsorption for 1 mg/L fluoride solution**

EKL-R102					EKL-D01				
Concentration: 1 mgF <sup>-</sup> /L									
Mass (g)	Particle Size (μm)	Mean adsorption	%	Mean Adsorption capacity (mg/g)	Mas s (g)	Particle Size (μm)	Mean adsorption	%	Mean Adsorption capacity (mg/g)
10	500-1000	50.893		5.58	10	500-1000	28.39		2.90
10	1000-2000	57.272		6.28	10	1000-2000	31.55		3.23
10	2000-6350	32.942		3.61	10	2000-6350	16.14		1.65
50	500-1000	42.639		4.68	50	500-1000	32.86		3.36
50	1000-2000	44.657		4.90	50	1000-2000	27.28		2.79
50	2000-6350	47.022		5.16	50	2000-6350	24.56		2.51
100	500-1000	28.187		3.09	100	500-1000	20.76		2.12
100	1000-2000	29.538		3.24	100	1000-2000	24.15		2.47
100	2000-6350	40.347		4.43	100	2000-6350	23.60		2.41

The mean % fluoride adsorption for sample EKL-R102 and EKL-D01 in 1 mg/L solution (Table 4.4) is 41.50% and 25.48% respectively.

**Table 4.5: Percentage fluoride adsorption for 5 mg/L fluoride solution**

EKL-R102						EKL-D01					
Concentration: 5 mgF/L											
Mas s (g)	Particle (µm	Size	Mean adsorption	%	Mean Adsorption capacity (mg/g)	Mas s (g)	Particle (µm)	Size	Mean adsorption	%	Mean Adsorption capacity (mg/g)
10	500-1000		49.962		25.23	10	500-1000		29.17		14.46
10	1000-2000		45.369		22.91	10	1000-2000		32.54		16.12
10	2000-6350		25.640		12.95	10	2000-6350		37.54		18.60
50	500-1000		54.962		27.75	50	500-1000		40.95		20.29
50	1000-2000		62.958		31.79	50	1000-2000		36.69		18.18
50	2000-6350		34.663		17.50	50	2000-6350		14.58		7.22
100	500-1000		28.186		14.23	100	500-1000		30.02		14.87
100	1000-2000		50.442		25.47	100	1000-2000		15.93		7.89
100	2000-6350		20.219		10.21	100	2000-6350		18.95		9.39

The mean % fluoride adsorption for sample EKL-R102 and EKL-D01 in 5 mg/L solution (Table 4.5) is 41.38% and 28.48% respectively.

**Table 4.6: Percentage fluoride adsorption for 10 mg/L fluoride solution**

EKL-R102						EKL-D01					
Concentration: 10 mgF-/L											
Mas s (g)	Particle (µm)	Size	Mean adsorption	%	Mean Adsorption capacity (mg/g)	Mas s (g)	Particle (µm)	Size	Mean adsorption	%	Mean Adsorption capacity (mg/g)
10	500-1000		47.448		25.23	10	500-1000		41.80		14.46
10	1000-2000		40.764		22.91	10	1000-2000		41.25		16.12
10	2000-6350		39.793		12.95	10	2000-6350		17.73		18.60
50	500-1000		46.123		27.75	50	500-1000		31.50		20.29
50	1000-2000		50.962		31.79	50	1000-2000		35.51		18.18
50	2000-6350		36.429		17.50	50	2000-6350		36.67		7.22
100	500-1000		49.627		14.23	100	500-1000		48.57		14.87
100	1000-2000		45.229		25.47	100	1000-2000		50.68		7.89
100	2000-6350		43.981		10.21	100	2000-6350		41.52		9.39

The mean % fluoride adsorption for sample EKL-R<sub>102</sub> and EKL-D01 in 10 mg/L solution (Table 4.6) is 44.48% and 38.36% respectively.

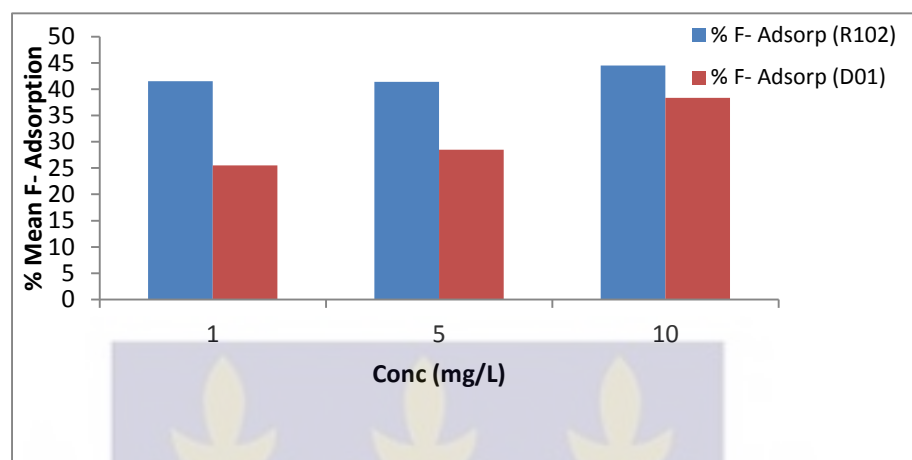


**Fig 4.38** Plot of percentage fluoride adsorption for varying fluoride concentrations

Percentage adsorption appreciated marginally for sample EKL-R<sub>102</sub> (41.50% - 44.48%) and sample EKL-D01 (25.48% - 38.36%) (Fig. 4.38) for concentrations 1, 5 and 10 mg/L respectively. It can be deduced that, the higher the concentration of the adsorbate, the higher the % fluoride adsorption (Kebede et al., 2014). This study confirmed the observation made by Malakootian et al. (2011) that initial fluoride concentration influences the amount of adsorbate adsorbed per unit mass of the adsorbent,  $q$  (mg/g).

#### **4.4.7 Effect of pH of Fluoride - Limestone Mixture on Percentage Mean Fluoride Adsorption**

The Table (4.7) gives the variation of pH of the different limestone samples and their corresponding % mean fluoride adsorption.

**Table 4.7: pH variation of F<sup>-</sup> - Limestone mixture with % mean fluoride adsorption**

Type of Limestone	Conc.of F <sup>-</sup> Solution	pH of F <sup>-</sup> - Limestone Mixture	% Mean Fluoride Adsorption
EKL-R <sub>1</sub> 02	1	7.65 - 7.80	41.50
EKL-R <sub>1</sub> 02	5	8.15 - 8.40	41.38
EKL-R <sub>1</sub> 02	10	8.27 - 8.40	44.48
EKL-D01	1	9.38 - 9.50	25.48
EKL-D01	5	9.20 - 9.60	28.48
EKL-D01	10	9.44 - 9.60	27.93

Sample EKL- R<sub>1</sub>02 gave a higher % mean fluoride adsorption of 42.45% for pH range (7.65 – 8.40) compared to 27.30 in EKL-D01 of pH range (9.38 – 9.60) (Table 4.7). This was due to the competition between the hydroxide (OH<sup>-</sup>) and fluoride ions (F<sup>-</sup>) for adsorption sites (Karthikeyan and Elango, 2007)

#### **4.4.8 Effect of Varying Adsorbent Dose on Percentage Mean Fluoride Adsorption**

The evaluation of the adsorbent dose on adsorption efficiency was carried out by varying the adsorbent mass (10, 50 and 100 g) for the same volume (100 mL) of fluoride solution for the two limestone samples. The results were found to be as follows.

**Table 4.8: Variation of Adsorbent Dose on % Fluoride Adsorption for Sample EKL-R102**

Mass (g)	% F <sup>-</sup> Adsorption (500 – 1000 $\mu$ m)	% F <sup>-</sup> Adsorption (1000 – 2000 $\mu$ m)	% F <sup>-</sup> Adsorption (2000 – 6350 $\mu$ m)	Conc. of soln. (mg/L)
10	50.89	57.27	32.94	1
50	42.64	44.66	47.02	
100	28.19	29.54	40.35	
10	49.96	45.37	25.64	5
50	54.96	62.96	34.66	
100	28.19	50.44	20.22	
10	47.45	40.76	39.79	10
50	46.12	50.96	36.43	
100	49.63	45.23	43.98	

Grain size 2000-6350  $\mu$ m (1 mg/L), grain size 1000-2000  $\mu$ m ( 5 mg/L) and all three grain sizes in the 10 mg/L solution gave an appreciable increase in % fluoride adsorption with respect to increasing adsorbent dose. On the other hand, grain sizes 500-1000  $\mu$ m (1 and 5 mg/L), grain size 1000-2000  $\mu$ m (1 mg/L) and grain size 2000-6350  $\mu$ m (5 mg/L) showing a decrease trend in % fluoride adsorption (Table 4.8).

**Table 4.9: Variation of Adsorbent Dose on % Fluoride Adsorption for Sample EKL-D01**

Mass (g)	% F <sup>-</sup> Adsorption (500 – 1000 $\mu$ m)	% F <sup>-</sup> Adsorption (1000 – 2000 $\mu$ m)	% F <sup>-</sup> Adsorption (2000 – 6350 $\mu$ m)	Conc. of soln. (mg/L)
10	28.38	31.55	16.14	1
50	32.86	27.28	24.56	
100	20.76	24.15	23.60	
10	29.17	32.54	37.54	5
50	40.95	36.69	14.58	
100	30.02	15.93	18.95	
10	41.80	41.25	17.73	10
50	31.50	35.51	36.67	
100	48.57	50.68	41.52	

All the three grain sizes of sample EKL-D01 in concentration 10 mg/L gave an appreciable increase in % fluoride adsorption with respect to increasing adsorbent dose. Grain sizes 500-1000  $\mu\text{m}$  (1 mg/L), grain size 1000-2000  $\mu\text{m}$  (1 and 5 mg/L) and grain size 2000-6350  $\mu\text{m}$  (5 mg/L) recorded a decrease in % fluoride adsorption with respect to increasing adsorbent dose (Table 4.9)

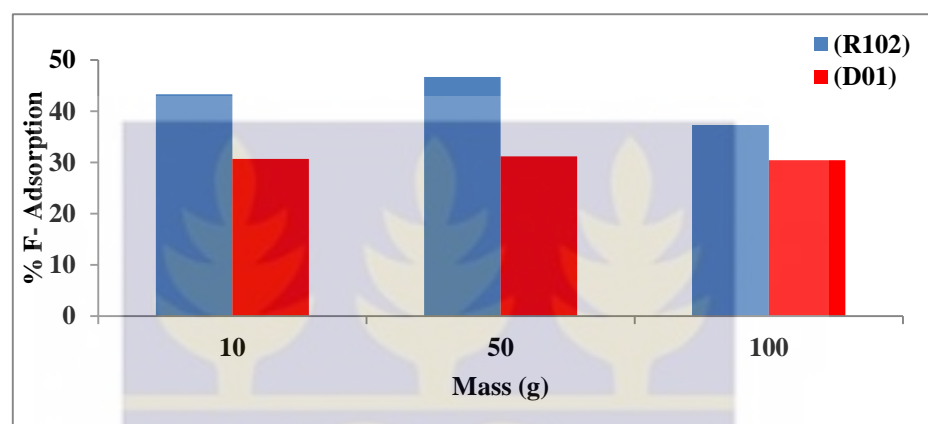


**Fig 4.39** Plot of % F<sup>-</sup> Adsorption against varying mass of samples

When a comparative analysis of the different masses was done when the concentration of the solution was kept constant, a mean percentage adsorption for sample EKL- R<sub>102</sub> for masses 10, 50 and 100 g gave 43.33%, 46.71% and 37.31% respectively. On the other hand, sample EKL-D01 recorded 30.68%, 31.18% and 30.46% for the mean percentage adsorption for masses 10, 50 and 100 respectively.

Although different masses in different concentrations gave different % adsorptions (Table 4.8 and 4.9), the mean % adsorption shows 50 g mass (EKL-R<sub>102</sub>) recording the highest mean % fluoride adsorption. This trend suggests that after a certain dose of the adsorbent, the maximum adsorption is attained and the amount of ions bound to the adsorbent and the amount of free ions remains constant (equilibrium) even with



further addition of the dose of the adsorbent. This is similar to studies reported by Abdel-Ghani *et al.*, (2007); Alok Mittal, (2006); and Murat Teker *et al.*, (1999).

The 100 g mass recorded the lowest mean % adsorption in the two samples. This may be attributed to the inability of more adsorbing sites to be exposed as the magnetic rod could not evenly stir the mixture uniformly. Also, the volume of the beaker in which the mixture (100 g) was contained could also have an influence on the exposure of more adsorbing sites of the adsorbents ((Dorris *et al.*, 2003)).

#### **4.5 Column Adsorption Experiment**

The results of the physico-chemical and anion analysis conducted on the ten (10) real water samples from the Bongo district is presented in Table 4.10

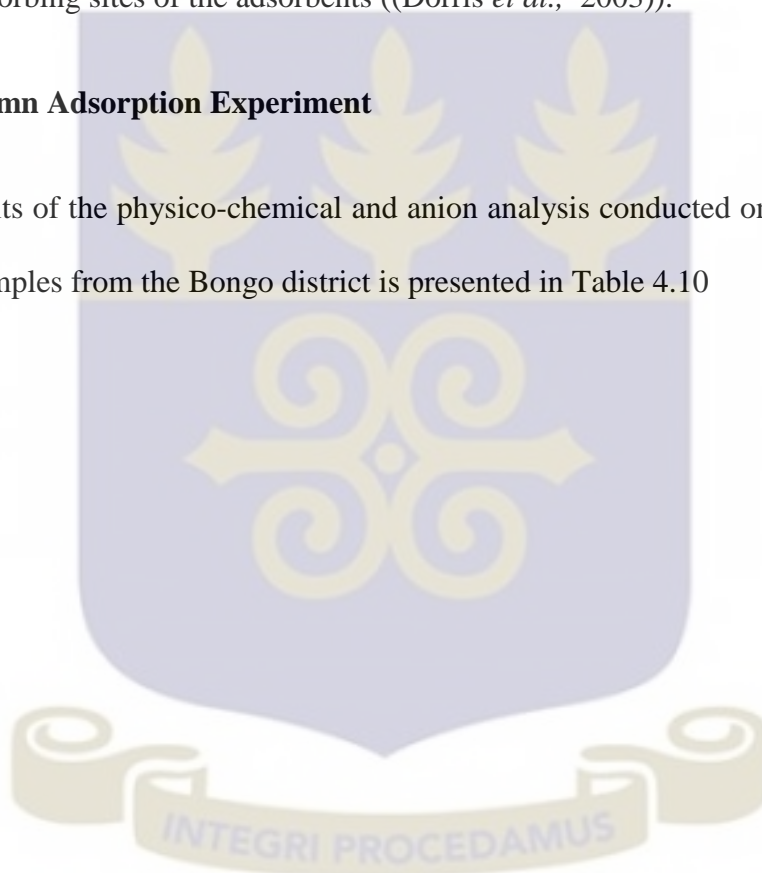


**Table 4.10 Physico-chemical and Anion Analysis of water samples from Bongo district**

	Sample ID										WHO (2003)
	A	B	C	D	E	F	G	H	I	J	
pH	8.25	7.74	7.95	8.34	8.24	8.17	8.08	8.30	8.22	8.06	6.5-8.5
EC	286	287	453	422	388	319	211	329	394	434	1400
Sal	0.1	0.1	0.2	0.2	0.2	0.1	0.1	0.1	0.2	0.2	-
TDS	127.0	126.0	200.0	186.0	170.9	140.2	92.0	144.4	173.0	189.6	1000
Turb	4	0	0	0	0	0	0	1	0	0	5
Col	0	0	0	0	0	0	0	0	0	0	15
F <sup>-</sup>	17.187	10.657	5.406	3.816	3.562	6.152	6.192	7.478	3.379	3.350	1.5
Cl <sup>-</sup>	11.430	14.017	39.573	20.273	27.452	8.872	2.166	18.934	24.114	23.407	250
NO <sub>3</sub> <sup>-</sup>	64.611	52.005	198.035	122.193	80.072	36.802	13.917	80.456	96.508	72.742	50
SO <sub>4</sub> <sup>2-</sup>	8.249	10.689	42.358	46.471	48.188	51.988	-	10.286	22.916	21.875	250
PO <sub>4</sub> <sup>3-</sup>	<0.001	0.024	<0.001	0.015	<0.001	0.014	<0.001	<0.001	<0.001	0.0084	3

[A = BAB1, B = BAB2, C = BNB3, D = BNB4, E = BNB5, F = BNB6, G = BNB7, H = BNN8, I = BZB9, J = BAB10]

#### 4.5.1 Anion Analysis from Column Adsorption Experiment

Based on the usage of the boreholes in the communities, Samples BNB6 and BNN8 were selected for the Column Adsorption experiment. Although, Samples BAB1 and BAB2 recorded the highest fluoride concentration, they are not used for this study because, they are not been used by the communities and are referred to as capped boreholes.

The water samples were run over three mini-column beds of height 20, 30 and 40 cm loaded with limestone samples EKL-R<sub>102</sub>. Aliquots were taken from each set-up at every 15-minutes interval for the 90-minutes duration. Fluoride and other anions were determined with the ICS-90 Ion Chromatographic System (APPENDIX H3). A plot of residual fluoride concentration with time is shown (Fig. 4.40 and 4.41).

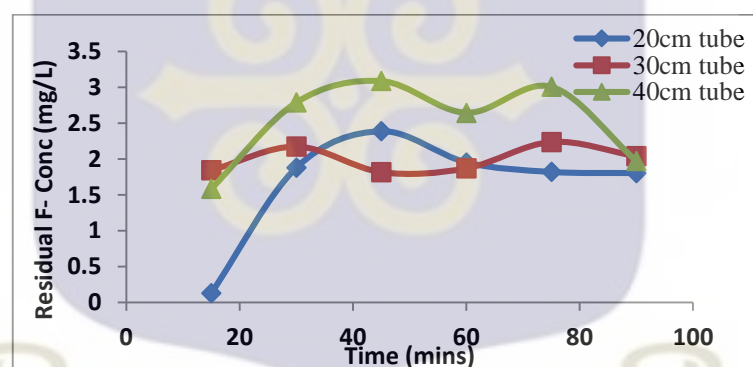


**Fig 4.40** Plot of Residual F<sup>-</sup> Concentration against Time for water sample BNB6

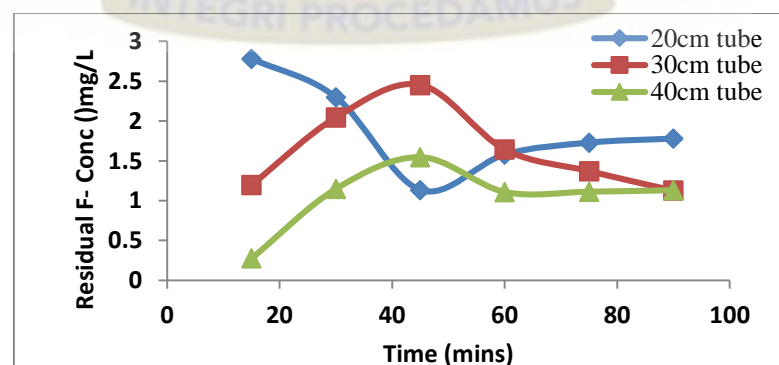


**Fig 4.41** Plot of Residual F<sup>-</sup> Concentration against Time for water sample BNN8

The adsorbent in mini-column bed (433.939 g) with height 40 cm gave a maximum mean percentage adsorption of approximately 86% as compared to 78% and 74% for bed heights 30 and 20 cm respectively.

The high adsorption was due to the presence of more adsorption sites present for the fluoride ions (adsorbate) to get attached. The three set-ups were able to reduce the fluoride content below WHO recommended level of 1.5 mg/L.

The reduction occurred at different times in each set-up. The 20 cm mini-column bed attained equilibrium with a maximum residual fluoride reduction of 1.13 at the 45<sup>th</sup> minute (Fig 4.41) after which the concentration begins to appreciate due to saturation of the adsorption sites. The mean percentage adsorption gave approximately 75%. In the 30 cm mini-column bed, equilibrium is attained at the 90<sup>th</sup> minutes that gave residual fluoride concentration of 1.13 mg/L. Though the reaction did not give a clear uniform path, it rises and falls at different times but the maximum reduction occurred at the 90<sup>th</sup> minutes.

One of the three set-ups (20 cm height mini-column bed) was able to reduce fluoride concentration in the water sample (BNB6) from 6.1519 mg/L to 0.13 mg/L within the first fifteen minutes (Fig. 4.39). The 30 and 40 cm column heights recorded 1.84 and 1.59 mg/L residual fluoride concentrations also at the 15<sup>th</sup> minute of the 90 minutes duration.

Comparing the efficiency of the adsorbent in each set-up for the two water sample defluoridation processes, average percentage fluoride adsorption that occurred in water sample BNN8 was approximately 80% as compared to 67% in BNB6. Despite

the same adsorbent been used in the two processes, the variation might be due to the concentrations of the co-existing anions present in the water samples.

**Table 4.11 Summary of the effect of co-existing anions in the water samples before and after the defluoridation process.**

Parameters	BNB6			BNN8		
	Initial	Final	% Adsorbed	Initial	Final	% Adsorbed
F <sup>-</sup>	6.152	2.058	66.55	7.478	1.526	79.60
Cl <sup>-</sup>	8.872	7.519	15.25	18.934	16.166	14.62
SO <sub>4</sub> <sup>2-</sup>	51.988	15.152	70.85	10.286	8.247	19.83
NO <sub>3</sub> <sup>-</sup>	36.802	27.959	24.03	80.456	33.10	58.85
PO <sub>4</sub> <sup>3-</sup>	0.014	< 0.001	-	< 0.001	< 0.001	-

Initial concentrations of Cl<sup>-</sup> and NO<sub>3</sub><sup>-</sup> in BNN8 are higher than in sample BNB6 (Table 4.12), while initial concentrations of SO<sub>4</sub><sup>2-</sup> and PO<sub>4</sub><sup>3-</sup> are much higher in sample BNB6 than BNN8. The effect of these anions on fluoride adsorption are in the order PO<sub>4</sub><sup>3-</sup> > SO<sub>4</sub><sup>2-</sup> > Cl<sup>-</sup> (Nabizadeh *et al.*, 2015)

The percentage of sulphate ion adsorbed (19.83%) onto the adsorbent in water sample BNN8 was lower compared to the percentage of sulphate ion adsorbed (70.85%) in sample BNB6. The greater the sulphate ion adsorbed onto the adsorbent, the lower the removal of fluoride from the water sample (Nabizadeh *et al.*, 2015).

The findings of the current study are consistent with those of Shao-Xiang *et al.*, (2009) who examined the effects of coexisting ions on fluoride removal by manganese oxide-coated alumina. From his study, NO<sub>3</sub><sup>-</sup> and Cl<sup>-</sup> showed negligible

effect on the removal of fluoride. However, other common coexisting ions affected fluoride removal in the order of  $\text{PO}_4^{3-} > \text{SO}_4^{2-}$ .

Some anions could enhance columbic repulsion forces and compete with fluoride for the active sites, readily decreasing the adsorption (Wambu et al., 2012). Generally, multivalent anions are absorbed more readily than monovalent anions. The impact of major anions on fluoride adsorption followed the order of  $\text{CO}_3^{2-} > \text{PO}_4^{3-} > \text{SO}_4^{2-} > \text{Cl}^-$  (Onyango *et al.*, 2004).

The results of this study indicate that sulphate is the greatest competitor for fluoride followed by nitrate and chloride. Similar phenomenon has been observed in the case of fluoride removal by nano-magnesia (Onyango et al., 2004). The adsorption mechanism of the anions onto adsorbents is significantly dependent on the physico-chemical properties of anions and their interaction with the adsorbent surface. Properties of anions such as the solubility, ionic radius, hydration energy and bulk diffusion coefficient are crucial for the selective adsorption of anions (Onyango *et al.*, 2004).

Johnston and Heijnen, (2002), in their study corroborated that, competition of ions adsorbing onto the active sites of the adsorbents are associated with the size of the ion, surface charges on the adsorbent which become more negative at high pH, and differential pore development on the heterogeneous adsorbent.



## CHAPTER FIVE

### CONCLUSION AND RECOMMENDATIONS

#### 5.1 CONCLUSION

##### 5.1.1 Mineralogy

Phase identification of the crystal nature of the limestone samples achieved using XRD revealed that the limestone samples from Oterkpolu were dominated by Calcite minerals, with some a few amount of Dolomite minerals [Calcite – 95%, Silicon oxide –5% for sample EKL-R<sub>1</sub>02 and Calcite – 68%, Dolomite – 22%, Silicon oxide – 10% for sample EKL-D01]. Petrographic Thin Section was used to identify the percentage (%) mineral composition of the limestone samples. Based on the results obtained, the limestone samples with the following compositions were selected for the study: EKL-R<sub>1</sub>02 gave Calcite – 96%, Quartz – 4% whiles EKL-D01 also gave Calcite – 85%, Quartz – 15%.

The Petrographic Thin Section also revealed that some of the samples may have undergone a little deformation or metamorphism, evidenced by fractures, veins and crystalline quartz in the micrograph of the Petrographic Thin Section slides.

During sample collection at the Oterkpolu limestone deposit site, the reaction between hydrochloric acid (a mineral acid) and the limestone sample was used to aid identification of the calcium carbonate (calcite). Limestone samples that gave a fizzing reaction on reaction with mineral acid [10% v/v HCl] were selected for the study because that indicates the limestone sample is made up of calcium carbonate (calcite).

### 5.1.2 Radiological Safety

Assessment of naturally occurring radionuclides was carried out on the limestone samples to be used for the defluoridation process to evaluate the hazards these may have on the defluoridated water to be used by the public. The Activity Concentration of the samples were measured using High Purity Germanium (HPGe) based gamma-ray spectrometer. The mean activity concentrations for  $^{238}\text{U}$ ,  $^{232}\text{Th}$  and  $^{40}\text{K}$  were found to be  $2.0 \pm 1.5$ ,  $1.7 \pm 1$  and  $21.9 \pm 13.4$  Bq/kg respectively for eight (8) limestone samples from Oterkpolu.

The Annual Effective Dose (AED) represents the stochastic health risk to the whole body when the sum of each organ or tissue is being irradiated. This was also found to be 0.13 mSv/yr. The recommended value by UNSCEAR, (2000) is 0.40 mSv/yr. Since the estimated Annual Effective Dose calculated is lower than the recommended value, there seems to be no potential radiological health hazard associated with Oterkpolu limestone to be used in the water defluoridation process.

### 5.1.3 Particle Size - % Adsorption

Limestone samples were divided into three groups of grain sizes. These are 500-1000, 1000-2000 and 2000-6350  $\mu\text{m}$ . This was done to determine the rate of adsorption of fluoride onto the different adsorbent surfaces since the nature of sample (particle size) determines the surface area available for the fluoride ions to adhere to.

The mean percentage fluoride adsorption (for the first 60<sup>th</sup> minute) for sample EKL-R<sub>102</sub> for concentration of 1, 5 and 10 mg/L for grain sizes 500-1000  $\mu\text{m}$ , 1000-2000  $\mu\text{m}$  and 2000-6350  $\mu\text{m}$  were 44.22%, 47.63% and 35.67% respectively. Sample EKL-D01 for the same concentrations and grain sizes were 33.77%, 32.84% and 25.70%

respectively. From the results, the optimum grain size that gave an optimum percentage fluoride adsorption was 1000-2000  $\mu\text{m}$ .

#### **5.1.4 Resident Time - % Absorption**

The resident time for the adsorption process was to determine the time equilibrium was established. The equilibrium time determines when maximum fluoride was removed from the solution by the adsorbent. After this time, fluoride ions are again released into the medium to increase the concentration.

The optimum resident time suitable for maximum fluoride removal was within the first 60<sup>th</sup> minute although a few samples gave a resident time of 45 minutes,

#### **5.1.5 Adsorbent Dose - % Adsorption**

The mass of the adsorbent dose determines the adsorption rate as this factor determines the number of active sites present for adsorption.

From the study, the mean percentage adsorption for sample EKL-R<sub>102</sub> for mass 10, 50 and 100 g (keeping concentration of solution constant) were 43.33%, 46.71% and 37.31% respectively. On the other hand, when grain size was kept constant, the mean percentage adsorption for the same sample gave 43.34% 46.71 and 37.31 respectively.

For sample EKL-D<sub>01</sub>, when concentration was kept constant, the mean percentage adsorption for mass 10, 50 and 100 g was 30.68%, 31.18% and 30.46% respectively.

When grain size was kept constant, the mean percentage fluoride adsorption gave 30.67%, 31.33 and 30.41% for 10, 50 and 100 g adsorbent dose.

From the results obtained, the 50 gram mass recorded the highest mean percentage adsorption.

#### **5.1.6 Fluoride Concentration - % Adsorption**

Fluoride concentrations were varied (1, 5 and 10 mg/L) in this study to cater for circumstances where the fluoride concentrations in affected communities are below the minimum WHO level of 1.5 mg/L and extreme situations where the concentration is up to 10 mg/L.

From the study, increasing the concentration of the solution from 1-10 mg/L recorded a marginal increase in the mean percentage adsorption for the two adsorbents. Thus, sample EKL-R<sub>1</sub>02 increased from 41.50% to 44.48% while sample EKL-D01 increased from 25.48% - 38.36%.

#### **5.1.7 pH - % Adsorption of Mixture (Limestone - Fluoride solution)**

The pH of a medium is important in predicting the efficiency of adsorption since there is a competition among hydrogen ions ( $H^+$ ), hydroxide ions ( $OH^-$ ) and fluoride ions ( $F^-$ ) onto the adsorbent surface.

The pH range for sample EKL-R<sub>1</sub>02 and EKL-D01 were found to be 7.65-8.40 and 9.20-9.60 respectively. Sample EKL-R<sub>1</sub>02 recorded a mean percentage adsorption of 42.45 as against 27.30 for sample EKL-D01.

From the results, it can be deduced that, media with low pH value enhances more adsorption sites for fluoride ions to adsorb onto the adsorption sites of the adsorbent since the positively charged adsorbent attracts fluoride ions electrostatically than in high pH media where  $OH^-$  compete with the fluoride ions leading to a lower defluoridation.

### 5.1.8 Column Adsorption

The developed defluoridation technique was used on real water samples from affected communities in northern Ghana to test the efficiency and efficacy of the adsorbent in a natural situation.

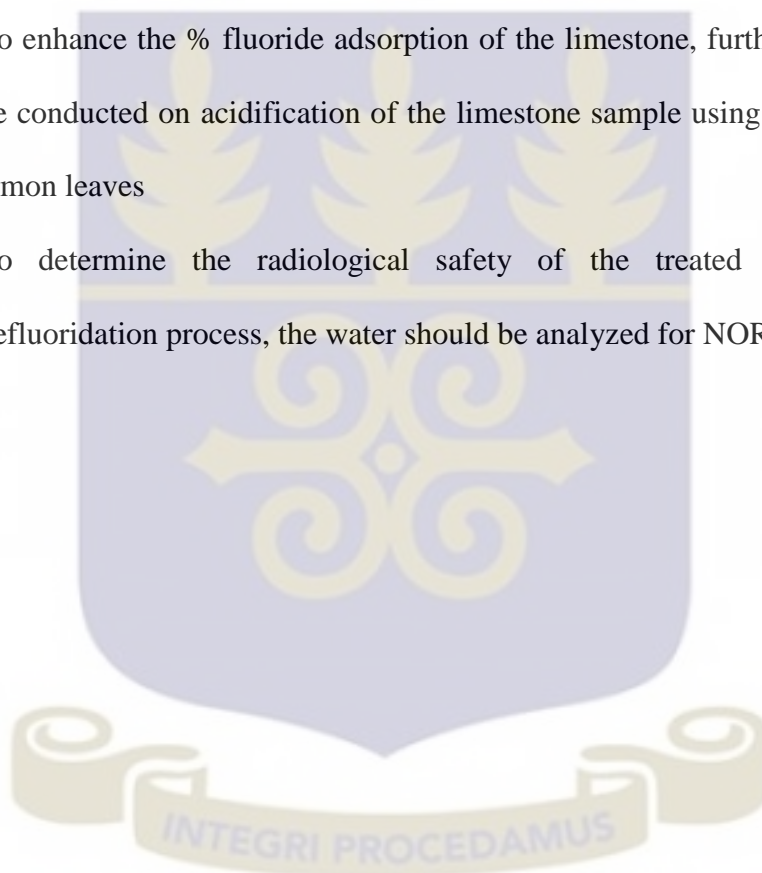
Water samples were taken from the Bongo district of the upper east region of Ghana. The district was chosen based on the high reported incidence of fluorosis as a result of high fluoride concentrations in their ground waters. Groundwater from ten (10) communities in the Bongo district was collected.

Two samples (BNB6 and BNN8) recorded 6.2 and 7.5 mg/L fluoride concentrations. The pHs of the samples before the defluoridation process were 8.17 and 8.30 respectively. After the defluoridation process, fluoride concentrations in the two water samples were reduced to 2.0 and 1.5 mg/L respectively constituting 67% and 80% mean percentage fluoride reduction.

Three mini-column glass beds of heights 20, 30 and 40 cm were loaded with limestone sample EKL-R<sub>102</sub> of masses (251.20, 376.80, 502.40 g) respectively. Running the water samples on the column beds, aliquots of the filtrate solution were taken at 15 minutes intervals for duration of 90 minutes. Maximum fluoride reduction occurred between the first 45 minutes. Column bed with height 40 cm recorded maximum percentage fluoride reduction of 86% for water sample BNN8 whiles column bed of height 20 cm recorded a percentage fluoride adsorption of 73% for water sample BNB6.

## 5.2 RECOMMENDATIONS

1. As a result of the unavailability of facilities and the limited time for the study, chemical analysis on the adsorbent was not carried out. I recommend subsequent studies should incorporate the chemical analysis of the adsorbent to make better inference.
2. Other studies can also assess the effectiveness of the other limestone sites in Ghana.
3. To enhance the % fluoride adsorption of the limestone, further studies should be conducted on acidification of the limestone sample using Citric Acid from lemon leaves
4. To determine the radiological safety of the treated water after the defluoridation process, the water should be analyzed for NORMs again.





## REFERENCES

- Abdelgawad**, A.M.; Watanabe, K.; Takeuchi, S.; Mizuno, T. (2009). The origin of fluoride-rich groundwater in Mizunami area, Japan—Mineralogy and geochemistry implications. *Eng. Geol.* 108, 76–85.
- Abdel-Ghani**, N.T.M. Hefray, G.A.F. EL-Chaghaby (2007). Removal of Lead from aqueous solution using low cost abundantly available adsorbent. *Int. J. Environ. Sci. Tech.* 4(1): 67-73
- Abe**, I., Iwasaki, S., Tokimoto, T., Kawasaki, N., Nakamura, T. and Tanada, S. (2004) Adsorption of fluoride ions onto carbonaceous materials, *J. Colloid Interface Sci.* 275: 35–39.
- Abugri** D. A and Pelig-Ba K.B. (2011). ‘Assessment of Fluoride in tropical surface soils used for crop cultivation. *African Journal of Environmental Science and Technology* 5(9): 653-660
- Afenya**, P. M. (1982). “Ghana’s mineral resources for small-scale mining industries”. In: JM Neilson (editor) Strategies for small-scale mining and mineral industries. AGID Rep. 8:24-28
- Agalga**, R. (2012). Evaluation of the concentration of naturally occurring radioactive materials in the Tono irrigation dam and associated radiological hazards. M.Phil Thesis, Radiation Protection, University of Ghana, School of Nuclear and Allied Sciences, Kwabenya.
- Ahamad**, K.U., Jawed, M., (2012). Breakthrough studies with mono-and binary-metal ion systems comprising of Fe (II) and As (III) using community prepared wooden charcoal packed columns. *Desalination* 285, 345-351
- Alok Mital** (2006). Removal of the dye, Amaranth from waste water using hen feathers as potential adsorbent. *Electron. J. Environment. Agric, Food Chem.* 5(2): 1296-1305

- Amor**, Z. Bariou, B. Mameri, N. Toky, M. Nicolas, S. and Elmidaoui, S. (2001). Fluoride removal from brackish water by electrodialysis, *Desalination* 133: 215–223.
- Anim-Gyampo**, M., Zango, M. S., & Apori, N. (2012). The Origin of Fluoride in Groundwaters of Paleozoic Sedimentary Formations of Ghana- A preliminary Study in Gushiegu District. *Research Journal of Environmental and Earth Science*, 4(5): 546-552.
- Anongura**, R. S., Louw, A. J., & Chikte, U. M. E. (2003). Dental fluorosis in a district of Ghana, West Africa. *J. Dental Res.*, 83(Special Issue B): 27 (SA Division IADR).
- Anongura**, R. S. (1995). Fluorosis survey of Bongo District, Upper East Region. A report submitted to the Upper Region Community Water Project.
- Apambire**, W. B., Boyle, D. R. and Michel, F.A. (1997). Geochemistry, genesis and health implications of fluoriferous groundwaters in the upper regions of Ghana. *Environmental Geology* 33 (1): 13-24.
- APHA**, (1992). Standard Methods For The Examination of Water and Waste Water. American Public Health Association, 1881<sup>th</sup> ed., Academic Press. Washington D.C. pp. 214-218,
- APHA**, (1998). Standard Methods For The Examination of Water and Wastewater. 20<sup>th</sup> edition. Washington, USA: American Public Health Association
- Atiemo**, E. (2012). “Studies of effect of selected local admixtures on essential properties of cement for housing construction”. MPhil Thesis, Civil and Geomatic Engineering, KNUST.
- Atipoka** F. A, (2009). “Water Supply Challenges in rural Ghana”. *Desalination* 248: 212-217
- Awudu**, A.R., Darko, E.O., Schandorf, C., Hayford, E.K., Abekoe, M.K., and Ofori-

- Dansoh, (2010). Determination of activity concentration levels of  $^{238}\text{U}$ ,  $^{232}\text{Th}$  and  $^{40}\text{K}$  in drinking water in a gold mine in Ghana. *Operational Radiation Safety Health Physics Journal* 99(2): pp149-153
- Ayoob, S., & Gupta, A. K.** (2006). Fluoride in drinking water: A review on the status and stress effects. *Critical Reviews in Environmental Science and Technology*, 36(6), 433-487.
- Banks, D., Reimann, C., Røyset, O., Skarphagen, H. and Sæther, O.M.** (1995). Natural concentrations of major and trace elements in some Norwegian Bedrock groundwaters, *Appl. Geochem.*10: 1–16.
- Beck, J. W., Edwards, R. L., Ito, E., Taylor, F. W., Recy, J., Rougerie, F., Joannot, P., Henin, C.** (1992). Sea-surface temperature from coral skeletal strontium/calcium ratios. *Science* 257 (5070): 644-647
- Beraki, B. M.** (2014). Investigation of Household Defluoridation of Water Using Local Materials as Sorbent Media: A case of Keren Community in Eritrea. MSc Thesis, Department of Civil Engineering, Jomo Kenyatta University of Agriculture and Technology, Kenya.
- Bhargava, D. S., & Killedar, D. J.** (1992). Fluoride adsorption on fishbone charcoal through a moving media adsorber. *Water Research*, 26(6): 781-788.
- Bhatnagar, A., Kumar, E., & Sillanpää, M.** (2011). Fluoride removal from water by adsorption—a review *Chemical Engineering Journal*, 171(3): 811-840.
- Bhongsuwan, T., Pisapak, P., and Duerast, H.** (2011). Result of alpha track detection of radon in soil gas in the Khlong Marui Fault Zone, southern Thailand: A possible earthquake precursor. *Songklanakarin Journal of Science and Technology* 33(5): 609-616
- Brindha, K. and Elango L.** (2013). Geochemistry of fluoride rich groundwater in weathered granitic rock region, southern india. *Water Qual. Expo. Health*;

5:127-138

**Browne, D.;** Whelton, H.; Mullane, D.O. (2005), Fluoride metabolism and fluorosis.  
*J. Dent.* 33: 177–186.

**Business & Financial Times, BF&T,** (2013). Give us limestone? Dangote tells  
Government? January 21, 2013

**Chaturvedi, A. K.,** Yadava, K. P., Pathak, K. C., & Singh, V. N. (1990).

Defluoridation of water by adsorption on fly ash. *Water, Air, and Soil  
Pollution*, 49(1): 51-61.

**Chinoy, N. J.** (1991). “Effects of fluoride on physiology of animals and human  
beings”. *Indian Journal of Environmental Toxicology*. 1: 7-13

**Chowdhury, S.;** Husain, T.; Veitch, B.; Bose, N.; Sadiq, R. (2004). Human health  
risk assessment of naturally occurring radioactive materials in produced  
water- a case study, *Human and Ecological Risk Assessment* 10 (6): 1155-  
1171

**Citifmonline.com** (2014 edition). Bongo District to solve water problem. 28<sup>th</sup>  
December, 2014

**Climent, H.,** Tokonami S., Furukawa, M. (1999). Statistical analysis applied to  
Radon and natural events, *Radon in the living environment*, 19-23 (030),  
Athens, Greece.

**Crittenden, J.,** Trussell, R., Hand, D., Howe, K., Tchobanoglous, G. (2005). “Water  
treatment: Principles and design”. *Published by John Wiley and Sons, NY*

**Dahi, E.,** Bregnhøj, H. and Orio, L (1996). “ sorption isotherms of fluoride on  
flocculated alumina”. *In: Proceedings of the First International Workshop on  
Fluorosis and Defluoridation of Water, Tanzania, 2<sup>nd</sup> June 1997*, pp35-39.

**Dapaah-Siakwan, S** and Gyau-Boakye, P. (2000). Hydrogeologic and borehole  
yield in Ghana. *Journal of Hydrogeology*, 8: 405-416

- Darko** E. O. and Faanu A. (2007). Baseline radioactivity measurements in the vicinity of a gold processing plant. *J. appl. Sci. Technol.* 12(1&2): 18–24
- Das**, N., Pattanaik, P. and Das, R. (2005). “Defluoridation of drinking water using activated titanium rich bauxite”. *Journal of Colloid and Interface Science*, 292: 1-10.
- Dissanayake**, C. B. (1991). The Fluoride Problem in the Groundwater of Srilanka - Environmental Management and Health. *Intl. J. Environ. Studies*, 19: 195-203.
- Dorris**, K.L., YuL.J., Shukla S.S., Shukla A. Margrave J.L., (2003). Adsorption of Chromium from Aqueous solutions by Maple Sawdust. *J.Hazard. Mater.*, B100,3-63,.
- Duah** A. A, (2002). “Groundwater contamination in Ghana”. *Published by Talor and Francis Group, plc. London-UK*
- Dunham**, R. H. (1962). *Classification of carbonate rocks according to dispositional textures*, in Ham W. E (ed.), *Classification of carbonate rocks: Am. Assoc. Petroleum Geologists Mem.* 1,p. 108-121
- Dwamena-Boateng** P., Larmie S. A (2011). “Excess fluoride levels in groundwater supplies in the Upper East region of Ghana”. *In proceedings of the National workshop on water quality sustainability development and agenda 21.*
- Edmunds**, M. and Smedley, P. (2005). Fluoride in natural waters. In *Essentials of Medical Geology, Impacts of Natural Environment on Public Health*, Elsevier Academic Press
- Emeka**, (2010). Ionizing radiation, man and the environment. Inaugural lecture, University of Jos, Nigeria. UNIJOS Inaugural Lecture 43.
- Eneida**, S.C., Celia, R.G.T and Teresa, M.K.R (2005). Biosorption Chromium (III) by *Sargassum* sp. Biomass. *Electron. J. Biotechnol.* 5:1-7



- Eyobel, M. D.** (2006). *Removal of Fluoride from Water Using Granular Aluminium Hydroxide: Adsorption in a Fixed Bed Column*. M.Sc. Thesis, Environmental Science Program, Addis Ababa University, Ethiopia.
- Fan, X.** Parker, D.J. Smith, M.D. (2003). Adsorption kinetics of fluoride on low cost materials, *Water Res.* 37: 4929–4937.
- Fawell, J.,** Bailey, K., Chilton, J., Dahi, E., Fewtrell, L. and Magara, Y., (2006). Fluoride in Drinking water, World Health Organisation, IWA Publishing, Alliance House, 12 Caxton Street, London SW1H 0QS, UK.
- Folk, R. L.** (1974). *Petrology of Sedimentary Rocks*. Austin, Texas: Hemphill.
- Frimpong, C.K.,** Nsiah, K., Awunyo-Vitor, D. And Dongsogo, J. (2013). “Soluble Fluoride levels in drinking water-A major risk factor of dental fluorosis among children in Bongo community of Ghana” *Ghana Medical Journal*, 4(1): pp16-23.
- Fufa, F,** Alemayehu, E., and Deboch, B. (2014). “Defluoridation of groundwater using gypsiferous limestone”. *Journal of Environmental and Occupational Science*. Vol 3. DOI:10.5455/jeos.20140314041743
- Gaciri, S.J.** and Davies, T.C. (1993). The occurrence and geochemistry of fluoride in some natural waters of Kenya, *J. Hydrol.* 143: 395–412.
- Gao, S.,** Sun, R., Wei, Z., Zhao, H., Li, H. and Hua, F. (2009). “Size-dependent defluoridation properties of synthetic hydroxyapatite”. *Journal of Fluorine Chemistry* 130: 550-556
- Ghana** Districts (2006), Yilo Krobo Municipal Demographic Characteristics. Available at: <http://www.ghanadistricts.com/districts/Yilo> Krobo. Assessed on May, 2016.
- Ghana** News Agency, GNA, (2014). Bongo District Assembly inaugurates WASH Team. 24<sup>th</sup> April, 2015



- Ghorai**, S., and Pant, K. K., (2004). “Investigations on the column performance of fluoride sorption by activated alumina in a fixed-bed”. *Chem. Eng. J.*, 98: 165-173
- Gilmore**, G., Hemingway, J. D. (1995). Practical Gamma-Ray Spectrometry (New York: Wiley)
- Greenwood**, N.N., Earnshaw, A., (1998). Chemistry of elements (2<sup>nd</sup>) edition. Pp 804 Oxford: Butterworth. ISBN 0-7506-3365-4
- GSS** (Ghana Statistical Service) (2011). Multiple Indicator Cluster Survey. Final Report.
- Harrison**, P. T. C. (2005). “Fluoride in water: a UK perspective”. *Journal of Fluorine Chemistry*. 126: 1448-1456
- Hichour**, M. Persin, F. Sandeaux, J. and Gavach, C. (2000). Fluoride removal from water by Donnan analysis, *Sep. Purif. Technol.* 18: 1–11.
- Iddrisu**, Y. (1987). “Rock phosphate prospects in Ghana. In: Wachira JK and AJG Notholt (eds.) Agrogeology in Africa. *Commonwealth Sci. Council, Technical Publ. Series* 226: 67-76
- Islam** M., R.K. Patel (2007), Evaluation of removal efficiency of fluoride from aqueous solution using quick lime, *Journal of Hazardous Materials* 143: 303–310.
- Islam**, M. and Patel, R. K. (2011). “Thermal activation of basic oxygen furnace slag and evaluation of its fluoride removal efficiency”. *Chemical Engineering Journal*. 169:68-7
- Johnston**, R. and Heijnen, H. (2002) Safe Water Technology for Arsenic Removal Report. World Health Organization, WHO, Geneva.
- Jusoh**, A., Shiungb, L. S., Alia, N. and Noor, M. J. M. M. (2007). “A simulation study of the removal efficiency of granular activated carbon on cadmium and

lead”. *Desalination* 206: 9-16

**Karthikeyan M**, Elango K. P, (2007). “Defluoridation of water using aluminium impregnated activated newspaper carbon” *Environmental Science: An Indian Journal*, 2: 187-193.

**Kebede, B.**, Beyene, A., Fufa, F., Megersa, M., and Behm, M. (2014). Experimental evaluation of sorptive removal of fluoride from drinking water using iron ore. *Appl. Water Sc.* DOI 10.1007/s13201-014-0210-x

**Kesse, G. O.** (1975). Limestone deposits in Ghana. Ghana Geological Survey Report No. 75/4, pp 16.

**Kesse, G. O.** (1985). The mineral and rock resources of Ghana. Balkema, Rotterdam, 610pp

**Krmar, M.**, J. Slivka, E. Varga, I. Bikit and M. Veskovic, (2009). Correlations of natural radionuclides in sediments from Danube. *Journal of Geochemical Explorations*. 100(1): 20-24

**Kurnaz, A.**, Keser, R., Okumusoglu, N.T., Karahan, G., Cevic, U. (2007). Determination of radioactivity levels and hazards of soils and segment samples in Firtini valley (Turkey). *Applied Radiation Isotopes*, 65(11): 1218-1289

**Levy S. M.**, and Guha-Chowdhury N. (1999), Total fluoride intake and implications for dietary fluoride supplementation. *Journal of Public Health Dentistry* 59: 211-23

**Li, Y.H.** Wang, S. Cao, A. Zhao, D. Zhang, X. Xu, C. Luan, Z. Ruan, D. Liang, J. Wu, D. and Wei, B. (2001). Adsorption of fluoride from water by amorphous alumina supported on carbon nanotubes, *Chem. Phys. Lett.* 350: 412–416.

**Li, Y. H.**, Wang, S., Zhang, X., Wei, J., Xu, C., Luan, Z., & Wu, D. (2003). Adsorption of fluoride from water by aligned carbon nanotubes. *Materials Research Bulletin*, 38(3): 469-476.

- MacDonald, A.M., Davies, J. (2000).** *A brief review of groundwater for rural supply in sub-Saharan Africa.* British Geological Survey, pp. 30 (WC/00/033).
- Macomber, Roger (1996).** *Organic chemistry..* Sausalito: University Science Books. pp. 230. ISBN 0-7487-6420-8
- Mahramanlioglu M., I. Kizilcikli, I.O. Bicer (2002),** Adsorption of fluoride from aqueous solution by acid treated spent bleaching earth, *Journal of Fluorine Chemistry* 115: 41–47.
- Malakootian, M., Moosazadeh, M., Yousefi, N., Fatehizadeh, A. (2011).** “Fluoride removal from aqueous solution by pumice: case study on Kuhbonana water”. *African Journal of Environmental Science and Technology* 5(4): 299-306
- Masarik, J. And Beer, J. (1999).** Simulation of particle uses and cosmogenic nuclide production in the earth’s atmosphere. *Journal of Geophysical Research*, 104(10): 12009-12111.
- Matiullah A. A., Rehman Shakeel Ur, Rehman Shafi Ur and Faheem M. (2004).** Measurement of radioactivity in the soil of Bahawalpur division, Pakistan. *Rad. Prot. Dosimetry* 112(3): 443–447.
- McKay, G. (1995).** *Use of Adsorbents for the Removal of Pollutants from Wastewaters.* CRC Press, Boca Raton, New York, London and Tokyo.
- Meenakshi, R. C. and Maheshwari, L. (2006).** Fluoride in drinking water and its removal. *J. Hazardous Materials*, B137: 456-463
- Merdanoglu B. and Altinsoy N. (2006).** Radioactivity concentrations and dose assessment for soil samples from Kestanbol Granite area, Turkey. *Rad. Prot. Dosimetry*, 121(4): 399–405.
- Miretzky, P., Muñoz, C., & Carrillo-Chávez, A. (2008).** Fluoride removal from aqueous solution by Ca-pretreated macrophyte biomass. *Environmental Chemistry*, 5(1): 68-72.

- Mishra, P.C., Behera, P.C., and Patel, R.K** (2005). Contamination of water due to major industries and open refuse dumping in the steel city of Orissa- a case study. *Journal of Environmental Science and Engineering*, 47(2): 141-154.
- Mohan, D., Pittman Jr., C.U.**, (2007). Arsenic removal from water/wastewater using adsorbents- critical review. *J. Hazard. Mater.* 142, 1-53
- Mohan, S.V., Karthikeyan, J.**, (1997). Removal of lignin and tannin aqueous solution by adsorption onto activated charcoal. *Environ. Poll.* 97, 183-197
- Mohapatra, M. Anand, S. Mishra, B.K. Dion E. Giles, Singh P.** (2009). Review of fluoride removal from drinking water. *Journal of Environmental Management* 91: 67–77
- Murat, T., Mustafa, I. and Onger, S.** (1999). Adsorption of Copper and Cadmium ions by activated carbon from rice Hulls. *Turk. J. Chem.* 23: 185-191
- Murray, J.** (1986). Appropriate use of fluoride for human health. *World Health Organization*. Geneva; 1986: 77- 89.
- Mwampashi, E. S.** (2011). “Adsorptive removal of fluoride”. *M.Sc Thesis, UNESCO-IHE, Delft, Netherlands*
- Nabizadeh, R., Jahangiri-rad, M. and Sadjadi, S.** (2015). Modelling the Effects of competing anions on fluoride removal by functionalized polyacrylonitrile coated with iron oxide nanoparticles. *S. Afr. J. Chem.* 68: 201-207
- Nagendra Rao, C.R** (2003). “Fluoride and Environment” in Martin J. Bunch, V. Madha Suresh and T. Vasantha Kumaran, eds, *Proceedings of the 3<sup>rd</sup> International Conference on Environment and Health, Chennai, India, 15-17 December*, Department of Geography, University of Madras and Faculty of Environmental Studies, York University. 386-399.
- Onyango, M. S., Kojima, Y., Aoyi, O., Bernardo, E. C., & Matsuda, H.** (2004). Enhanced removal of Cr (VI) from aqueous solution using polypyrrole/Fe<sub>3</sub>O<sub>4</sub> magnetic nano-composite. *J. Colloid Interface Sci.*, 279(2): 341–50.

**Onyango, M. S., Kojima, Y., Aoyi, O., Bernardo, E. C., & Matsuda, H. (2004).**

Adsorption equilibrium modeling and solution chemistry dependence of fluoride removal from water by trivalent-cation- exchanged zeolite F-9. *Journal of Colloid and Interface Science*, 279(2): 341-350.

**Paudyal, H., Pangen, B., Inoue, K., Kawakita, H., Ohto, K., Harada, H. and Alam,**

S.(2011). “Adsorptive removal of fluoride from aqueous solution using orange waste loaded with multi-valent metal ions”. *Journal of Hazardous Materials* 192: 676-682

**Pelig-Ba, K.B (1987).** Hydrochemical study of groundwater in some aquifers in the Upper Regions of Ghana. Joint 13<sup>th</sup> Biennial Conference in West African Science Association and the 15<sup>th</sup> Biennial Conference of the Ghana Science Association, University of Ghana, August 1987, Ghana

**Pelig-Ba, K.B. (1998).** Trace elements in ground water from some crystalline rocks in the Upper Regions of Ghana. *Water, Air Soil Pollution*. 103: 71-89.

**Pietrelli L (2005).** Fluoride wastewater treatment by adsorption onto metallurgical grade alumina. *Anal Chim*, 95:303-312

**Ponsot, I. Falcone, R. Bernardo, E (2013).** Stabilization of fluorine-containing Industrial waste by production of sintered glass-ceramics. *Ceram. Int.*, 39: 6907–6915.

**Population and Housing Census, PHS, (2010).** Summary report of final results. Ghana Statistical Service, (GSS), 2012 Publication.

**Population and Housing Census, PHS, (2010).** District Analytical Report, Yilo Krobo Municipal. Ghana Statistical Service.

**Ramasamy, V., Suresh, G., Meenakshisundaram, V, and Gajendran, V. (2009).**

Evaluation of natural radioanuclide content in rivers, sediments and excess lifetime canser risk due to Gamma radioactivity. *Research Journal of*



*Environmental and Earth Sciences*. 1(1): 6-10

- Ramos**, R.L. Turrubiartes, J.O. and Castillo, M.A.S. (1999). Adsorption of fluoride from aqueous solution on aluminium-impregnated carbon, *Carbon* 37: 609–617.
- Rao** Nagendra, C.R. (2003). ‘Fluoride and Environment – A Review’ in Martin J. Bunch, V. Madha Suresh and T. Vasantha Kumaran, eds., *Proceedings of the Third International Conference on Environment and Health, Chennai, India, 15-17 December, 2003*. Chennai: Department of Geography, University of Madras, Faculty of Environmental Studies, York University. Pp 386-399.
- Raymond**, D. Letterman (1999). (Ed) *Water Quality and Treatment- A Handbook of Community Water Supplies*, (5<sup>th</sup> ed.). McGraw-Hill publication. New York, pp. 158.
- Reardon**, E.J. and Wang, Y. (2000). A Limestone Reactor for fluoride removal from wastewaters, *Environ. Sci. Technol.* 34: 3247–3253.
- Reddy**, N.B. and Prasad, K.S.S. (2003). Pyroclastic fluoride in ground waters in some parts of Tadpatri Taluk, Anantapur district, Andhra Pradesh, *Indian J. Environ. Health* 45: 285–288.
- Regassa** E. Namara, Leah Horowitz, Ben Nyamadi and Boubacar Barry (2011). Irrigation Development in Ghana: Post experience, emerging opportunities and future directions. Ghana Strategy Support Program (GSSP). GSSP working paper No. 0027 March 2011.
- RGNDWM (1993)**. *Prevention and control of fluorosis. Vol. II. Water quality and defluoridation techniques*. New Delhi, India, Rajiv Gandhi National Drinking Water Mission
- Ruiz**, T. Persin, F. Hichour, M. Sandeaux, J. (2003). Modelisation of fluoride removal in Donnan dialysis, *J. Membr. Sci.* 212: 113–121.



- Sarkar, M., Banerjee, A., Pramanick, P.P., and Sarkar, A.S. (2006).** Use of laterite for the removal of fluoride from contaminated drinking water. *Journal of Colloid and Interface Science* 302 (2006) 432-441
- Shao-Xiang, T., Shu-Guang, W., Wen-Xin, G., Xian-Wei L. and Bao-Yu, G. (2009)** Removal of fluoride by hydrous manganese oxide-coated alumina: performance and mechanism. *J. Hazard. Mater.* 168: 1004–1011
- Shen, F., Chen, X., Gao, P., & Chen, G. (2003).** Electrochemical removal of fluoride ions from industrial wastewater. *Chemical Engineering Science*, 58(3): 987-993.
- Shomar, B., Muller, G., Yahya, A., Aska, S., Sansur, R. (2004).** “Fluoride in groundwater, soil and infused black tea and the occurrence of dental fluorosis among school children of the Gaza strip”. *Journal of Water Health*, 2(1): 23-35.
- Singh, A.K., Prakash D. and Shahi S.K. (2013),** Decolourization of the textile dye (Brown GR) by isolated *Aspergillus* strain from meerut region, *Int. Res. J. Environment Science.*, 2(2): 25-29.
- Singh, G. Kumar, B. Sen, P.K. and Majumdar, J. (1999).** Removal of fluoride from spent pot liner leachate using ion exchange. *Water Environ. Res.*, 71: 36-42.
- Smedley PL, Edmunds WM, West JM, Gardner SJ, Pelig-Ba K.B (1995).** Vulnerability of shallow groundwater quality due to natural geochemical environment. 2. Health problems related to groundwater in the Obuasi and Bolgatanga areas, Ghana. British Geological Survey, BGS Technical Report WC/95/43.
- Smet, J., (1990).** Fluoride in drinking water. In: Frencken, LE (Ed.), Endemic Fluorosis in Developing Countries – Causes, Effects and Possible Solution: Report of a Symposium Held in Delft, The Netherlands. Netherlands

Organisation for Applied Scientific Research.

- Solomon**, A. O, Ike, E.E, Ashano, E.C and Jwanbot, D.I. (2002). Natural background radiation characteristics of basalts on Jos Plateau and radiological implication of the use of the rock for house constructin. *African Journal of Natural Sciences*, 5(1): 40-43
- Srimurali**, M., Pragathi, A., & Karthikeyan, J. (1998). A study on removal of fluorides from drinking water by adsorption onto low-cost materials. *Environmental Pollution*, 99(2): 285-289.
- Streat**, M., Hellgardt, K., Newton, N.L.R., (2008). Hydrous ferric oxide as an adsorbent in water treatment. Part 2. Adsorption studies. *Process Saf. Environ. Prot.* 86, 11-20
- Stumm**, W., and Morgan, J.J. (1996). Aquatic chemistry: chemical equilibria and rates in natural waters. Wiley, New York.
- Sujana**, M.G., Thakur, R.S., and Rao, S.B. (1997). Removal of fluoride from aqueous solution by using alum sludge. *Journal of Colloid and Interface Science* 206, 94-101 (1998).
- Suneetha**, M., Sundar, B.S and Ravindhranath, K. (2015). “Removal of fluoride from polluted waters using active carbon derived from barks of *vitex negundo* plant”. *Journal of Analytical Science and Technology*. 6:15
- Suresh** K. Nath and Robin K. Dutta. (2010). Enhancement of Limestone Defluoridation of Water by Acetic and Citric Acids in Fixed Bed Reactor. *Clean – Soil, Air, Water*, 38 (7): 614–622
- Suresh** K Nath & Robin K Dutta (2010), ‘Fluoride removal from water using crushed limestone’ *Indian Journal of Chemical Technology*, (17): 120-125
- Tchomgui**-Kamga E, Ngameni E, Darchen A (2010). Evaluation of removal efficiency of fluoride from aqueous solution using new charcoals that contain

calcium compounds. *J. Colloid Interf Sci*, 346:494–499

**Tor, A** (2006). “Removal of fluoride from an aqueous solution by using montmorillonite”. *Desalination*, 201: 267–276.

**Tripathy, S.S. Srivastava, S.B. Bersillon, J.L. and Gopal, K.** (2004). Removal of fluoride from drinking water by using low cost adsorbents, in: Proceedings of the 9th FECS Conference and 2nd SFC Meeting on Chemistry and the Environment, Bordeaux, France, 352.

**UNSCEAR** (2000). Sources and effect of ionizing radiation. United Nations Scientific Committee on the Effect of Atomic Radiation, United Nations, New York.

**USEPA** (1989). Risk Assessment Guidance for Superfund, vol. 1: Human Health Evaluation Manual (Part A). EPA/540/1-89002. Washington D.C: US. Environmental Protection Agency, Office of Emergency Response

**USEPA** (1995). Guidance for Risk Characterization at the U.S. Environmental Protection Agency. Washinton, D.C: U.S. Environmental Protection Agency, Science Policy Council

**USEPA** (2003). Integrated Risk Information System. Cincinnati, OH: U.S. Environmental Protection Agency, Environmental Criteria and Assessment Office. <http://www.epa.gov/iris>

**USEPA** (1996). Low stress (low flow), Purging and Sampling Procedure for the collection of Groundwater Samples from monitoring wells, U.S. EPA, Region I, Standard Operating Procedure: GW 0001, pp13

**USEPA** (2006). Technical report on Technologically Enhanced Naturally Occurring Radioactive Materials from Uranium Mining Volume 1: Mining and Reclamation Background, EPA 402-R-05-007, January 2006

**Vaaramaa, K. and Lehto, J.** (2003). Removal of metals and anions from drinking

water by ion exchange, *Desalination* 155: 157–170.

**Valdez-Jiménez, L.;** Soria Fregozo, C.; Miranda Beltrán, M.L.; Gutiérrez Coronado, O.; Pérez Vega, M.I (2011). Effects of the fluoride on the central nervous system. *Neurología*, 26: 297–300.

**Virk, H.S.,** Vivek Walia, Anad Kumar Sharma, Naresh Kumar and Rajv Kumar (2000). Correlation of radon anomalies with microseismic events in Kangara and Chamba valleys of N-W Himalaya. *Geophysical International*, 39(3): 221-227

**Wambu, E.W.,** Onindo, C.O., Ambusso, W., and Muthakia, G.K. (2012). Removal of fluoride from aqueous solutions by adsorption using siliceous mineral of a Kenyan origin. *Soil Air Water*. DOI: 10.1002/clean.201100171

**Wang, R. Li, H.Na., and Y. Wang** (1995). Study of new adsorbents for fluoride removal from waters. *Water Qual. Res. J. Canada*, 30: 81-88

**Wang, Y., & Reardon, E. J.** (2001). Activation and regeneration of a soil sorbent for defluoridation of drinking water. *Applied Geochemistry*, 16(5): 531-539.

**Wang, Y.,** Sikora, S., and Kim, H. (2012). Evaluation of mineral substrates for in situ iron removal from groundwater. *Environ Earth Sci* (2013) 69: 2247-2255

**Wasay, S. A.,** Haran, M., & Tokunaga, S. (1996). Adsorption of fluoride, phosphate, and arsenate ions on lanthanum-impregnated silica gel. *Water Environment Research*, 68(3): 295-300.

**WHO** (1984). Guidelines for Drinking Water Quality. *World Health Organization*, Geneva, 1(2).

**WHO** (2001). Water-Related Diseases. Fluorosis: The Diseases and how it Affects People. Geneva: World Health Organization. Available at: [http://www.who.int/water\\_sanitation\\_health/diseases/fluorosis/en/](http://www.who.int/water_sanitation_health/diseases/fluorosis/en/): Assessed on: May, 2016

- WHO** (2002). World Water Day 2001: Oral Health. Geneva:World Health Organization. Available at: [http://www.who.int/entity/water\\_sanitation\\_health/en/oralhealth.htm](http://www.who.int/entity/water_sanitation_health/en/oralhealth.htm): Assessed on: May, 2016.
- WHO**, (1985). Guidelines for Drinking Water Quality, vol. 3. World Health Organization, Geneva, pp. 1–2.
- WHO**. (2006). *Fluoride in Drinking-Water*. Published by IWA Publishing, London, UK. World Health Organization.
- WHO** *Guidelines for Drinking Water Quality* (2006). First Addendum to Third Edition (Vol 1 Recommendations), (3rd ed.). Geneva, Switzerland: World Health Organization, pp. 375–377.
- WHO** (2008). Guidelines for Drinking-Water Quality, 3<sup>rd</sup> edition (Vol. 1). WHO, Geneva, Recommendations.
- WRC**, Distribution of fluoride-rich groundwater in Eastern and Mogwase region of Northern and North-west province, WRC Report No. 526/1/01 1.1 9.85 Pretoria, 2001.
- Xiang**, Q. (2003), “Effect of fluoride in drinking water on children’s intelligence”. Fluoride 36: 84-94; Available at: <http://www.fluoridealert.org/health/cancer>: Assessed on: May, 2016
- Yadaz**, A.K., Abbasssi, R., Gupta, A., and Dadashzadeh, M. (2012). Removal of fluoride from aqueous solution and groundwater by weheat straw, sawdust and activated bagasse carbon of sugarcane. *Ecological Engineering* 52 (2013) 211-218
- Yoseph**, A. W. (2007). Fluoride Removal from Water with Aluminium Oxide Hydroxide: A Pilot Study for Household Application. M.Sc. Thesis, *Environmental Science Program*, Addis Ababa University, Ethiopia.



## APPENDIX A

## A1: Peak and Pattern list of limestone sample EKL-Bk03 from XRD Analysis

**Peak List**

Pos. [°2Th.]	Height [cts]	FWHMLeft [°2Th.]	d-spacing [Å]	Rel. Int. [%]
20.8791	169.09	0.1181	4.25467	0.98
22.0481	212.87	0.1181	4.03165	1.24
24.0846	367.95	0.1181	3.69517	2.14
26.6647	760.50	0.1574	3.34319	4.42
27.9150	125.58	0.1574	3.19622	0.73
30.9732	17219.33	0.1968	2.88727	100.00
33.5616	576.87	0.1574	2.67027	3.35
35.3333	389.39	0.1574	2.54034	2.26
37.3822	618.53	0.1574	2.40568	3.59
39.4719	38.35	0.2362	2.28300	0.22
41.1496	1756.82	0.1968	2.19372	10.20
43.8165	233.99	0.1968	2.06618	1.36
44.9435	974.10	0.1968	2.01696	5.66
49.2514	205.02	0.2362	1.85015	1.19
50.5342	1205.30	0.1968	1.80616	7.00
51.0818	1356.29	0.2362	1.78807	7.88
58.8866	174.74	0.1968	1.56834	1.01
59.7946	337.24	0.2755	1.54668	1.96
62.0031	25.07	0.6298	1.49679	0.15
63.4247	261.67	0.2362	1.46662	1.52
64.5227	207.76	0.1181	1.44429	1.21
65.1639	126.42	0.2755	1.43162	0.73
66.0605	69.28	0.3936	1.41435	0.40
67.4013	353.14	0.1574	1.38944	2.05
70.4832	218.75	0.1574	1.33605	1.27
72.8887	83.84	0.3149	1.29778	0.49
74.7920	71.52	0.3149	1.26941	0.42
76.9734	120.97	0.4723	1.23879	0.70
79.7351	43.96	0.3936	1.20268	0.26
82.5994	83.86	0.3149	1.16809	0.49
86.6694	70.39	0.3149	1.12339	0.41
87.8762	183.30	0.1968	1.11105	1.06

**Pattern List**

Visible Ref.Code	Score	Cpd Name	Displ. [°2Th]	Scale Fac.	Chem. Formula
98-017-1518	62	Dolomite	0.000	0.954	C2 Ca1 Mg1 O6
03-065-0466	36	Silicon Oxide	0.000	0.036	O2 Si

## A2: Peak and Pattern list of limestone sample EKA-B01 from XRD Analysis

**Peak List**

Pos. [°2Th.]	Height [cts]	FWHMLeft [°2Th.]	d-spacing [Å]	Rel. Int. [%]
8.7057	144.80	0.6298	10.15753	2.31
12.4842	136.01	0.2362	7.09042	2.17
19.7516	66.83	0.2362	4.49491	1.07
20.8773	298.35	0.1181	4.25502	4.77
21.9990	71.21	0.2362	4.04054	1.14
23.0946	296.88	0.1574	3.85128	4.74
23.9914	109.63	0.2362	3.70931	1.75
25.2437	45.52	0.4723	3.52806	0.73
26.6617	1668.30	0.1574	3.34356	26.66
27.9472	204.11	0.1181	3.19262	3.26
29.4505	4563.86	0.1574	3.03299	72.92
30.7670	6258.35	0.1574	2.90615	100.00
33.2454	81.46	0.3149	2.69494	1.30
35.0489	87.47	0.4723	2.56030	1.40
36.0222	397.14	0.1574	2.49332	6.35
36.5532	118.91	0.1181	2.45831	1.90



37.2778	155.96	0.1968	2.41217	2.49
39.4819	592.57	0.1968	2.28245	9.47
40.9538	362.72	0.1968	2.20375	5.80
42.4651	92.74	0.1968	2.12875	1.48
43.2271	476.83	0.1968	2.09298	7.62
44.7120	171.45	0.2362	2.02686	2.74
47.5743	421.63	0.1968	1.91138	6.74
48.5611	463.83	0.1968	1.87482	7.41
50.1314	316.61	0.1968	1.81972	5.06
50.9448	177.08	0.4723	1.79256	2.83
56.6696	64.02	0.2362	1.62431	1.02
57.4257	166.32	0.2755	1.60471	2.66
59.9987	118.70	0.3149	1.54191	1.90
60.7325	129.97	0.1181	1.52502	2.08
61.5364	86.86	0.2362	1.50701	1.39
63.1687	90.07	0.3936	1.47195	1.44
64.7757	129.45	0.3149	1.43926	2.07
65.6984	73.38	0.3936	1.42127	1.17
67.1529	78.04	0.3149	1.39398	1.25
70.3954	49.92	0.4723	1.33750	0.80
72.9962	55.42	0.2362	1.29614	0.89
81.6524	37.06	0.6298	1.17922	0.59
83.8549	73.07	0.3936	1.15377	1.17

**Pattern List**

Visible Code	Ref. Score	Cpd Name	Displ. [°2Th]	Scale Fac.	Chem. Formula
01-086-2334	65	Calcium Carbonate	0.000	0.431	Ca( C O <sub>3</sub> )
01-085-0795	48	Silicon Oxide	0.000	0.272	SiO <sub>2</sub>
98-017-1525	52	Dolomite	0.000	0.601	C <sub>2</sub> Ca1 Mg1 O <sub>6</sub>
01-070-9131	13	Calcium Magnesium	..0.000	0.261	Ca0.23 Mg1.77( Si..
01-073-2361	23	Calcium Magnesium	..0.000	0.533	Ca Mg ( C O <sub>3</sub> ) <sub>2</sub>

**A3: Peak and Pattern list of limestone sample EKA-R01 from XRD Analysis****Peak List**

Pos.[°2Th.]	Height [cts]	FWHMLLeft[°2Th.]	d-spacing [Å]	Rel. Int. [%]
8.8459	460.77	0.1574	9.99681	14.92
17.7474	122.91	0.1574	4.99774	3.98
19.7060	197.07	0.1968	4.50522	6.38
20.8591	393.26	0.1574	4.25869	12.74
22.0356	88.59	0.2362	4.03391	2.87
23.0862	245.36	0.1181	3.85266	7.95
24.0898	103.50	0.3936	3.69439	3.35
26.6456	2310.09	0.1181	3.34555	74.81
27.8820	148.40	0.2362	3.19993	4.81
29.4370	3087.94	0.1574	3.03435	100.00
30.7413	2357.41	0.1968	2.90851	76.34
30.9692	1635.19	0.1181	2.88763	52.95
33.1629	227.90	0.1968	2.70146	7.38
34.9357	213.16	0.2362	2.56833	6.90
36.0130	293.56	0.1574	2.49393	9.51
36.5553	179.72	0.1181	2.45817	5.82
37.2608	109.40	0.3936	2.41324	3.54
39.4583	431.87	0.1574	2.28376	13.99
41.0197	245.12	0.3149	2.20036	7.94
42.4331	104.59	0.2362	2.13029	3.39
43.1930	369.14	0.1574	2.09455	11.95
44.8147	140.37	0.3149	2.02245	4.55
47.5487	333.33	0.2362	1.91235	10.79
48.5327	327.47	0.2362	1.87585	10.60
50.1122	333.58	0.1574	1.82037	10.80
50.9666	152.58	0.4723	1.79184	4.94
56.5817	62.11	0.2362	1.62663	2.01
57.4269	157.95	0.1968	1.60468	5.12
59.9537	174.34	0.1968	1.54295	5.65
60.7226	88.52	0.2362	1.52525	2.87
61.5958	92.57	0.3149	1.50570	3.00
64.6855	112.49	0.3149	1.44105	3.64

68.2058	96.04	0.2362	1.37500	3.11
70.4073	62.57	0.4723	1.33731	2.03
73.0696	46.80	0.9446	1.29502	1.52
81.4833	39.49	0.6298	1.18124	1.28

**Pattern List**

Visible Ref. Code	Score	Cpd Name	Displ. [ $^{\circ}$ 2Th]	Scale Fac.	Chem. Formula
01-086-2334	64	Calcium Carbonate	0.000	0.739	Ca ( C O <sub>3</sub> )
03-065-0466	55	Silicon Oxide	0.000	0.696	Si O <sub>2</sub>
01-074-7802	33	Calcium Magnesium	.. 0.000	0.695	Ca (Ca <sub>0.13</sub> Mg <sub>0.87</sub> ..
01-089-20	Potassium Sodium C..	0.000	0.203	(K <sub>0.727</sub> Na <sub>0.170</sub> C..	

**A4: Peak and Pattern list of limestone sample EKL-R<sub>102</sub> from XRD Analysis****Peak List**

Pos. [ $^{\circ}$ 2Th.]	Height [cts]	FWHMLeft [ $^{\circ}$ 2Th.]	d-spacing [Å]	Rel. Int. [%]
20.7131	26.69	0.4723	4.28838	0.26
23.0777	573.13	0.1181	3.85406	5.54
24.8817	99.54	0.1181	3.57857	0.96
25.8847	312.63	0.1181	3.44214	3.02
26.6572	316.09	0.1181	3.34412	3.06
27.9444	116.94	0.1574	3.19293	1.13
28.7504	219.09	0.1181	3.10522	2.12
29.4456	10343.67	0.1968	3.03348	100.00
31.4925	145.81	0.1968	2.84083	1.41
36.0192	890.85	0.1574	2.49352	8.61
39.4548	1181.59	0.1968	2.28395	11.42
42.6186	98.83	0.1968	2.12144	0.96
43.2106	1043.98	0.1968	2.09374	10.09
47.1510	294.04	0.1574	1.92755	2.84
47.5502	953.92	0.2362	1.91229	9.22
48.5445	1086.77	0.2362	1.87543	10.51
56.5793	155.05	0.1181	1.62669	1.50
57.4320	445.84	0.1574	1.60455	4.31
60.7022	302.12	0.1574	1.52571	2.92
61.5111	90.93	0.2362	1.50757	0.88
63.1353	80.47	0.3149	1.47265	0.78
64.7170	259.24	0.1968	1.44042	2.51
65.7063	104.29	0.3149	1.42111	1.01
69.2340	53.09	0.3936	1.35707	0.51
70.3721	49.94	0.4723	1.33789	0.48
72.9801	102.70	0.3149	1.29638	0.99
76.3956	34.11	0.3149	1.24671	0.33
77.2411	62.92	0.3936	1.23516	0.61
81.6010	79.97	0.3149	1.17984	0.77
83.8193	138.53	0.1968	1.15417	1.34
84.9009	56.41	0.3149	1.14221	0.55

**Pattern List**

Visible Ref. Code	Score	Cpd Name	Displ. [ $^{\circ}$ 2Th]	Scale Fac.	Chem. Formula
01-086-2334	76	Calcium Carbonate	0.000	0.675	Ca ( C O <sub>3</sub> )
01-081-1665	31	Silicon Oxide	0.000	0.057	Si O <sub>2</sub>

**A5: Peak and Pattern list of limestone sample EKA-Y04 from XRD Analysis****Peak List**

Pos. [°2Th.]	Height [cts]	FWHMLeft [°2Th.]	d-spacing [Å]	Rel. Int. [%]
8.7857	138.26	0.4723	10.06517	0.92
19.7546	79.54	0.2362	4.49425	0.53
20.8510	432.49	0.1181	4.26033	2.89
22.0100	64.09	0.2362	4.03854	0.43
23.9567	194.68	0.1574	3.71461	1.30
26.6393	2116.28	0.1181	3.34632	14.13
27.7825	69.50	0.2362	3.21117	0.46
29.4277	805.70	0.1574	3.03528	5.38
30.7525	14972.42	0.1968	2.90748	100.00
33.3278	119.73	0.3936	2.68847	0.80
35.0405	160.98	0.3149	2.56089	1.08
36.5378	89.67	0.1968	2.45931	0.60
37.2445	279.26	0.2362	2.41425	1.87
39.4636	177.43	0.1574	2.28346	1.19
40.9211	726.92	0.2755	2.20543	4.86
42.4807	87.64	0.1574	2.12801	0.59
43.7316	56.92	0.2362	2.07000	0.38
44.7119	400.29	0.1574	2.02686	2.67
49.1599	58.90	0.2362	1.85338	0.39
50.1077	550.41	0.1574	1.82052	3.68
50.7603	583.87	0.3149	1.79864	3.90
55.1028	10.92	0.7872	1.66673	0.07
58.7317	51.87	0.3936	1.57211	0.35
59.5991	151.85	0.2362	1.55128	1.01
59.9570	182.92	0.2362	1.54288	1.22
61.7710	28.62	0.4723	1.50185	0.19
63.2300	95.63	0.4723	1.47067	0.64
64.3101	84.01	0.9446	1.44855	0.56
67.2413	111.14	0.3936	1.39236	0.74
68.2208	65.64	0.2362	1.37474	0.44
70.4225	42.73	0.6298	1.33706	0.29
72.7874	31.87	0.7085	1.29934	0.21
76.9974	26.31	0.9446	1.23846	0.18
79.8314	33.13	0.6298	1.20147	0.22
81.4034	18.47	0.4723	1.18220	0.12
87.7561	68.23	0.6298	1.11226	0.46

**Pattern List**

Visible	Score	Cpd	Displ.	Scale	Chem.
Ref. Code		Name	[°2Th]	Fac.	Formula
98-017-1525	57	Dolomite	0.000	0.712	C2 Ca1 Mg1 O6
01-087-2096	53	Silicon Oxide	0.000	0.140	Si O2
98-015-2200	23	Ankerite	0.000	0.649	C2 Ca1 Fe0.33 Mg0...
98-006-8547	13	Muscovite 2M1	0.000	0.023	H2 Al2.97 Fe0.03 K...

**A6: Peak and Pattern list of limestone sample EKL-D01 from XRD Analysis****Peak List**

Pos. [°2Th.]	Height [cts]	FWHMLeft [°2Th.]	d-spacing [Å]	Rel. Int. [%]
23.0841	596.77	0.1181	3.85301	6.79
26.6495	744.73	0.1181	3.34507	8.47
27.9428	143.91	0.1181	3.19311	1.64
29.4406	8791.41	0.1968	3.03398	100.00
30.7558	1351.91	0.1574	2.90717	15.38
31.5028	128.89	0.2362	2.83992	1.47
34.8469	23.21	0.4723	2.57467	0.26
36.0077	822.46	0.1574	2.49429	9.36
37.3973	35.98	0.4723	2.40474	0.41

39.4512	1030.15	0.1574	2.28415	11.72
40.9351	85.06	0.2755	2.20471	0.97
43.2028	1047.24	0.1968	2.09410	11.91
44.7549	83.24	0.1574	2.02502	0.95
47.1220	255.25	0.1574	1.92867	2.90
47.5392	882.72	0.2362	1.91271	10.04
48.5415	847.98	0.2362	1.87553	9.65
50.1074	108.26	0.1574	1.82054	1.23
56.5906	127.13	0.1968	1.62640	1.45
57.4279	335.51	0.1968	1.60466	3.82
60.6981	218.37	0.1968	1.52580	2.48
63.1640	64.82	0.3149	1.47205	0.74
64.6883	238.03	0.2362	1.44100	2.71
65.7157	98.16	0.3149	1.42093	1.12
69.2500	50.16	0.2362	1.35680	0.57
70.2864	73.55	0.3149	1.33931	0.84
72.9795	81.27	0.3149	1.29639	0.92
76.3689	46.50	0.3149	1.24708	0.53
77.2558	55.62	0.3149	1.23496	0.63
81.5665	75.34	0.3936	1.18025	0.86
83.8475	107.60	0.3149	1.15385	1.22

### Pattern List

Visible Ref.Code	Score	Cpd Name	Displ. [°2Th]	Scale Fac.	Chem. Formula
01-086-2334	77	Calcium Carbonate	0.000	0.684	Ca( C O3 )
01-070-3755	31	Silicon Oxide	0.000	0.092	Si O2
98-017-1525	40	Dolomite	0.000	0.113	C2 Ca1 Mg1 O6

### A7: Peak and Pattern list of limestone sample EKL-Y03 from XRD Analysis

#### Peak List

Pos. [°2Th.]	Height [cts]	FWHMLeft [°2Th.]	d-spacing [Å]	Rel. Int. [%]
6.0886	191.76	0.6298	14.51627	2.44
8.8873	287.67	0.1574	9.95036	3.66
12.2515	86.82	0.4723	7.22451	1.10
17.8134	113.60	0.2362	4.97939	1.44
19.7402	136.34	0.3149	4.49748	1.73
20.8575	641.04	0.1574	4.25901	8.15
23.0770	205.41	0.1181	3.85418	2.61
26.6484	2823.15	0.1181	3.34520	35.89
27.8676	137.51	0.2362	3.20156	1.75
29.4431	3673.48	0.1574	3.03373	46.70
30.7571	7865.73	0.1574	2.90705	100.00
33.3617	58.78	0.4723	2.68581	0.75
34.9814	139.60	0.3936	2.56508	1.77
36.0172	230.60	0.1574	2.49365	2.93
36.5450	209.40	0.1181	2.45884	2.66
37.2096	136.57	0.1968	2.41644	1.74
39.4613	521.37	0.1968	2.28359	6.63
40.9344	293.58	0.1968	2.20475	3.73
42.4540	126.80	0.1574	2.12928	1.61
43.2208	360.67	0.1574	2.09327	4.59
44.7147	214.52	0.1968	2.02675	2.73
47.5707	317.81	0.1968	1.91152	4.04
48.5622	319.12	0.1968	1.87478	4.06
50.1286	527.53	0.1574	1.81981	6.71
50.7575	247.79	0.2362	1.79873	3.15
57.4919	131.21	0.3149	1.60302	1.67
59.9965	170.45	0.2362	1.54196	2.17
61.5343	117.31	0.2362	1.50706	1.49
64.7815	85.35	0.2362	1.43915	1.09
65.7250	74.33	0.3149	1.42076	0.94
68.2469	108.98	0.3149	1.37427	1.39
72.9735	31.34	0.9446	1.29648	0.40
80.0032	32.62	0.4723	1.19933	0.41
81.5876	51.26	0.4723	1.18000	0.65
83.9750	55.29	0.4723	1.15243	0.70

**Pattern List**

Visible Ref.Code	Score	Cpd Name	Displ. [°2Th]	Scale Fac.	Chem. Formula
01-087-2096	61	Silicon Oxide	0.000	0.360	Si O <sub>2</sub>
98-042-3568	57	Calcium Carbonate	0.000	0.421	C <sub>1</sub> Ca <sub>1</sub> O <sub>3</sub>
00-041-0586	47	Calcium Iron Magne..	0.000	0.990	Ca(Fe+2, Mg) ..
98-007-9027	24	Muscovite 2M1	0.000	0.074	H <sub>2</sub> Al <sub>2.82</sub> Ba <sub>0.01</sub> F..

**A8: Peak and Pattern list of limestone sample EKL-Y01 from XRD Analysis****Peak List**

Pos.[°2Th.]	Height [cts]	FWHMLeft[°2Th.]	d-spacing [Å]	Rel. Int. [%]
8.8863	641.54	0.1181	9.95142	11.47
12.4858	112.72	0.2362	7.08951	2.02
17.7959	187.32	0.1574	4.98424	3.35
19.7498	165.68	0.3149	4.49532	2.96
20.8775	533.33	0.1181	4.25498	9.54
23.0958	409.39	0.1574	3.85108	7.32
24.2157	89.43	0.2362	3.67546	1.60
25.1366	44.30	0.5510	3.54286	0.79
26.6663	2377.87	0.1574	3.34300	42.52
27.9702	362.74	0.1181	3.19004	6.49
29.4604	5591.91	0.1574	3.03199	100.00
30.7839	524.92	0.3149	2.90459	9.39
33.1766	160.49	0.1574	2.70037	2.87
34.9652	159.26	0.3149	2.56623	2.85
36.0391	597.81	0.1574	2.49218	10.69
36.5793	140.39	0.1181	2.45661	2.51
37.5253	51.36	0.4723	2.39683	0.92
39.4694	861.53	0.1968	2.28314	15.41
40.9459	54.56	0.4723	2.20416	0.98
42.4649	140.77	0.1574	2.12877	2.52
43.2222	647.08	0.1968	2.09321	11.57
45.6361	71.93	0.4723	1.98794	1.29
47.1929	172.09	0.1181	1.92594	3.08
47.5795	638.15	0.1968	1.91119	11.41
48.5581	620.78	0.1968	1.87493	11.10
50.1414	282.62	0.1181	1.81938	5.05
54.0684	34.27	0.4723	1.69615	0.61
56.6850	105.03	0.2362	1.62391	1.88
57.4512	261.85	0.1574	1.60406	4.68
59.9713	155.02	0.1181	1.54254	2.77
60.7330	187.07	0.1574	1.52501	3.35
61.5414	106.55	0.3149	1.50690	1.91
64.0757	63.10	0.2362	1.45328	1.13
64.7074	160.52	0.1574	1.44062	2.87
65.7539	102.05	0.3936	1.42020	1.83
68.2752	99.06	0.3149	1.37377	1.77
70.3667	85.82	0.3149	1.33798	1.53
73.0082	60.21	0.6298	1.29595	1.08
81.6160	63.73	0.2362	1.17966	1.14
83.8335	117.84	0.1181	1.15401	2.11

**Pattern List**

Visible Ref.Code	Score	Cpd Name	Displ. [°2Th]	Scale Fac.	Chem. Formula
01-085-0796	53	Silicon Oxide	0.000	0.430	Si O <sub>2</sub>
98-017-1524	31	Dolomite	0.000	0.094	C <sub>2</sub> Ca <sub>1</sub> Mg <sub>1</sub> O <sub>6</sub>
01-086-2334	63	Calcium Carbonate	0.000	0.512	Ca( C O <sub>3</sub> )
98-003-4406	25	Muscovite 2M1	0.000	0.091	H <sub>4</sub> Al <sub>5.74</sub> Fe <sub>0.26</sub> K..

**A9: Peak and Pattern list of limestone sample EKA-R02 from XRD Analysis****Peak List**

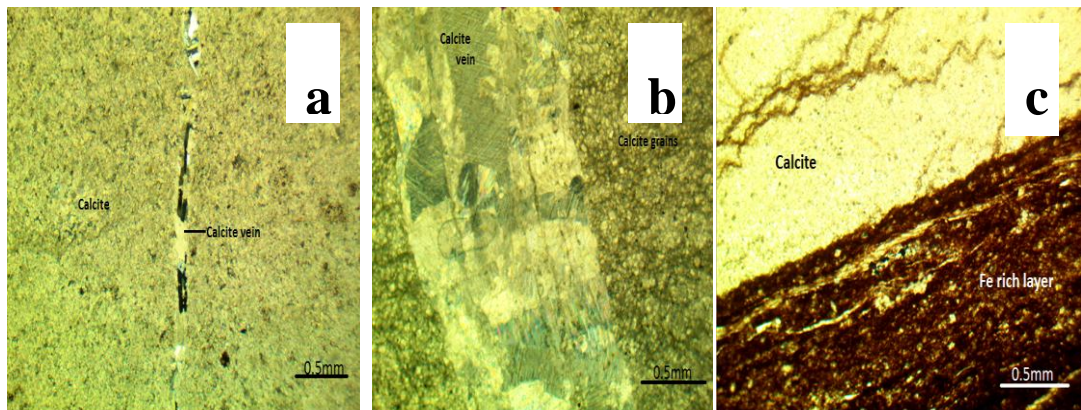
Pos. [°2Th.]	Height [cts]	FWHMLeft [°2Th.]	d-spacing [Å]	Rel. Int. [%]
8.7573	129.07	0.6298	10.09773	1.24
20.8955	90.42	0.1181	4.25137	0.87
23.0991	627.45	0.1574	3.85053	6.02
26.6585	481.37	0.1181	3.34396	4.62
27.9618	101.08	0.1181	3.19098	0.97
29.4547	10414.21	0.1574	3.03257	100.00
31.4897	140.85	0.1574	2.84107	1.35
36.0243	919.79	0.1968	2.49317	8.83
39.4605	1271.67	0.1968	2.28363	12.21
43.2100	1166.05	0.1968	2.09377	11.20
47.1602	301.52	0.1574	1.92719	2.90
47.5476	986.10	0.2755	1.91239	9.47
48.5468	1011.67	0.2755	1.87534	9.71
56.6115	197.14	0.1968	1.62584	1.89
57.4485	403.02	0.1574	1.60413	3.87
60.7171	266.18	0.1574	1.52537	2.56
63.1496	81.11	0.3149	1.47235	0.78
64.6966	264.47	0.2362	1.44083	2.54
65.6985	117.15	0.3149	1.42126	1.12
69.3024	35.08	0.3936	1.35590	0.34
70.3539	77.82	0.3149	1.33819	0.75
72.9498	117.43	0.1574	1.29685	1.13
76.3870	41.58	0.3149	1.24683	0.40
77.2734	68.47	0.4723	1.23472	0.66
81.5967	81.59	0.4723	1.17989	0.78
83.8584	116.68	0.3936	1.15373	1.12
84.8859	63.26	0.4723	1.14237	0.61

**Pattern List**

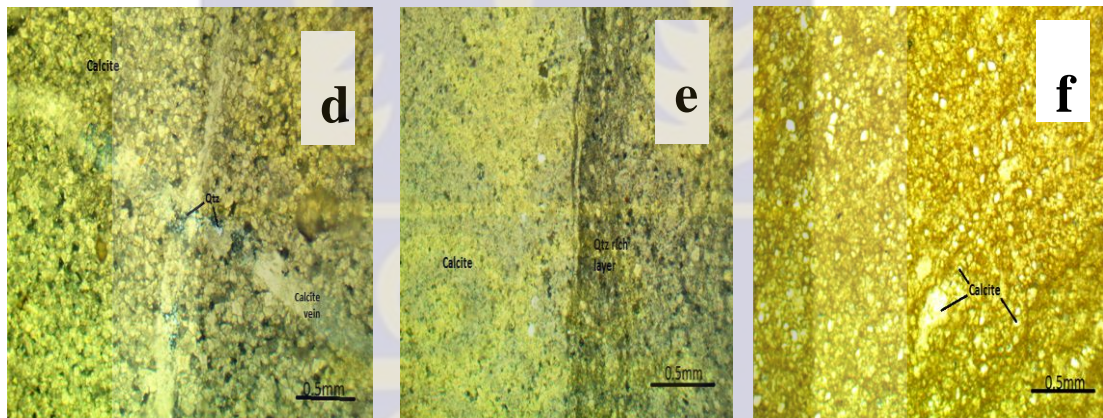
Visible Ref.Code	Score	Cpd Name	Displ. [°2Th]	Scale Fac.	Chem. Formula
01-086-2334	80	Calcium Carbonate	0.000	0.592	Ca( C O3 )
01-083-2199	9	Sodium Calcium Man..	0.000	0.021	Ca0.34 Mn1.65 Na H..
01-078-1252	17	Silicon Oxide	0.000	0.041	Si O2



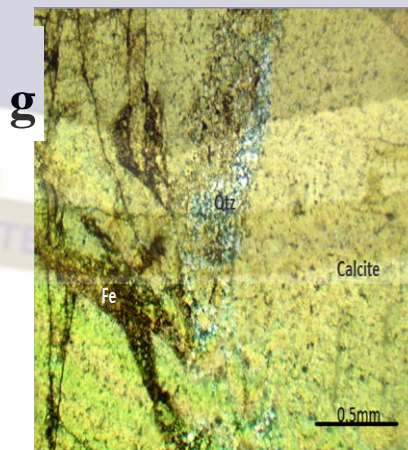
## APPENDIX B: Petrographic Thin Section of limestone samples



(i) : Photomicrograph of limestone samples (a) EKA-Bk03, (b) EKA-B01 and (c) EKL-R102



(ii) Photomicrograph of limestone samples (d) EKA-Y04, (e) EKL-D01 and (f) EKL-Y03



(iii) Photomicrograph of limestone samples (g) EKA-R02

**APPENDIX C: Activity Concentrations of Samples****C1: Activity concentration of limestone sample EKA-B01**

	Radionuclide	Energy (keV)	Net Area	$\gamma$ -Yield	Counting Time	Mass (kg)	Efficiency	Activity
<b>U-238 series</b>	Pb-214	295.2	5562.56	0.193	36000	1.5809	0.2635	1.9218968
		<b>351.932</b>	9830.33	<b>0.376</b>	36000	1.5809	0.234141	1.961982
		241.997	2674.3	0.0743	36000	1.5809	0.301147	2.1000812
	Bi-214	<b>609.312</b>	7594.95	<b>0.461</b>	36000	1.5809	0.161915	1.7878487
		1120.287	1542.96	0.151	36000	1.5809	0.107535	1.6696348
		<b>1764.494</b>	1277.82	<b>0.154</b>	36000	1.5809	0.079245	1.8398067
<b>Th-232 series</b>	Pb-212	<b>238.632</b>	5467.14	<b>0.433</b>	36000	1.5809	0.303994	0.7297943
	Tl-208	<b>583.191</b>	1839.99	<b>0.845</b>	36000	1.5809	0.166753	0.2294447
		510.77	1612.14	0.226	36000	1.5809	0.182293	0.6875689
	Ac-228	338.32	1186.06	0.1127	36000	1.5809	0.240431	0.7691046
		911.204	1330.02	0.258	36000	1.5809	0.123548	0.733153
		968.971	830.47	0.158	36000	1.5809	0.118549	0.7790444
	Ra-224	240.986	2743.67	0.041	36000	1.5809	0.301995	3.8935073
<b>K-40</b>	K-40	<b>1460.83</b>	9860.68	<b>0.11</b>	36000	1.5809	0.089968	17.507319

**C2: Activity concentration of limestone sample EKA-Bk03**

	Radionuclide	Energy (keV)	Net Area	$\gamma$ -Yield	Counting Time	Mass (kg)	Efficiency	Activity
<b>U-238 series</b>	Pb-214	<b>295.224</b>	1718.81	0.193	36000	1.6418	0.263485	0.571862
		<b>351.932</b>	2965.78	<b>0.376</b>	36000	1.6418	0.234141	0.569967
	Bi-214	<b>609.312</b>	2402.72	<b>0.461</b>	36000	1.6418	0.161915	0.544619
<b>Th-232 series</b>	Pb-212	<b>238.632</b>	2130.02	<b>0.433</b>	36000	1.6418	0.303994	0.273784
	Tl-208	<b>510.77</b>	1129.42	0.226	36000	1.6418	0.182293	0.463824
<b>K-40</b>	K-40	<b>1460.83</b>	3169.55	<b>0.11</b>	36000	1.6418	0.089968	5.418693

**C3: Activity concentration of limestone sample EKA-R01**

	Radionuclide	Energy (keV)	Net Area	$\gamma$ -Yield	Counting Time	Mass (kg)	Efficiency	Activity
<b>U-238 series</b>	Pb-214	295.2	1395.24	0.193	36000	1.5586	0.2635	0.4889608
		<b>351.932</b>	2433.47	<b>0.376</b>	36000	1.5586	0.234141	0.492632
		241.997	878.86	0.0743	36000	1.5586	0.301147	0.700028
	Bi-214	<b>609.312</b>	1834.97	<b>0.461</b>	36000	1.5586	0.161915	0.4381316
<b>Th-232 series</b>	Pb-212	<b>238.632</b>	7491.01	<b>0.433</b>	36000	1.5586	0.303994	1.0142625
	Tl-208	<b>583.191</b>	2548.45	<b>0.845</b>	36000	1.5586	0.166753	0.3223358
		510.77	1677.75	0.226	36000	1.5586	0.182293	0.7257891
	Ac-228	338.32	1348.02	0.1127	36000	1.5586	0.240431	0.8866349
		911.204	1647.22	0.258	36000	1.5586	0.123548	0.9209961
		968.971	1011.36	0.158	36000	1.5586	0.118549	0.9623072
	Ra-224	240.986	878.86	0.041	36000	1.5586	0.301995	1.2650234
<b>K-40</b>	K-40	<b>1460.83</b>	17232.86	<b>0.11</b>	36000	1.5586	0.089968	31.034151

**C4: Activity concentration of limestone sample EKA-R02**

	Radionuclide	Energy (keV)	Net Area	$\gamma$ -Yield	Counting Time	Mass (kg)	Efficiency	Activity
<b>U-238 series</b>	Pb-214	<b>351.932</b>	2032.87	0.376	36000	1.5778	0.234141	0.406527
	Bi-214	<b>609.312</b>	1532.62	<b>0.461</b>	36000	1.5778	0.161915	0.361487
<b>Th-232 series</b>	Pb-212	<b>238.632</b>	3896.18	<b>0.433</b>	36000	1.5778	0.303994	0.521113
	Tl-208	<b>583.191</b>	1135.59	0.845	36000	1.5778	0.166753	0.141885
		<b>510.77</b>	1383.08	1.226	36000	1.5778	0.182293	0.591035
<b>K-40</b>	K-40	<b>1460.83</b>	7678.66	<b>0.11</b>	36000	1.5778	0.089968	13.66

**C5: Activity concentration of limestone sample EKA-Y04**

	Radionuclide	Energy (keV)	Net Area	$\gamma$ -Yield	Counting Time	Mass (kg)	Efficiency	Activity
<b>U-238 series</b>	Pb-214	295.2	5889.6	0.193	36000	1.5477	0.2635	2.078542
		<b>351.932</b>	9819.31	<b>0.376</b>	36000	1.5477	0.234141	2.001822
		241.997	3038.37	0.0743	36000	1.5477	0.301147	2.437161
	Bi-214	<b>609.312</b>	8054.82	<b>0.461</b>	36000	1.5477	0.161915	1.936776
		1120.287	1750.34	0.151	36000	1.5477	0.107535	1.93467
		<b>1764.494</b>	1492.19	<b>0.154</b>	36000	1.5477	0.079245	2.194544
<b>Th-232 series</b>	Pb-212	<b>238.632</b>	4420.47	<b>0.433</b>	36000	1.5477	0.303994	0.602735
	Tl-208	<b>583.191</b>	1482.73	<b>0.845</b>	36000	1.5477	0.166753	0.188861
		510.77	1614.27	0.226	36000	1.5477	0.182293	0.703246
		911.204	1045.59	0.258	36000	1.5477	0.123548	0.588729
	Ra-224	240.986	3038.37	0.041	36000	1.5477	0.301995	4.404204
<b>K-40</b>	K-40	<b>1460.83</b>	8053.43	<b>0.11</b>	36000	1.5809	0.089968	14.60533

**C6: Activity concentration of limestone sample EKL-Y03**

	Radionuclide	Energy (keV)	Net Area	$\gamma$ -Yield	Counting Time	Mass (kg)	Efficiency	Activity
<b>U-238 series</b>	Pb-214	295.2	3770.15	0.193	36000	1.5787	0.2635	1.304424
		<b>351.932</b>	6590.99	<b>0.376</b>	36000	1.5787	0.234141	1.317293
		241.997	2088.97	0.0743	36000	1.5787	0.301147	1.642718
	Bi-214	<b>609.312</b>	5102.06	<b>0.461</b>	36000	1.5787	0.161915	1.202697
		1120.287	1075.09	0.151	36000	1.5787	0.107535	1.164975
		<b>1764.494</b>	1020.41	<b>0.154</b>	36000	1.5787	0.079245	1.471235
<b>Th-232 series</b>	Pb-212	<b>238.632</b>	9320.48	<b>0.433</b>	36000	1.5787	0.303994	1.2459
	Tl-208	<b>583.191</b>	3065.88	<b>0.845</b>	36000	1.5787	0.166753	0.382845
		510.77	2223.76	0.226	36000	1.5787	0.182293	0.949743
	Ac-228	338.32	1856.42	0.1127	36000	1.5787	0.240431	1.205479



		911.204	2162.9	0.258	36000	1.5787	0.123548	1.193927
		968.971	1189.78	0.158	36000	1.5787	0.118549	1.11766
	Ra-224	240.986	2066.81	0.041	36000	1.5787	0.301995	2.937071
<b>K-40</b>	K-40	<b>1460.83</b>	17831.52	<b>0.11</b>	36000	1.5787	0.089968	31.70341

### C7: Activity concentration of limestone sample EKL-D01

	Radionuclide	Energy (keV)	Net Area	$\gamma$ -Yield	Counting Time	Mass (kg)	Efficiency	Activity
<b>U-238 series</b>	Pb-214	295.2	14196.33	0.193	36000	1.4757	0.2635	5.254577
		<b>351.932</b>	25386.36	<b>0.376</b>	36000	1.4757	0.234141	5.427923
		241.997	7245.75	0.0743	36000	1.4757	0.301147	6.095588
	Bi-214	<b>609.312</b>	19144.47	<b>0.461</b>	36000	1.4757	0.161915	4.827869
		1120.287	4114.59	0.151	36000	1.4757	0.107535	4.769795
		<b>1764.494</b>	3476.67	<b>0.154</b>	36000	1.4757	0.079245	5.362562
<b>Th-232 series</b>	Pb-212	<b>1238.11</b>	1541.97	<b>0.0579</b>	36000	1.4757	0.100546	4.985771
		<b>238.632</b>	4068.2	<b>0.433</b>	36000	1.4757	0.303994	0.581767
		<b>583.191</b>	1307.22	<b>0.845</b>	36000	1.4757	0.166753	0.17463
	Tl-208	510.77	1529.72	0.226	36000	1.4757	0.182293	0.698927
		911.204	919.72	0.258	36000	1.4757	0.123548	0.543123
		240.986	7245.75	0.041	36000	1.4757	0.301995	11.01536
<b>K-40</b>	K-40	<b>1460.83</b>	6312.86	<b>0.11</b>	36000	1.4757	0.089968	12.0073

**C8: Activity concentration of limestone sample EKL-R102**

	Radionuclide	Energy (keV)	Net Area	$\gamma$ -Yield	Counting Time	Mass (kg)	Efficiency	Activity
<b>U-238 series</b>	Pb-214	295.2	1847.85	0.193	36000	1.3911	0.2635	0.725551
		<b>351.932</b>	3254.88	<b>0.376</b>	36000	1.3911	0.234141	0.738258
		241.997	1368	0.0743	36000	1.3911	0.301147	0.738258
	Bi-214	<b>609.312</b>	2558.15	<b>0.461</b>	36000	1.3911	0.161915	1.220838
<b>Th-232 series</b>	Tl-208	<b>583.191</b>	3633.63	<b>0.845</b>	36000	1.3911	0.166753	0.684349
		510.77	2056.66	0.226	36000	1.3911	0.182293	0.514931
	Ac-228	338.32	2065.82	0.1127	36000	1.3911	0.240431	0.996832
		911.204	2459	0.258	36000	1.3911	0.123548	1.540427
		968.971	1515.81	0.158	36000	1.3911	0.118549	1.615954
	Ra-224	240.986	1369.08	0.041	36000	1.3911	0.301995	2.207923
<b>K-40</b>	K-40	<b>1460.83</b>	24482.38	<b>0.11</b>	36000	1.3911	0.089968	49.39835





## C9: Certificate of Reference material for radiological analysis

**CZECH METROLOGY INSTITUTE**  
INSPECTORATE FOR IONIZING RADIATION  
Ráztová 3, 102 00 Praha 10

## CERTIFICATE

Cont. No. 9031 - OL - 146/14	Type: MIRS 2	Prod. No. 050214-1425039	
Radiounit	Half life days	Activity kBq	Combined standard uncertainty, %
Am-241	157000	4,694	1.1
Cd-109	462,6	14,34	1.4
Co-139	137,5	1,335	1.1
Co-57	271,26	1,156	1.1
Co-60	1925,4	2,697	1.1
Co-137	11019	2,689	1.3
Sr-115	115,1	4,000	2.2
Se-85	64,78	4,570	1.3
Y-88	106,6	5,323	1.2

Mass: 980,0 g      Density: 0,98 g/cm<sup>3</sup>      Volume: 1000 cm<sup>3</sup>  
 Radioactive impurities: gamma < 0,1 %  
 Reference date: 20.3.2014      Homogeneity better than: 1 %

**Description:**  
 Radioactive material is homogeneously dispersed in silicone resin. Composition of the matrix: C - 0,034 H - 0,0056 O - 0,214 % - 1,379 (mass ratio).  
**Measuring method:**  
 Preparation from standard SR solutions whose activities were determined by suitable absolute method. Final control is based on gamma spectrometry on HPGe detector.  
**Note:**  
 As the criterion of homogeneity standard deviation of the activity value of 1 cm<sup>3</sup> element was chosen (p=3). The volume is calculated from the mass and the density.

Date of the certificate issue: 25.3.2014      Validity: 5 years

**Customer:**  
 CANBERRA-PACKARD CENTRAL EUROPE  
 Wernersiedlung 6  
 A-2432 Schwandorf  
 Austria

**Control:** RNDr. Richard Bladovský, CSc., RNDr. Pavel Dvůřák, CSc.

Tel.: +420 266 020 497      Fax: +420 266 020 466

## Appendix

Uncertainty of declared quantity is processed in accordance with the recommendation ISO 1993 "Guide to the Expression of Uncertainty in Measurement".

Uncertainty of the result, described by a combined standard uncertainty on confidence level  $P = 68,3 \%$ , is expressed as a square root of the sum of the second power of type A and type B standard uncertainties.

Type A standard uncertainty is experimental standard deviation of the mean  $\bar{x}_0$  of a set of values of measured quantity influencing immediately to the activity (number of counts, counting current etc.).

$$s_x = \sqrt{\frac{1}{n(n-1)} \sum_{i=1}^n (x_i - \bar{x})^2}$$

$$\bar{x} = \frac{1}{n} \sum_{i=1}^n x_i$$

$n$  = number of repeated measurements  
 $x_i$  = measured values  
 $\bar{x}$  = average of measured values

Type B standard uncertainty is usually determined by methods another than statistical ones. It is expressed as a square root of sum of second power of standard uncertainties of quantity values which influence results of measurement, e.g. uncertainties of half-life, weight, dead time of the device, geometrical factor, height, standard etc. Standard uncertainties are in the most cases determined by a qualified estimation (for instance on a basis of a long-time observation, from a description of used measuring device etc.).

**A**  
CANBERRA

### DETECTOR SPECIFICATION AND PERFORMANCE DATA

**Specifications**

Detector Model	GM4020	Serial number	h34130
Cryostat Model	2500SL		
Preamplifier Model	2002CSL		

The purchase specifications and therefore the warranted performance of this detector are as follows:

Nominal volume \_\_\_\_\_ cc      Relative efficiency \_\_\_\_\_ %

Resolution \_\_\_\_\_ keV (FWHM) at 1.33 MeV  
 \_\_\_\_\_ keV (FWHM) at 1.33 MeV  
 1.10 keV (FWHM) at 122 keV  
 \_\_\_\_\_ keV (FWHM) at \_\_\_\_\_ keV

Peak/Compton \_\_\_\_\_      Cryostat well diameter \_\_\_\_\_ mm      Well depth \_\_\_\_\_ mm  
 Cryostat description or Drawing Number if special 2500SL

**Physical Characteristics**

Geometry \_\_\_\_\_ Coaxial one open end, closed end, beam window

Diameter	60,5 mm	Active volume	cc
Length	61,5 mm	Crystal well depth	mm
Distance from window (outside)	6 mm	Crystal well diameter	mm

**Electrical Characteristics**

Depletion voltage \_\_\_\_\_ Vdc      Vdc \_\_\_\_\_ Vdc  
 Recommended bias voltage Vdc \_\_\_\_\_ Vdc  
 Leakage current at recommended bias \_\_\_\_\_ nA  
 Preamplifier test point voltage at recommended voltage \_\_\_\_\_ Vdc

**Resolution and Efficiency**

With amp time constant of \_\_\_\_\_  $\mu$ s

Isotope	<sup>57</sup> Co	<sup>60</sup> Co
Energy (keV)	122	1332
FWHM (keV)	578	192
FWHM (keV)		3.51
Peak/Compton	63.4:1	
Rel. Efficiency	44.2%	

- Tests are performed following IEEE standard test ANSIEEE M325-1996  
 - Standard Canberra electronics used - See Germanium detector manual Section 7

Tested by: \_\_\_\_\_ Date: January 29, 2014  
 Approved by: \_\_\_\_\_ Date: January 29, 2014

12432007

1/1

GD4ME001/P

**APPENDIX D: Batch Adsorption Analysis**D1: % fluoride adsorption of sample EKL-R<sub>1</sub>02 in 1 mg/L NaF solution.

Mass of sample (g)	Particle size (µm)	Initial F <sup>-</sup> Conc measured[Co] (mg/L)	Residual F <sup>-</sup> Conc[Ct] (mg/L)	Time (min)	% Adsorption	% Mean Adsorption (first 60 <sup>th</sup> min)	Adsorption capacity
10.003	500-1000	1.0973	0.7655	15	30.24	50.8931	3.3170
10.005	500-1000	1.0973	0.6243	30	43.11		4.7286
10.002	500-1000	1.0973	0.3124	45	71.53		7.8466
10.001	500-1000	1.0973	0.4532	60	58.70		6.4391
10.002	500-1000	1.0973	0.7213	75	34.27		3.7589
10.004	500-1000	1.0973	1.0973	90	11.34		1.2436
10.006	1000-2000	1.0973	0.7105	15	35.25	57.2724	3.8668
10.004	1000-2000	1.0973	0.5871	30	46.50		5.1005
10.004	1000-2000	1.0973	0.3257	45	70.32		7.7137
10.002	1000-2000	1.0973	0.2521	60	77.03		8.4495
10.001	1000-2000	1.0973	1.0102	75	7.94		0.8707
10.004	1000-2000	1.0973	1.0509	90	4.23		0.4639
10.001	2000-6350	1.0973	0.5217	15	52.46	32.9422	5.7543
10.000	2000-6350	1.0973	0.6732	30	38.65		4.2397
10.003	2000-6350	1.0973	0.7852	45	28.44		3.1201
10.003	2000-6350	1.0973	0.9632	60	12.22		1.3406
10.006	2000-6350	1.0973	1.0038	75	8.52		0.9347
10.004	2000-6350	1.0973	1.0021	90	8.68		0.9517
Mass of sample (g)	Particle size (µm)	Initial F <sup>-</sup> Conc measured[Co] (mg/L)	Residual F <sup>-</sup> Conc[Ct] (mg/L)	Time (min)	% Adsorption	% Mean Adsorption (first 60 <sup>th</sup> min)	Adsorption capacity
50.004	500-1000	1.0973	0.8442	15	23.07	42.6387	2.5302
50.002	500-1000	1.0973	0.6875	30	37.35		4.0968
50.004	500-1000	1.0973	0.6373	45	41.92		4.5986
50.003	500-1000	1.0973	0.3487	60	68.22		7.4838
50.001	500-1000	1.0973	0.8423	75	23.24		2.5492
50.002	500-1000	1.0973	0.9321	90	15.06		1.6515
50.006	1000-2000	1.0973	0.7329	15	33.21	44.6573	3.6429
50.004	1000-2000	1.0973	0.6285	30	42.72		4.6866
50.002	1000-2000	1.0973	0.4502	45	58.97		6.4691
50.001	1000-2000	1.0973	0.6175	60	43.73		4.7966
50.002	1000-2000	1.0973	0.8761	75	20.16		2.2113
50.002	1000-2000	1.0973	1.0010	90	8.78		0.9627
50.002	2000-6350	1.0973	0.6551	15	40.30	47.0222	4.4207
50.004	2000-6350	1.0973	0.6212	30	43.39		4.7596
50.004	2000-6350	1.0973	0.5471	45	50.14		5.5003
50.001	2000-6350	1.0973	0.5019	60	54.26		5.9522
50.005	2000-6350	1.0973	0.8563	75	21.96		2.4093
50.003	2000-6350	1.0973	0.9728	90	11.35		1.2446
Mass of sample (g)	Particle size (µm)	Initial F <sup>-</sup> Conc measured[Co] (mg/L)	Residual F <sup>-</sup> Conc[Ct] (mg/L)	Time (min)	% Adsorption	% Mean Adsorption (first 60 <sup>th</sup> min)	Adsorption capacity
100.000	500-1000	1.0973	0.8442	15	23.07	42.6387	2.5302
100.002	500-1000	1.0973	0.6875	30	37.35		4.0968
100.003	500-1000	1.0973	0.6373	45	41.92		4.5986
100.001	500-1000	1.0973	0.3487	60	68.22		7.4838
100.006	500-1000	1.0973	0.8423	75	23.24		2.5492
100.007	500-1000	1.0973	0.9321	90	15.06		1.6515
100.004	1000-2000	1.0973	0.7329	15	33.21		3.6429

100.005	1000-2000	1.0973	0.6285	30	42.72	44.6573	4.6866
100.002	1000-2000	1.0973	0.4502	45	58.97		6.4691
100.003	1000-2000	1.0973	0.6175	60	43.73		4.7966
100.005	1000-2000	1.0973	0.8761	75	20.16		2.2113
100.007	1000-2000	1.0973	1.0010	90	8.78		0.9627
100.002	2000-6350	1.0973	0.6551	15	40.30	47.0222	4.4207
100.004	2000-6350	1.0973	0.6212	30	43.39		4.7596
100.001	2000-6350	1.0973	0.5471	45	50.14		5.5003
100.001	2000-6350	1.0973	0.5019	60	54.26		5.9522
100.003	2000-6350	1.0973	0.8563	75	21.96		2.4093
100.001	2000-6350	1.0973	0.9728	90	11.35		1.2446

D2: % fluoride adsorption of sample EKL-R<sub>102</sub> in 5 mg/L NaF solution

Mass of sample (g)	Particle size (µm)	Initial F <sup>-</sup> Conc measured[Co] (mg/L)	Residual F <sup>-</sup> Conc[Ct] (mg/L)	Time (min)	% Adsorption	% Mean Adsorption (first 60 <sup>th</sup> min)	Adsorption capacity
10.002	500-1000	5.0506	3.4666	15	31.84	49.96	15.8368
10.001	500-1000	5.0506	2.9810	30	40.98		20.6919
10.003	500-1000	5.0506	2.3066	45	54.33		27.4345
10.004	500-1000	5.0506	1.3547	60	73.18		36.9516
10.002	500-1000	5.0506	2.7413	75	45.72		23.0883
10.000	500-1000	5.0506	4.4356	90	12.18		6.1488
10.002	1000-2000	5.0506	4.1849	15	17.14	45.37	8.6552
10.001	1000-2000	5.0506	2.6734	30	47.07		23.7672
10.000	1000-2000	5.0506	2.2037	45	56.37		28.4633
10.000	1000-2000	5.0506	1.9748	60	60.90		30.7518
10.003	1000-2000	5.0506	2.3972	75	52.54		26.5286
10.004	1000-2000	5.0506	2.0739	90	58.94		29.7610
10.002	2000-6350	5.0506	2.7840	15	44.88	25.64	
10.001	2000-6350	5.0506	3.7496	30	25.76		22.6615
10.003	2000-6350	5.0506	3.9334	45	22.12		13.0074
10.000	2000-6350	5.0506	4.5555	60	9.80		11.1698
10.000	2000-6350	5.0506	3.7726	75	25.30		4.9500
10.004	2000-6350	5.0506	2.0534	90	59.34		29.9660
Mass of sample (g)	Particle size (µm)	Initial F <sup>-</sup> Conc measured[Co] (mg/L)	Residual F <sup>-</sup> Conc[Ct] (mg/L)	Time (min)	% Adsorption	% Mean Adsorption (first 60 <sup>th</sup> min)	Adsorption capacity
50.003	500-1000	5.0506	2.6712	15	47.11	54.96	23.7892
50.001	500-1000	5.0506	2.5713	30	49.09		24.7880
50.001	500-1000	5.0506	2.1127	45	58.17		29.3731
50.003	500-1000	5.0506	1.7436	60	65.48		33.0634
50.000	500-1000	5.0506	3.6812	75	27.11		13.6913
50.005	500-1000	5.0506	3.9084	90	22.62		11.4197
50.005	1000-2000	5.0506	2.4247	15	51.99	62.96	26.2537
50.002	1000-2000	5.0506	2.2542	30	55.37		27.9584
50.000	1000-2000	5.0506	1.6272	45	67.78		34.2272
50.006	1000-2000	5.0506	1.1773	60	76.69		38.7253
50.000	1000-2000	5.0506	3.9911	75	20.98		10.5929
50.000	1000-2000	5.0506	3.2791	90	35.08		17.7115
50.002	2000-6350	5.0506	2.5710	15	49.10	34.66	24.7910
50.001	2000-6350	5.0506	3.7994	30	24.77		12.5095
50.000	2000-6350	5.0506	3.5678	45	29.36		14.8250
50.000	2000-6350	5.0506	3.2614	60	35.43		17.8884
50.003	2000-6350	5.0506	3.5417	75	29.88		15.0860
50.000	2000-6350	5.0506	3.2978	90	34.70		17.5245

Mass of sample (g)	Particle size (µm)	Initial F <sup>-</sup> Conc measured[Co] (mg/L)	Residual F <sup>-</sup> Conc[Ct] (mg/L)	Time (min)	% Adsorption	% Mean Adsorption (first 60 <sup>th</sup> min)	Adsorption capacity
100.003	500-1000	5.0506	3.8411	15	23.95	28.19	12.0926
100.002	500-1000	5.0506	3.4149	30	32.39		16.3537
100.000	500-1000	5.0506	3.5173	45	30.36		15.3299
100.005	500-1000	5.0506	3.7349	60	26.05		13.1544
100.000	500-1000	5.0506	2.0094	75	60.21		30.4059
100.000	500-1000	5.0506	3.0998	90	38.63		19.5041
100.002	1000-2000	5.0506	3.3606	15	33.46	50.44	16.8966
100.004	1000-2000	5.0506	2.3515	30	53.44		26.9856
100.000	1000-2000	5.0506	2.2386	45	55.68		28.1144
100.000	1000-2000	5.0506	2.0613	60	59.19		29.8870
100.007	1000-2000	5.0506	2.6714	75	47.11		23.7872
100.000	1000-2000	5.0506	2.9827	90	40.94		20.6749
100.002	2000-6350	5.0506	4.7412	15	6.13	20.22	3.0934
100.004	2000-6350	5.0506	4.1127	30	18.57		9.3771
100.000	2000-6350	5.0506	3.6824	45	27.09		13.6793
100.004	2000-6350	5.0506	3.5814	60	29.09		14.6891
100.000	2000-6350	5.0506	3.8410	75	23.95		12.0963
100.001	2000-6350	5.0506	3.5515	90	29.68		14.9880

D3: % fluoride adsorption of sample EKL-R<sub>102</sub> in 10 mg/L NaF solution.

Mass of sample (g)	Particle size (µm)	Initial F <sup>-</sup> Conc measured[Co] (mg/L)	Residual F <sup>-</sup> Conc[Ct] (mg/L)	Time (min)	% Adsorption	% Mean Adsorption (first 60 <sup>th</sup> min)	Adsorption capacity
10.003	500-1000	10.1726	6.0761	15	40.27	47.4476	40.9568
10.005	500-1000	10.1726	5.6827	30	44.14		44.8945
10.002	500-1000	10.1726	5.6221	45	44.73		45.4914
10.001	500-1000	10.1726	4.0029	60	60.65		61.6723
10.002	500-1000	10.1726	7.7931	75	23.39		23.7902
10.004	500-1000	10.1726	8.8365	90	13.13		13.3610
10.006	1000-2000	10.1726	6.8015	15	33.14	40.7637	33.7043
10.004	1000-2000	10.1726	6.4512	30	36.58		37.2103
10.004	1000-2000	10.1726	5.6719	45	44.24		45.0070
10.002	1000-2000	10.1726	5.1789	60	49.09		49.9370
10.001	1000-2000	10.1726	6.5058	75	36.05		36.6570
10.004	1000-2000	10.1726	8.8312	90	13.19		13.4086
10.001	2000-6350	10.1726	6.6754	15	34.38	39.7932	34.9650
10.000	2000-6350	10.1726	6.6298	30	34.83		35.4245
10.003	2000-6350	10.1726	5.0143	45	50.71		51.5675
10.003	2000-6350	10.1726	6.1789	60	39.26		39.9370
10.006	2000-6350	10.1726	6.9995	75	31.19		31.7310
10.004	2000-6350	10.1726	8.4802	90	16.64		16.9172

Mass of sample (g)	Particle size (µm)	Initial F <sup>-</sup> Conc measured[Co] (mg/L)	Residual F <sup>-</sup> Conc[Ct] (mg/L)	Time (min)	% Adsorption	% Mean Adsorption (first 60 <sup>th</sup> min)	Adsorption capacity
50.004	500-1000	10.1726	6.2541	15	38.52	46.1227	7.8365
50.002	500-1000	10.1726	5.9027	30	41.97		8.5396
50.004	500-1000	10.1726	5.2584	45	48.31		9.8282
50.003	500-1000	10.1726	4.5077	60	55.69		11.3291
50.001	500-1000	10.1726	7.6603	75	24.70		5.0246
50.002	500-1000	10.1726	8.4207	90	17.22		3.5034
50.006	1000-2000	10.1726	6.0344	15	40.68		8.2756
50.004	1000-2000	10.1726	5.3942	30	46.97		9.5564



50.002	1000-2000	10.1726	4.4393	45	56.36	50.9624	11.4666
50.001	1000-2000	10.1726	4.0857	60	59.84		12.1723
50.002	1000-2000	10.1726	7.4160	75	27.10		5.5132
50.002	1000-2000	10.1726	8.4197	90	17.23		3.5058
50.002	2000-6350	10.1726	6.9566	15	31.61		6.4317
50.004	2000-6350	10.1726	6.2906	30	38.16		7.7638
50.004	2000-6350	10.1726	5.0797	45	50.06	36.4287	10.1858
50.001	2000-6350	10.1726	7.5405	60	25.87		5.2642
50.005	2000-6350	10.1726	7.3408	75	27.84		5.6632
50.003	2000-6350	10.1726	8.0572	90	20.80		4.2308

Mass of sample (g)	Particle size (µm)	Initial F <sup>-</sup> Conc measured[Co] (mg/L)	Residual F <sup>-</sup> Conc[Ct] (mg/L)	Time (min)	% Adsorption	% Mean Adsorption (first 60 <sup>th</sup> min)	Adsorption capacity
100.000	500-1000	10.1726	6.0291	15	40.73		4.1434
100.002	500-1000	10.1726	5.5775	30	45.17		4.5950
100.003	500-1000	10.1726	4.7422	45	53.38		5.4304
100.001	500-1000	10.1726	4.1481	60	59.22	49.6272	6.0242
100.006	500-1000	10.1726	7.7651	75	23.67		2.4075
100.007	500-1000	10.1726	9.1726	90	9.83		1.0000
100.004	1000-2000	10.1726	6.6003	15	35.12		3.5722
100.005	1000-2000	10.1726	5.8207	30	42.78		4.3517
100.002	1000-2000	10.1726	5.0113	45	50.74	45.2293	5.1613
100.003	1000-2000	10.1726	4.8541	60	52.28		5.3185
100.005	1000-2000	10.1726	6.9612	75	31.57		3.2212
100.007	1000-2000	10.1726	8.9621	90	11.90		1.2105
100.002	2000-6350	10.1726	6.3789	15	37.29		3.7936
100.004	2000-6350	10.1726	5.8219	30	42.77		4.3505
100.001	2000-6350	10.1726	5.2904	45	47.99	43.9806	4.8822
100.001	2000-6350	10.1726	5.3033	60	47.87		4.8691
100.003	2000-6350	1.0973	7.6533	75	24.77		2.5193
100.001	2000-6350	1.0973	8.8235	90	13.26		1.3491

#### D4: % fluoride adsorption of sample EKL-D01 in 1 mg/L NaF solution

Mass of sample (g)	Particle size (µm)	Initial F <sup>-</sup> Conc measured[Co] (mg/L)	Residual F <sup>-</sup> Conc[Ct] (mg/L)	Time (min)	% Adsorption	% Mean Adsorption (first 60 <sup>th</sup> min)	Adsorption capacity
10.003	500-1000	1.0230	1.0010	15	2.15		0.2200
10.005	500-1000	1.0230	0.8672	30	15.23		1.5577
10.002	500-1000	1.0230	0.5902	45	42.31		4.3271
10.001	500-1000	1.0230	0.4721	60	53.85	28.3847	5.5079
10.002	500-1000	1.0230	0.6453	75	36.92		3.7762
10.004	500-1000	1.0230	0.9783	90	4.37		0.4469
10.006	1000-2000	1.0230	0.9871	15	3.51		0.3589
10.004	1000-2000	1.0230	0.8372	30	18.16		1.8576
10.004	1000-2000	1.0230	0.5439	45	46.83		4.3271
10.002	1000-2000	1.0230	0.4329	60	57.68	31.5469	5.5079
10.001	1000-2000	1.0230	1.6734	75	34.17		3.7762
10.004	1000-2000	1.0230	0.8217	90	19.68		2.0126
10.001	2000-6350	1.0230	1.0080	15	1.47		0.1500
10.000	2000-6350	1.0230	0.9782	30	4.38		0.4479
10.003	2000-6350	1.0230	0.7329	45	28.36	16.1364	2.9004
10.003	2000-6350	1.0230	0.7126	60	30.34		3.1034
10.006	2000-6350	1.0230	1.8267	75	19.19		1.9626
10.004	2000-6350	1.0230	0.9864	90	3.58		0.3559

Mass of sample (g)	Particle size (µm)	Initial F <sup>-</sup> Conc measured[Co] (mg/L)	Residual F <sup>-</sup> Conc[Ct] (mg/L)	Time (min)	% Adsorption	% Mean Adsorption (first 60 <sup>th</sup> min)	Adsorption capacity
50.004	500-1000	1.0230	0.9943	15	2.81	32.8641	0.2869
50.002	500-1000	1.0230	0.5481	30	46.42		4.7481
50.004	500-1000	1.0230	0.6750	45	34.02		3.4793
50.003	500-1000	1.0230	0.5298	60	48.21		4.9310
50.001	500-1000	1.0230	0.7851	75	23.26		2.3785
50.002	500-1000	1.0230	1.0154	90	0.74		0.0760
50.006	1000-2000	1.0230	0.9431	15	7.81	27.2776	0.7988
50.004	1000-2000	1.0230	0.7593	30	25.78		2.6365
50.002	1000-2000	1.0230	0.6581	45	35.67		3.6483
50.001	1000-2000	1.0230	0.6153	60	39.85		4.0762
50.002	1000-2000	1.0230	0.7359	75	28.06		2.8704
50.002	1000-2000	1.0230	0.8761	90	14.36		1.4687
50.002	2000-6350	1.0230	0.8621	15	15.73	24.5552	1.6087
50.004	2000-6350	1.0230	0.8218	30	19.67		2.0116
50.004	2000-6350	1.0230	0.6541	45	36.06		3.6883
50.001	2000-6350	1.0230	0.7492	60	26.76		2.7375
50.005	2000-6350	1.0230	0.8789	75	14.09		1.4407
50.003	2000-6350	1.0230	1.0032	90	1.94		0.1980
Mass of sample (g)	Particle size (µm)	Initial F <sup>-</sup> Conc measured[Co] (mg/L)	Residual F <sup>-</sup> Conc[Ct] (mg/L)	Time (min)	% Adsorption	% Mean Adsorption (first 60 <sup>th</sup> min)	Adsorption capacity
100.000	500-1000	1.0230	0.8961	15	1.27	20.7551	1.2687
100.002	500-1000	1.0230	0.7654	30	2.58		2.5755
100.003	500-1000	1.0230	0.7432	45	2.80		2.7974
100.001	500-1000	1.0230	0.8380	60	1.85		1.8496
100.006	500-1000	1.0230	0.7201	75	3.03		3.0284
100.007	500-1000	1.0230	0.9126	90	1.10		1.1038
100.004	1000-2000	1.0230	0.8756	15	1.47	24.1544	1.4737
100.005	1000-2000	1.0230	0.8219	30	2.01		2.0106
100.002	1000-2000	1.0230	0.7651	45	2.58		2.5785
100.003	1000-2000	1.0230	0.6410	60	3.82		3.8192
100.005	1000-2000	1.0230	0.8616	75	1.61		1.6137
100.007	1000-2000	1.0230	0.9128	90	1.10		1.1018
100.002	2000-6350	1.0230	0.8812	15	1.42	23.6022	1.4177
100.004	2000-6350	1.0230	0.8127	30	2.10		2.1026
100.001	2000-6350	1.0230	0.7219	45	3.01		3.0104
100.001	2000-6350	1.0230	0.7104	60	3.13		3.1254
100.003	2000-6350	1.0230	0.8903	75	1.33		1.3267
100.001	2000-6350	1.0230	0.9921	90	0.31		0.3089

**D5: % fluoride adsorption of sample EKL-D01 in 5 mg/L NaF solution.**

Mass of sample (g)	Particle size (µm)	Initial F <sup>-</sup> Conc measured[Co] (mg/L)	Residual F <sup>-</sup> Conc[Ct] (mg/L)	Time (min)	% Adsorption	% Mean Adsorption (first 60 <sup>th</sup> min)	Adsorption capacity
10.003	500-1000	4.9561	3.8412	15	22.50	29.1726	11.1468
10.005	500-1000	4.9561	3.7364	30	24.61		12.1946
10.002	500-1000	4.9561	3.8122	45	23.08		11.4367
10.001	500-1000	4.9561	2.6513	60	46.50		23.0434
10.002	500-1000	4.9561	3.5593	75	28.18		13.9652
10.004	500-1000	4.9561	4.1582	90	16.10		7.9774
10.006	1000-2000	4.9561	4.6521	15	6.13	37.56	3.0394
10.004	1000-2000	4.9561	3.0948	30	37.56		18.6093



10.004	1000-2000	4.9561	2.8264	45	42.97	32.5352	21.2927
10.002	1000-2000	4.9561	2.8012	60	43.48		21.5447
10.001	1000-2000	4.9561	4.6231	75	6.72		3.3293
10.004	1000-2000	4.9561	4.8731	90	1.67		0.8298
10.001	2000-6350	4.9561	4.8391	15	2.36		1.1698
10.000	2000-6350	4.9561	3.7859	30	23.61		11.6997
10.003	2000-6350	4.9561	2.2799	45	54.00	37.5391	26.7566
10.003	2000-6350	4.9561	1.4776	60	70.19		34.7780
10.006	2000-6350	4.9561	3.0795	75	37.86		18.7622
10.004	2000-6350	4.9561	4.6867	90	5.44		2.6935

Mass of sample (g)	Particle size (µm)	Initial F <sup>-</sup> Conc measured[Co] (mg/L)	Residual F <sup>-</sup> Conc[Ct] (mg/L)	Time (min)	% Adsorption	% Mean Adsorption (first 60 <sup>th</sup> min)	Adsorption capacity
50.004	500-1000	4.9561	3.9283	15	20.74		10.2759
50.002	500-1000	4.9561	3.3567	30	32.27		15.9908
50.004	500-1000	4.9561	2.2835	45	53.93		26.7207
50.003	500-1000	4.9561	2.1373	60	56.88	40.9526	28.1824
50.001	500-1000	4.9561	3.9061	75	21.19		10.4979
50.002	500-1000	4.9561	4.1822	90	15.62		7.7375
50.006	1000-2000	4.9561	3.9065	15	21.18		10.4939
50.004	1000-2000	4.9561	3.3911	30	31.58		15.6469
50.002	1000-2000	4.9561	3.1288	45	36.87	36.6937	18.2693
50.001	1000-2000	4.9561	2.1237	60	57.15		28.3183
50.002	1000-2000	4.9561	2.7422	75	44.67		22.1346
50.002	1000-2000	4.9561	4.5833	90	7.52		3.7273
50.002	2000-6350	4.9561	4.7546	15	4.07		2.0146
50.004	2000-6350	4.9561	4.3074	30	13.09		6.4857
50.004	2000-6350	4.9561	4.1918	45	15.42	14.5770	7.6415
50.001	2000-6350	4.9561	3.6808	60	25.73		12.7504
50.005	2000-6350	4.9561	3.9079	75	21.15		10.4799
50.003	2000-6350	4.9561	4.3884	90	11.45		5.6759

Mass of sample (g)	Particle size (µm)	Initial F <sup>-</sup> Conc measured[Co] (mg/L)	Residual F <sup>-</sup> Conc[Ct] (mg/L)	Time (min)	% Adsorption	% Mean Adsorption (first 60 <sup>th</sup> min)	Adsorption capacity
100.000	500-1000	4.9561	4.4688	15	9.83		4.8720
100.002	500-1000	4.9561	3.7352	30	24.63		12.2066
100.003	500-1000	4.9561	2.9127	45	41.23		20.4299
100.001	500-1000	4.9561	2.7571	60	44.37	30.0165	21.9856
100.006	500-1000	4.9561	3.5452	75	28.47		14.1062
100.007	500-1000	4.9561	4.4587	90	10.04		4.9730
100.004	1000-2000	4.9561	4.8754	15	1.63		0.8068
100.005	1000-2000	4.9561	4.4201	30	10.81		5.3589
100.002	1000-2000	4.9561	3.8541	45	22.24	15.9314	11.0178
100.003	1000-2000	4.9561	3.5165	60	29.05		14.3931
100.005	1000-2000	4.9561	4.7611	75	3.93		1.9496
100.007	1000-2000	4.9561	4.8897	90	1.34		0.6639
100.002	2000-6350	4.9561	4.4460	15	10.29		5.0910
100.004	2000-6350	4.9561	3.7315	30	24.71		12.2436
100.001	2000-6350	4.9561	3.9839	45	19.62	18.9463	9.7201
100.001	2000-6350	4.9561	3.9070	60	21.17		10.4889
100.003	2000-6350	4.9561	4.3410	75	12.41		6.1498
100.001	2000-6350	4.9561	4.6063	90	7.06		3.4973

D6: % fluoride adsorption of sample EKL-D01 in 10 mg/L NaF solution.

Mass of sample (g)	Particle size (µm)	Initial F <sup>-</sup> Conc measured[Co] (mg/L)	Residual F <sup>-</sup> Conc[Ct] (mg/L)	Time (min)	% Adsorption	% Mean Adsorption (first 60 <sup>th</sup> min)	Adsorption capacity
10.003	500-1000	9.9518	6.6468	15	33.21	41.8005	33.0434
10.005	500-1000	9.9518	4.4742	30	55.04		54.7705
10.002	500-1000	9.9518	4.2127	45	57.67		57.3738
10.001	500-1000	9.9518	7.8339	60	21.28		21.1705
10.002	500-1000	9.9518	8.2214	75	17.39		17.3005
10.004	500-1000	9.9518	8.5614	90	13.97		13.9040
10.006	1000-2000	9.9518	6.4541	15	35.15	41.2458	34.9700
10.004	1000-2000	9.9518	6.2194	30	37.50		37.3203
10.004	1000-2000	9.9518	5.4867	45	44.87		44.6510
10.002	1000-2000	9.9518	5.2282	60	47.46		47.2360
10.001	1000-2000	9.9518	7.9727	75	19.89		19.7851
10.004	1000-2000	9.9518	9.5082	90	4.46		4.4342
10.001	2000-6350	9.9518	8.6150	15	13.43	17.7317	13.3653
10.000	2000-6350	9.9518	8.4017	30	15.58		15.4994
10.003	2000-6350	9.9518	8.1342	45	18.26		18.1705
10.003	2000-6350	9.9518	7.5978	60	23.65		23.5400
10.006	2000-6350	9.9518	7.9544	75	20.07		19.9740
10.004	2000-6350	9.9518	8.8241	90	11.33		11.2725
Mass of sample (g)	Particle size (µm)	Initial F <sup>-</sup> Conc measured[Co] (mg/L)	Residual F <sup>-</sup> Conc[Ct] (mg/L)	Time (min)	% Adsorption	% Mean Adsorption (first 60 <sup>th</sup> min)	Adsorption capacity
50.004	500-1000	9.9518	6.3917	15	35.77	31.4968	7.1198
50.002	500-1000	9.9518	6.4882	30	34.80		6.9271
50.004	500-1000	9.9518	6.2341	45	37.36		7.4353
50.003	500-1000	9.9518	8.1552	60	18.05		3.5930
50.001	500-1000	9.9518	8.8471	75	11.10		2.2094
50.002	500-1000	9.9518	8.6941	90	12.64		2.5151
50.006	1000-2000	9.9518	6.1153	15	38.55	35.5134	7.6722
50.004	1000-2000	9.9518	6.0360	30	39.35		7.8313
50.002	1000-2000	9.9518	6.3671	45	36.02		7.1694
50.001	1000-2000	9.9518	7.1519	60	28.13		5.5991
50.002	1000-2000	9.9518	8.9554	75	10.01		1.9928
50.002	1000-2000	9.9518	9.7098	90	2.43		0.4840
50.002	2000-6350	9.9518	6.9624	15	30.04	36.6682	5.9786
50.004	2000-6350	9.9518	6.2725	30	36.97		7.3585
50.004	2000-6350	9.9518	6.3465	45	36.23		7.2106
50.001	2000-6350	9.9518	5.6292	60	43.44		8.6452
50.005	2000-6350	9.9518	8.7203	75	12.37		2.4629
50.003	2000-6350	9.9518	9.3905	90	5.64		1.1226
Mass of sample (g)	Particle size (µm)	Initial F <sup>-</sup> Conc measured[Co] (mg/L)	Residual F <sup>-</sup> Conc[Ct] (mg/L)	Time (min)	% Adsorption	% Mean Adsorption (first 60 <sup>th</sup> min)	Adsorption capacity
100.000	500-1000	9.9518	6.2595	15	37.10	48.5699	3.6922
100.002	500-1000	9.9518	4.9290	30	50.47		5.0227
100.003	500-1000	9.9518	4.7901	45	51.87		5.1617
100.001	500-1000	9.9518	4.4943	60	54.84		5.4572
100.006	500-1000	9.9518	8.6902	75	12.68		1.2616
100.007	500-1000	9.9518	9.6541	90	2.99		0.2977
100.004	1000-2000	9.9518	5.3004	15	46.74	50.6810	4.6513
100.005	1000-2000	9.9518	4.4186	30	55.60		5.5330
100.002	1000-2000	9.9518	4.4015	45	55.77		5.5503
100.003	1000-2000	9.9518	5.5120	60	44.61		4.4398
100.005	1000-2000	9.9518	7.7804	75	21.82		2.1712

100.007	1000-2000	9.9518	8.9122	90	10.45		1.0396
100.002	2000-6350	9.9518	6.4798	15	34.89		3.4719
100.004	2000-6350	9.9518	5.9819	30	39.89		3.9697
100.001	2000-6350	9.9518	5.3254	45	46.49	41.5184	4.6264
100.001	2000-6350	9.9518	5.4928	60	44.81		4.4588
100.003	2000-6350	9.9518	8.7283	75	12.29		1.2235
100.001	2000-6350	9.9518	9.3535	90	6.01		0.5983

## APPENDIX E: Preparation of NaF solutions

### E1: Preparation of Stock Anhydrous NaF Solution (100 mg/L)

From the formula;

$$\text{Concentration, } C, = \frac{\text{Amount of substance}}{\text{Volume}} \quad (3)$$

$$\text{Amount of substance, } n = \frac{\text{mass}}{\text{Molar mass}} \quad (4)$$

Putting the two equations together, we have;

$$\text{Mass of substance, } m = C \times M \times V$$

$$\text{Where; } C = 100 \text{ mgF}^-/\text{L}$$

$$M = 41.99 \text{ g/mol (22.990 + 18.998)}$$

$$V = 1000 \text{ cm}^3 \text{ or } 1 \text{ dm}^3 \text{ or } 1 \text{ L}$$

$$1 \text{ ppm} \equiv 1 \text{ mg/L; therefore, } 1000 \text{ ppm/F}^- = 1000 \text{ mg/F}^-$$

$$\% \text{ F}^- \text{ in NaF} = \frac{18.998}{41.988} \times 100 = 45.25\%$$

$$100 \text{ mg/F}^- = 45.25 \times \chi \text{ mg of NaF}$$

$$\chi \text{ mg of NaF} = \frac{100 \text{ mg/F}^-}{45.25/100} = 220.99 \text{ mg} \equiv 0.221 \text{ g}$$

**E2: Preparation of Diluted Anhydrous NaF Solution (1, 5 and 10 mg/L)**

From the relation,

$$C_1 \times V_1 = C_2 \times V_2 \quad (5)$$

Where;  $C_1$  = Initial Concentration of solution

$C_2$  = Final Concentration of solution

$V_1$  = Initial Volume of solution

$V_2$  = Final Volume of solution

For a concentration of 1 mgF<sup>-</sup>/L;

$$V_1 = \frac{C_2 \times V_2}{C_1} = \frac{1 \text{ mg} \times 1000 \text{ cm}^3}{100 \text{ mg}} = 10 \text{ cm}^3$$

For a concentration of 5 mgF<sup>-</sup>/L;

$$V_1 = \frac{C_2 \times V_2}{C_1} = \frac{5 \text{ mg} \times 1000 \text{ cm}^3}{100 \text{ mg}} = 50 \text{ cm}^3$$

For a concentration of 10 mgF<sup>-</sup>/L;

$$V_1 = \frac{C_2 \times V_2}{C_1} = \frac{10 \text{ mg} \times 1000 \text{ cm}^3}{100 \text{ mg}} = 100 \text{ cm}^3$$

## APPENDIX F: Ion Chromatography

### Ion Chromatography

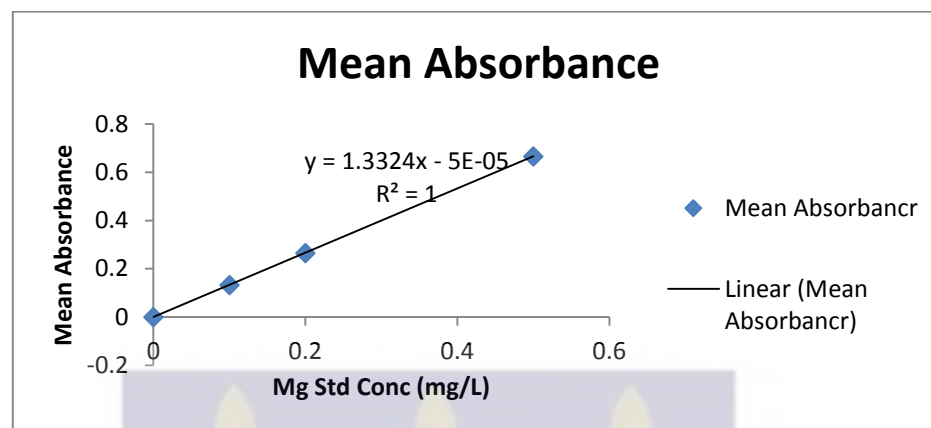
#### *Principle*

Water sample is injected into a stream of Carbonate-Bicarbonate ( $\text{Na}_2\text{CO}_3/\text{NaHCO}_3$ ) eluent and passed through a series of ion exchangers. The pressure transducer measures the system pressure at the point that the eluent flows from the pump head outlet valve into the pressure transducer. The compressor aids in cooling the system as it makes use of air (nitrogen gas) drawn from the surroundings.

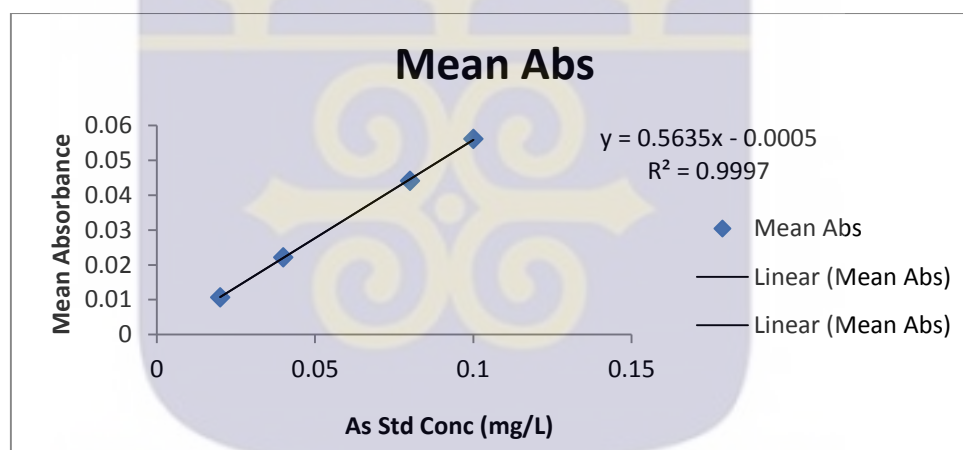
The anions of interest are separated on the basis of their relative affinities for a low capacity, strongly basic anion exchanger (guard and separator columns). The separated anions are directed onto a micro-membrane suppressor bathed in continuously flowing strongly acid solution (Regenerant solution). In the suppressor, the separated anions are converted to their highly conductive acid forms and the Carbonate-Bicarbonate eluent is converted to weakly conductive carbonic acid. The separated anions in their acid forms are measured by conductivity. They are identified on the basis of retention time as compared to standards. Quantitative analysis is by measuring the peak area or height.

## APPENDIX G: Standard Calibration Curve

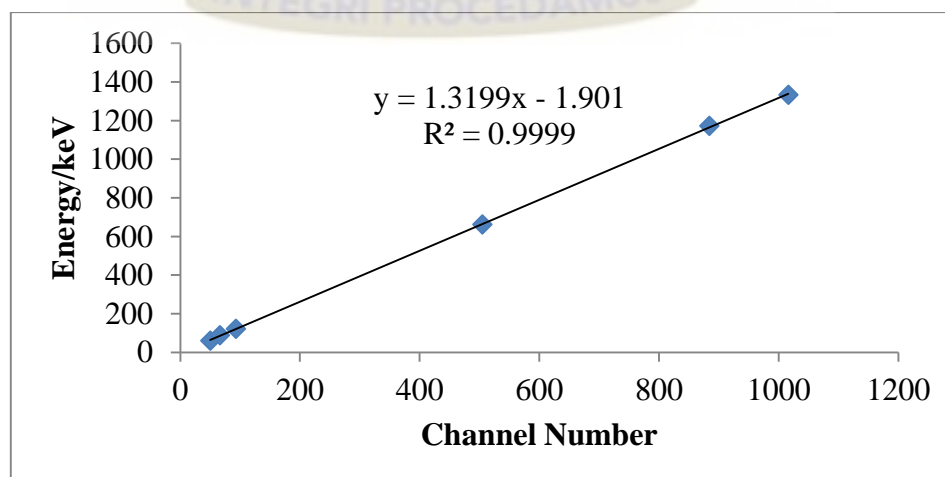
### APPENDIX G1: Magnesium (Mg) Calibration graph



### APPENDIX G2: Arsenic Calibration Curve

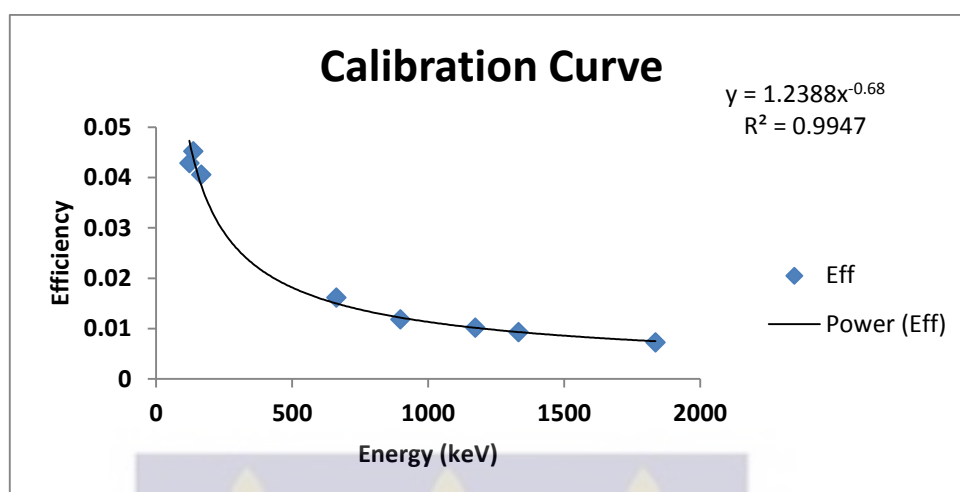


### APPENDIX G3: Energy Calibration Curve





APPENDIX G4: Efficiency Calibration Curve



### APPENDIX H: Batch Adsorption Analysis

APPENDIX H1: Results of comparing anions in water samples before and after column adsorption experiment

Parameters	Sample	Conc. Before Column Analysis (mg/L)	Height of Mini-Column bed (cm)	Volume of Mini-bed Column (cm <sup>3</sup> )	Mass of Adsorbent in Mini-bed Column (g)	Residual Conc. After Column Analysis (mg/L)						Mean % Adsorption
						Time Aliquots Were Taken (Mins)						
						15	30	45	60	75	90	
F <sup>-</sup>	BNN8	7.4781	20	251.20	217.751	2.7823	2.2985	1.1324	1.5782	1.7277	1.7790	74.82
			30	376.80	314.255	1.1981	2.0446	2.4526	1.6432	1.3714	1.1278	78.07
			40	502.40	433.939	0.2757	1.1477	1.5454	1.1093	1.1126	1.1317	85.91
	BNB6	6.1519	20	251.20	217.751	0.1301	1.8796	2.3876	1.953	1.8199	1.8036	72.98
			30	376.80	314.255	1.8430	2.1726	1.8161	1.8701	2.2370	2.0385	67.55
			40	502.40	433.939	1.5870	2.7897	3.0878	2.6451	3.0074	1.9722	59.12
Cl <sup>-</sup>	BNN8	18.9343	20	251.20	217.751	16.7032	14.0901	18.8629	15.8085	16.6779	18.2356	11.64
			30	376.80	314.255	13.2707	16.8549	17.3673	18.9034	16.1215	15.3839	13.82
			40	502.40	433.939	16.6105	13.0259	12.1327	16.0445	18.4893	16.4069	18.39
	BNB6	8.8715	20	251.20	217.751	8.1378	7.0772	8.0666	8.1196	6.5803	7.5403	14.48
			30	376.80	314.255	8.2117	8.1851	7.7532	7.1327	6.3294	6.5494	17.03
			40	502.40	433.939	8.7865	6.0071	7.5743	7.4426	7.9043	7.9394	14.23
NO <sub>3</sub> <sup>-</sup>	BNN8	80.4559	20	251.20	217.751	28.7064	32.8647	27.3536	24.7882	24.1629	34.8897	64.21
			30	376.80	314.255	29.7397	15.6413	31.4220	34.0818	34.4705	36.3429	62.36
			40	502.40	433.939	25.5516	26.8257	78.3549	32.9186	39.0939	38.7698	49.97
	BNB6	36.8015	20	251.20	217.751	27.7043	32.128	35.1536	30.5353	32.8512	23.2942	17.73

			30	376.80	314.255	35.0923	27.1781	30.4703	29.0818	19.9655	32.5311	21.05
			40	502.40	433.939	23.8601	23.703	28.8075	26.2261	24.2955	20.3841	33.30
SO <sub>4</sub> <sup>2-</sup>	BNN8	10.2861	20	251.20	217.751	2.8536	6.8647	6.8606	6.4488	6.8412	6.3917	41.25
			30	376.80	314.255	8.2130	8.2636	9.4456	9.7939	9.9944	10.0075	9.72
			40	502.40	433.939	9.8229	9.6488	8.3678	8.5674	10.0069	10.0477	8.51
	BNB6	51.9879	20	251.20	217.751	18.3589	16.407	1.6289	7.8591	8.3354	15.1713	78.28
			30	376.80	314.255	14.8643	4.6441	9.5094	28.6418	28.9672	30.2819	62.52
			40	502.40	433.939	46.0773	8.5346	7.4508	1.5188	10.2983	14.1865	71.77
PO <sub>4</sub> <sup>3-</sup>	BNN8	<0.001	20	251.20	217.751	2.2523	2.0523	0.0878	0.0102	0.0131	0.0061	
			30	376.80	314.255	<0.001	<0.001	<0.001	<0.001	<0.001	<0.001	
			40	502.40	433.939	<0.001	<0.001	<0.001	<0.001	<0.001	<0.001	
	BNB6	0.014	20	251.20	217.751	<0.001	<0.001	<0.001	<0.001	<0.001	<0.001	
			30	376.80	314.255	0.021	<0.001	0.9012	1.111	<0.001	<0.001	
			40	502.40	433.939	<0.001	<0.001	<0.001	<0.001	<0.001	<0.001	

